



UFBA

UNIVERSIDADE FEDERAL DA BAHIA
ESCOLA POLITÉCNICA
PROGRAMA DE PÓS-GRADUAÇÃO EM
ENGENHARIA INDUSTRIAL - PEI

DOUTORADO EM ENGENHARIA INDUSTRIAL

NATHÁLIA FREITAS FREIRE

**DEVELOPMENT OF BIOBASED POLYMERIC
NANOPARTICLES CONTAINING ACTIVE
PHARMACEUTICAL INGREDIENTS FOR
ANTICANCER APPLICATION**

PEI
PROGRAMA DE PÓS-GRADUAÇÃO EM
ENGENHARIA INDUSTRIAL - PEI
Salvador
2022



UNIVERSIDADE FEDERAL DA BAHIA
ESCOLA POLITÉCNICA
PROGRAMA DE PÓS-GRADUAÇÃO EM ENGENHARIA INDUSTRIAL

**DEVELOPMENT OF BIOBASED POLYMERIC NANOPARTICLES
CONTAINING ACTIVE PHARMACEUTICAL INGREDIENTS FOR
ANTICANCER APPLICATION**

NATHÁLIA FREITAS FREIRE

Salvador
2022

NATHÁLIA FREITAS FREIRE

**DEVELOPMENT OF BIOBASED POLYMERIC NANOPARTICLES
CONTAINING ACTIVE PHARMACEUTICAL INGREDIENTS FOR
ANTICANCER APPLICATION**

Tese de Doutorado apresentada ao Programa de Pós-Graduação em Engenharia Industrial (PEI), Escola politécnica da Universidade Federal da Bahia (UFBA), como requisito parcial para obtenção do grau de Doutora em Engenharia Industrial.

Orientadoras:

Prof.^a Dra. Elaine Cabral Albuquerque

Prof.^a Dra. Rosana Lopes Fialho

Coorientadores:

Prof.^a Dra. Claudia Sayer

Prof. Dr. Pedro Hermes de Araújo

Prof. Dr. Guillermo Velasco Díez

Salvador
2022

Ficha catalográfica elaborada pelo Sistema Universitário de Bibliotecas (SIBI/UFBA),
com os dados fornecidos pelo(a) autor(a).

Freitas Freire, Nathália

Development of biobased polymeric nanoparticles containing active pharmaceutical ingredients for anticancer application / Nathália Freitas Freire. -- Salvador, 2022.

125 f. : il

Orientadora: Elaine Cabral Albuquerque.

Coorientadora: Rosana Lopes Fialho.

Tese (Doutorado - Programa de Pós-graduação em Engenharia Industrial) -- Universidade Federal da Bahia, Escola Politécnica, 2022.

1. Monômeros de base biológica. 2. Nanopartículas de poli(tioéter-éster). 3. Polimerização por miniemulsão in situ via tiol-eno. 4. Emulsificação com evaporação de solvente. 5. Insumos farmacêuticos ativos (IFAs) . I. Cabral Albuquerque, Elaine. II. Lopes Fialho, Rosana. III. Título.

DEVELOPMENT OF BIOBASED POLYMERIC NANOPARTICLES CONTAINING ACTIVE PHARMACEUTICAL INGREDIENTS FOR ANTICANCER APPLICATION

Nathália Freitas Freire

Tese submetida ao corpo docente do programa de pós-graduação em Engenharia Industrial da Universidade Federal da Bahia como parte dos requisitos necessários para a obtenção do grau de doutor em Engenharia Industrial.

Examinada por:

Raquel de Melo Barbosa

Prof. Dra. Raquel de Melo Barbosa
Universidad de Granada

Documento assinado digitalmente
gov.br JOYCE BATISTA AZEVEDO
Data: 27/02/2023 15:55:04-0300
Verifique em <https://verificador.iti.br>

Prof. Dra. Joyce B. Azevedo
Universidade Federal da Bahia



Documento assinado digitalmente
Bruno Francisco Oechsler
Data: 15/02/2023 13:03:31-0300
CPF: ***.182.959-**
Verifique as assinaturas em <https://v.ufsc.br>

Prof. Dr. Bruno Francisco Oechsler
Universidade Federal de Santa Catarina

Islane Espírito Santo

Prof. Dra. Islane Espírito Santo
ITF Chemical LTDA

Prof. Dr. Guillermo D. Velasco
Universidad Complutense de Madrid

VELASCO DIEZ
GUILLERMO - 50443341V

Firmado digitalmente por VELASCO DIEZ GUILLERMO -
50443341V
Nombre de reconocimiento (DN): c=ES,
serialNumber=IDCES-50443341V, givenName=GUILLERMO,
sn=VELASCO DIEZ, cn=VELASCO DIEZ GUILLERMO -
50443341V
Fecha: 2023.02.17 16:55:14 +01'00'

Salvador, BA - BRASIL

2022

Para minha mãe, que me ensinou o verdadeiro significado de resiliência.

Acknowledgments

A gratidão é a memória do coração. Gostaria de agradecer ao Universo, pelo tempo e pela vida. A toda a minha família, por me dar doses diárias de amor. À minha mãe, você é a minha base, obrigada pelo incentivo e aconselhamento de todos os dias. À minha irmã, pelo notório carinho. Minhas sobrinhas Julia e Liz, que me encham de luz e vida. As minhas orientadoras, Dra. Elaine Cabral Albuquerque e Dra. Rosana Lopes Fialho. Obrigada pelos direcionamentos, por acreditarem e apostarem no meu potencial. Agradeço pela interação, o incentivo e a confiança! Aos professores Dr. Pedro Hermes Araújo e Dra. Claudia Sayer, meus coorientadores na Universidade Federal de Santa Catarina, pelo acolhimento e orientação de forma excepcional, por abrirem as portas do laboratório, incentivando e indicando, a todo momento, o caminho do conhecimento. A toda a família LCP, que proporcionou trabalho coletivo, me enchendo de ensinamentos diários e contínuos. Onde fui aprendendo a ser cientista. Foi realmente incrível poder trabalhar com vocês. Ao Leandro e ao centro de análises, por toda a ajuda. Ao professor Dr. Guillermo Velasco e a todos do Grupo de Señalización por Cannabinoides do Departamento Bioquímica y Biología Molecular da Universidad Complutense de Madrid, Espanha. Foi incrível aprender sobre o mundo celular, vocês são tão gentis, obrigado por compartilhar o conhecimento. Além disso, muito obrigada a todos os pesquisadores do departamento de Farmácia da Complutense, aprendi muito sobre as técnicas de cromatografia e os processos de liberação das nanopartículas.

A Theseu, Camila, Paulinho e a AMAME, pelas doações de amostras e por acreditarem no poder da ciência. A todos os meus amigos, os antigos e os novos, sempre me fazendo sentir viva, em momentos de dificuldade e diversão. À Coordenação de Aperfeiçoamento de Pessoal de Nível Superior (CAPES), pelo apoio financeiro e parceria no projeto. À Universidade Federal da Bahia, ao Programa de Pós-Graduação em Engenharia Industrial e à Escola Politécnica pela oportunidade.

Que nada nos limite.

Que nada nos defina.

Que nada nos sujeite.

Que a liberdade seja a nossa própria substância, já que viver é ser livre.

Simone de Beauvoir (1970)

Abstract

Vegetable oils are potential substitutes for petroleum derivatives, as they present themselves as a clean and environmentally friendly alternative and are available in high quantities at relatively low prices. Biomass-derived chemicals can be converted into monomers with unique structures, generating materials with new properties. Methyl 10-undecenoic acid, a castor oil derived, was shown to be a suitable starting material for the preparation of esters with alkene groups that can be lead in biodegradable polymers. The main objective of this research work is the study of the synthesis and physical, chemical, and biological characterization of polymeric particles derived from renewable sources, containing the active pharmaceutical ingredients (APIs) zinc phthalocyanine (ZnPc) and full-spectrum *Cannabis* extract (CN), both with promising action against cancer. At the first step of the work, the encapsulation of zinc phthalocyanine in poly(thioether-ester) (PTEe) nanoparticles via thiol-ene miniemulsion polymerization using a biobased α - ω -diene diester monomer (derived from castor oil) was obtained. Two different thiols were employed as comonomers. ZnPc loaded PTEe nanoparticles presented an average diameter of around 122 -145 nm and high encapsulation efficiency (> 95%) of ZnPc for both thiols. FTIR and thermal analyses showed that there was no significant interaction between the drug and the polymer, indicating that ZnPc is molecularly dispersed in the polymeric matrix. The ZnPc release profile in the nanoparticles showed an initial burst effect followed by a slow-release rate. Cytotoxicity studies showed that nanoparticles do not cause hemolytic damage and showed phototoxic effect in breast cancer cells at low concentrations of ZnPc. In second step, full-spectrum *Cannabis* extract was encapsulated in PTEe nanoparticles synthesized by thiol-ene *in situ* miniemulsion and solvent evaporation with the biobased monomer (1,3-propylene diundec-10-enoate). The Full-spectrum *Cannabis* extract was analyzed by physicochemical characterizations and also by biological *in vitro* studies such as cytotoxicity assay, hemolysis assay, apoptosis, and membrane potential to investigate the potential of nanoparticles for anticancer therapy treatments. With high encapsulation efficiency (> 97%) and an average diameter between 91 - 229 nm, the encapsulation of full-*Cannabis* extract in biobased nanoparticles was efficient to stimulate a cytotoxic effect on cancer cells line.

Keywords: Biobased monomer; Poly(thioether-ester) nanoparticles; Thiol-ene *in situ* miniemulsion polymerization; Solvent evaporation; Zinc phthalocyanine; Full-spectrum *Cannabis* extract; Cancer therapy; *in vitro* studies.

Resumo

Os óleos vegetais são potenciais substitutos dos derivados de petróleo, sendo uma alternativa limpa, ambientalmente amigável e de alta disponibilidade. Os produtos químicos derivados de biomassa podem ser convertidos em monômeros com estruturas únicas e novas propriedades. O ácido 10-undecenoico, derivado do óleo de rícino, apresenta-se como um potencial material para a preparação de ésteres que podem ser transformados em polímeros biodegradáveis. Esse projeto de pesquisa possui como objetivo estudar a síntese e a caracterização físico, química e biológica de nanopartículas poliméricas, derivadas de fontes renováveis, contendo os insumos farmacêuticos ativos (IFAs) ftalocianina de zinco e extrato de *Cannabis* completo, ambos com propriedades promissoras ação contra o câncer. Na primeira etapa do trabalho, obteve-se o encapsulamento de ftalocianina de zinco (ZnPc) em nanopartículas de poli(tioéter-éster) (PTEe) por polimerização em miniemulsão *in situ* via tiol-eno utilizando monômero α - ω -dieno diester de base biológica (derivado do óleo de rícino). Dois tióis diferentes foram empregados como comonômeros. As nanopartículas de PTEe carregadas de ZnPc apresentaram um diâmetro médio de 122 -145 nm e alta eficiência de encapsulamento (> 95%). As nanopartículas de PTEe contendo ZnPc apresentaram um diâmetro médio entre 122-145 nm e alta eficiência de encapsulamento (> 95%). As análises mostraram que não houve interação significativa entre a substância e a cadeia polimérica, indicando que o ZnPc está disperso na matriz. O perfil de liberação do ZnPc apresentou uma rápida liberação inicial (efeito burst) seguido de uma taxa de liberação lenta. Os estudos de citotoxicidade revelaram que as nanopartículas não causam danos hemolíticos e apresentaram efeito fototóxico em células de câncer de mama. Na segunda etapa do trabalho, o extrato completo de *Cannabis* foi encapsulado em nanopartículas poliméricas de PTEe pelas técnicas de miniemulsão *in situ* e evaporação de solvente, utilizando o monômero 1,3-propylene diundec-10-enoate. O extrato de *Cannabis* foi analisado por caracterizações físico-químicas e por estudos biológicos *in vitro*, como ensaio de citotoxicidade, ensaio de hemólise, apoptose e potencial de membrana para investigar o potencial das nanopartículas em tratamentos anticancerígenos. Com alta eficiência de encapsulamento (> 97%) e um diâmetro médio entre 91 - 229 nm, o encapsulamento de extrato de *Cannabis* em nanopartículas de base biológica foi eficiente para estimular um efeito citotóxico na linhagem de células cancerígenas.

Palavras-chave: Monômeros de base biológica; Nanopartículas de poli(tioéter-éster); Polimerização por miniemulsão *in situ* via tiol-eno; Evaporação de solvente; Ftalocianina de zinco; Extrato de *Cannabis* completo; Terapia anticancerígena; estudos *in vitro*.

List of Figures

FIGURE 1- DEMONSTRATION OF THE STRUCTURE OF POLYUNSATURATED TRIGLYCERIDE	8
FIGURE 2- FATTY ACIDS COMMONLY USED IN POLYMER CHEMISTRY: A) OLEIC ACID, B) LINOLEIC ACID, C) LINOLENIC ACID, D) ERUCIC ACID, E) PETROSELINIC ACID, F) RICINOLEIC ACID, G) VERNOLIC ACID, H) 10-UNDECENOIC ACID	9
FIGURE 3- CHEMICAL REACTIONS FOR THE PREPARATION OF A VARIETY OF DERIVATIVES OF CASTOR OIL	11
FIGURE 4- PRODUCTS OF THE THERMAL FRAGMENTATION OF RICINOLEIC ACID. 1) RICINOLEIC ACID, 2) 10-UNDECENOIC ACID, 3) HEPTANAL	11
FIGURE 5- SCHEMATIC REPRESENTATION OF VARIOUS TECHNIQUES FOR THE PREPARATION OF POLYMER NANOPARTICLES	14
FIGURE 6- SCHEME OF THE EMULSIFICATION-SOLVENT EVAPORATION	15
FIGURE 7- SCHEME OF THE MINIEMULSION PROCESS	17
FIGURE 8- THE MECHANISM FOR THE HYDROTHIOLATION OF A C=C BOND IN THE PRESENCE OF AN INITIATOR	18
FIGURE 9- MOLECULAR STRUCTURE OF ZINC PHTHALOCYANINE	25
FIGURE 10- MAIN CANNABINOIDS PRESENT IN CANNABIS SATIVA	27
FIGURE 11- BIOSYNTHETIC PATHWAY FOR THE PRODUCTION OF CANNABINOIDS AND MAIN BREAKDOWN PRODUCTS OF THC	28
FIGURE 12- TEM IMAGES OF ZNPc-PTEE NANOPARTICLES. A) DITHIOL+ZNPc; B) TETRATHIOL+ZNPc	40
FIGURE 13- FTIR SPECTRUM OF ZNPc LOADED POLYMERIC NANOPARTICLES	42
FIGURE 14- THERMAL DEGRADATION ANALYSIS (TGA) AND DIFFERENTIAL SCANNING CALORIMETRY (DSC) OF NANOPARTICLES SAMPLES OF DITHIOL AND TETRATHIOL POLYMERS AND ZNPc LOADED	43
FIGURE 15- THE RELEASE PROFILE OF ZNPc-PTEE NANOPARTICLES OBTAINED WITH DITHIOL AND TETRATHIOL IN pH 7.4. DATA REFER TO THE MEAN ± STANDARD DEVIATION (N =2) WITH AN EXPERIMENTAL ERROR OF ±10%	45
FIGURE 16- (A) CYTOTOXIC EFFECT OF FREE ZNPc AND ZNPc-PTEE NANOPARTICLES AT DIFFERENT CONCENTRATIONS IN NIH3T3 CELLS (B) HEMOLYSIS ASSAY. RELATIVE RATE OF	

HEMOLYSIS IN RBCs UPON INCUBATION (2H) WITH FREE ZNPc AND ZNPc-PTEe NANOPARTICLES AT DIFFERENT CONCENTRATIONS. DATA REPRESENT MEAN \pm SD (N = 3). (* P < 0.05) ONE-WAY ANOVA FOLLOWED BY TUKEY'S TEST.	47
FIGURE 17- PHOTOTOXICITY ASSAY AT DIFFERENT CONCENTRATIONS OF FREE ZNPc AND ZNPc-PTEe NANOPARTICLES ON MDA-MB231 CELL. DATA REPRESENT THE MEAN \pm SD (N = 3). (* P < 0.05) TWO WAY ANOVA FOLLOWED BY TUKEY'S TEST.	48
FIGURE 18- SYNTHESIS OF NANOPARTICLES AND ENCAPSULATION OF <i>CANNABIS</i> EXTRACT BY ME-PTEe AND SE-PTEe.	56
FIGURE 19- CHROMATOGRAM OF THE FULL-SPECTRUM <i>CANNABIS</i> EXTRACT AT A CONCENTRATION OF 25MG ML ⁻¹	62
FIGURE 20- TRANSMISSION ELECTRON MICROSCOPY (TEM) IMAGES OF CN-PTEe NANOPARTICLES. (A) ME1; (B) SE1.	64
FIGURE 21- FTIR SPECTRUM OF CN AND CN LOADED (A)ME-PTEe AND (B)SE-PTEe POLYMERIC NANOPARTICLES.	67
FIGURE 22- DIFFERENTIAL SCANNING CALORIMETRY-DSC: (A) ME-PTEe AND (B) SE-PTEe. THERMOGRAVIMETRY ANALYSIS-TGA: (C) ME-PTEe AND (D) SE-PTEe. PHYSICAL MIX (1:1) OF PTEe AND CN.	69
FIGURE 23- B16F10 (A) AND NIH3T3 (B) CELLS. IN VITRO CYTOTOXICITY ASSAY OF FREE CN AND CN ENCAPSULATED IN PTEe NANOPARTICLES, SE3 AND ME3. SIGNIFICANT DIFFERENCES ARE SHOWN ***P < 0.0001; ****P < 0.00001 - COMPARED TO THE CN GROUP AND #P < 0.01; ####P < 0.00001 - COMPARED TO THE CT GROUP - TWO-WAY ANOVA FOLLOWED BY TUKEY TEST).	71
FIGURE 24- HEMOLYSIS ASSAY ON HUMAN ERYTHROCYTES UPON INCUBATION WITH 10, 20 AND 30 NM GNPs SOLUTIONS AT DIFFERENT CONCENTRATIONS. DATA REPRESENT MEAN \pm SD (N = 3).	72
FIGURE 25- EFFECTS OF FREE CN AND CN ENCAPSULATED IN PTEe NANOPARTICLES (SE3 AND ME3) ON THE MITOCHONDRIAL MEMBRANE POTENTIAL OF B16F10 CELLS. CELLS WERE STAINED WITH TMRM AND HOESCHT AND ANALYZED BY FLUORESCENCE MYCROSCOPY.	73
FIGURE 26- FLOW CYTOMETRY ANALYSIS. B16F10 CELLS WERE STAINED WITH AN ANNEXIN V-FITC AND PROPIDIUM IODIDE (PI) AT DIFFERENT INCUBATION TIMES AFTER TREATMENT WITH MEL-B AT NEARLY THE IC50 CONCENTRATION. DATA ARE AVERAGE VALUE \pm STANDARD DEVIATION (N=3).	74
FIGURE 27- (A) BF16F10 MELANOMA CELLS WERE SEEDED IN 60-MM DIAMETER CULTURE DISHES, INCUBATED OVERNIGHT, AND TREATED WITH FREE CN AND CN ENCAPSULATED IN	

PTEE NANOPARTICLES (Se3) FOR 24 H AT THE CONCENTRATIONS INDICATED (5, 25, 50 MG.ML⁻¹). WHOLE-CELL EXTRACTS WERE PROCESSED FOR WESTERN BLOT ANALYSIS OF THE INDICATED ANTIBODIES. B-ACTIN PROTEIN LEVELS IN THE SAME EXTRACT WERE USED AS A CONTROL LOADING. DATA ARE AVERAGE VALUE ± STANDARD DEVIATION (N = 5). FOR STATISTICAL ANALYSIS WE PERFORMED UNPAIRED T TEST **P<0.01; ***P=0.0001; ****P<0.0001. THE BANDS SHOWN IN FIGURE 9A WERE SCANNED AS DIGITAL PEAKS AND THE AREAS OF THE PEAKS WERE REPORTED AS FOLD INDUCTION IN PERCENTAGE RESPECT TO THE VEICHL (CT), AS DESCRIBED IN MATERIAL AND METHODS. 76

FIGURE A.1- CALIBRATION CURVE OF ZINC PHTHALOCYANINE PRODUCED WITH DIMETHYLSULFOXIDE AS SOLVENT FOR ANALYSIS OF ENCAPSULATION EFFICIENCY. 103

FIGURE A.2- CALIBRATION CURVE OF CBD PRODUCED WITH METANOL AS SOLVENT FOR ANALYSIS OF ENCAPSULATION EFFICIENCY. 104

FIGURE A.3- CALIBRATION CURVE OF THC PRODUCED WITH METANOL AS SOLVENT FOR ANALYSIS OF ENCAPSULATION EFFICIENCY. 105

FIGURE A.4- CALIBRATION CURVE OF CBN PRODUCED WITH METANOL AS SOLVENT FOR ANALYSIS OF ENCAPSULATION EFFICIENCY. 106

FIGURE A.5- T98G (A), U87 (B) AND BF16F10 (C) CELLS. IN VITRO CYTOTOXICITY ASSAY OF FREE CN AND CN ENCAPSULATED IN PTEE NANOPARTICLES, Se3. ALL ASSAYS WERE PERFORMED AT EQUIVALENT TO THC CONCENTRATIONS. DATA ARE AVERAGE VALUE ± STANDARD DEVIATION (N = 3). FOR STATISTICAL ANALYSIS WE PERFORMED UNPAIRED T TEST *P<0.05; **P<0.01; ***P=0.0001; ****P<0.0001. 107

FIGURE A.6- DOT PLOT. FLOW CYTOMETRY ANALYSIS. B16F10 CELLS WERE STAINED WITH AN ANNEXIN V-FITC AND PROPIDIUM IODIDE (PI) AT DIFFERENT INCUBATION TIMES AFTER TREATMENT WITH CN, Se3 AND Me3 AT NEARLY THE IC50 CONCENTRATION. 108

SCHEME 1- SCHEMATIC REPRESENTATION OF THE ESTERIFICATION REACTION FOR SYNTHESIS OF RENEWABLE MONOMER AND THE STUDIED THIOL-ENE REACTION BETWEEN 1,3-PROPYLENE UNDEC-10-ENOATE WITH THIOL OR TETRATHIOL..... 35

List of Tables

TABLE 1- EXAMPLES OF CURRENTLY DEVELOPED NANOPARTICLES AS DRUG DELIVERY SYSTEMS FOR THE TREATMENT OF CANCER.	21
TABLE 2- INTENSITY MEAN DIAMETER: DROPLETS (DP_G) AND NANOPARTICLES (DP); POLYDISPERSITY INDEX: DROPLETS (PDI_G), NANOPARTICLES (PDI) OBTAINED BY DLS AND ENCAPSULATION EFFICIENCY (EE).	41
TABLE 3- MATHEMATICAL MODELS AND KINETIC PARAMETERS.	46
TABLE 4- RETENTION TIME, LINEAR RETENTION INDICES CALCULATED (LRI), THE MAJORITY IONS (M/Z), CHEMICAL FUNCTION, AND A MOLECULAR FORMULA OF EACH IDENTIFIED COMPOUND.	62
TABLE 5- INTENSITY MEAN DIAMETER: DROPLETS (DP_G) AND NANOPARTICLES (DP); POLYDISPERSITY INDEX: DROPLETS (PDI_G), NANOPARTICLES (PDI) OBTAINED BY DLS, AND WEIGHT AVERAGE BY GPC.....	65

List of Acronyms and Abbreviations

ANVISA - Brazilian Health Regulatory Agency

APIs- Active Pharmaceutical Ingredients

B16F10- Melanoma cells

CBD- Cannabidiol

CN- Full-spectrum *Cannabis* extract

CN-PTEe- Nanoparticles containing full-spectrum *Cannabis* extract

Dithiol- Butanedithiol

DLS- Dynamic light scattering

DMEM- Dulbecco's modified eagle medium

DMSO- Dimethyl sulfoxide

DSC- Differential Scanning Calorimetry

EE%- Encapsulation efficiency

FBS- Fetal bovine serum

FTIR- Fourier-transform infrared spectroscopy

GC/FID- Gas Chromatography with Flame-Ionization Detection

GC/MS- Gas Chromatograph coupled with mass spectrometer

GPC- Gel permeation chromatography

HPLC- High-performance liquid chromatograph

IUPAC- International Union of Pure and Applied Chemistry

MDA-MB231- Breast cancer cells

Me-PTEe- *in-situ* thiol-ene miniemulsion polymerization

MTT- 3-(4,5-dimethylthiazol-2-yl)-2,5-diphenyltetrazolium bromide

NIH3T3- Murine fibroblast

PBS- Phosphate Buffered Saline solution

PDT- Photodynamic therapy

PTEe- Poly(thioether-ester)

PTSA- p-toluenesulfonic acid monohydrate

RBCs- Human red blood

SDS- Sodium dodecyl sulfate

Se-PTEe- Miniemulsification with solvent evaporation

T98- Glioma cells

TEM- Transmission Electronic Microscopy

Tetrathiol- Pentaerythritol tetrakis

TGA - Thermal degradation analysis

THC- Delta-9-tetrahydrocannabinol

U87- Glioma cells

ZnPc- Zinc phthalocyanine

ZnPc-PTEe- Zinc phthalocyanine loaded in poly-thioether-ester

Table of Contents

<i>Chapter 1</i>	1
1.0 INTRODUCTION	1
1.1 OBJECTIVES	4
1.1.1 OBJECTIVE	4
1.1.2 SPECIFIC OBJECTIVES	4
<i>Chapter 2</i>	5
2.0 REVIEW	5
2.1 GREEN CHEMISTRY: MONOMERS AND POLYMERS FROM RENEWABLE RESOURCES	5
2.2 SYNTHESIS OF MONOMERS FROM VEGETABLE OILS	7
2.3 CASTOR OIL AS RENEWABLE RAW MATERIAL	10
2.4 NANOPARTICLES POLYMERIZATION TECHNIQUES	12
2.4.1 SOLVENT EVAPORATION TECHNIQUE	14
2.4.2 MINIEMULSION POLYMERIZATION	15
2.4.3 THIOL-ENE POLYMERIZATION	17
2.5 APPLICATION OF POLYMERIC NANOPARTICLES IN CANCER THERAPY	20
2.6 ANTICANCER ACTIVE PHARMACEUTICAL INGREDIENTS (APIs)	24
2.6.1 ZINC PHTHALOCYANINE	25
2.6.2 CANNABIS EXTRACT	26
2.7 FINAL CONSIDERATIONS	31
<i>Chapter 3</i>	32
3.0 ZINC PHTHALOCYANINE ENCAPSULATION VIA THIOL-ENE MINIEMULSION POLYMERIZATION AND IN VITRO PHOTOTOXICITY STUDIES	32
3.1 INTRODUCTION	32
3.2 EXPERIMENTAL PROCEDURE	35
3.2.1 MATERIALS	35
3.2.2 SYNTHESIS OF THE BIOBASED α,ω -DIENE-DIESTER MONOMER	36
3.2.3 SYNTHESIS OF ZnPc LOADED IN PTEe NANOPARTICLES VIA THIOL-ENE MINIEMULSION POLYMERIZATION	36
3.3 CHARACTERIZATION	37
3.3.1 PARTICLE SIZE, SURFACE CHARGE, AND MORPHOLOGY	37
3.3.2 FOURIER-TRANSFORM INFRARED SPECTROSCOPY	37
3.3.3 THERMAL ANALYSIS	37
3.3.4 ENCAPSULATION EFFICIENCY	37

3.4 IN VITRO STUDIES	38
3.4.1 RELEASE PROFILE STUDIES	38
3.4.2 CYTOTOXICITY ASSAY	38
3.4.3 PHOTOTOXICITY STUDIES	39
3.4.4 HEMOLYSIS ASSAY	39
3.5 RESULTS AND DISCUSSION.....	40
3.5.1 IN VITRO STUDIES.....	44
3.6 CONCLUSIONS	49
<i>Chapter 4</i>	50
4.0 PREPARATION AND CHARACTERIZATION OF FULL-SPECTRUM CANNABIS EXTRACT LOADED POLY(THIOETHER-ESTER) NANOPARTICLES: IN VITRO EVALUATION OF THEIR ANTITUMORAL EFFICACY.....	50
4.1 INTRODUCTION	50
4.2 MATERIAL AND METHODS.....	53
4.2.1 MATERIALS.....	53
4.2.2 SYNTHESIS OF THE BIOBASED A, Ω -DIENE-DIESTER MONOMER	54
4.2.3 SYNTHESIS OF PTEe NANOPARTICLES CONTAINING FULL-SPECTRUM CANNABIS EXTRACT VIA THIOL-ENE MINIEMULSION POLYMERIZATION (Me- PTEe)	54
4.2.4 SYNTHESIS OF PTEe NANOPARTICLES CONTAINING FULL-SPECTRUM CANNABIS EXTRACT VIA MINIEMULSIFICATION AND SOLVENT EVAPORATION (Se-PTEe)	55
4.3 CHARACTERIZATION.....	56
4.3.1 FULL-SPECTRUM CANNABIS EXTRACT CHARACTERIZATION, QUALITATIVE AND QUANTITATIVE	56
4.3.2 PARTICLE SIZE, SURFACE CHARGE, AND MORPHOLOGY.....	57
4.3.3 FOURIER-TRANSFORM INFRARED SPECTROSCOPY	57
4.3.4 THERMAL ANALYSIS	58
4.3.5 GEL PERMEATION CHROMATOGRAPHY.....	58
4.3.6 ENCAPSULATION EFFICIENCY	58
4.4 IN VITRO STUDIES: ANALYSIS OF THE EFFECT OF THE ENCAPSULATED CANNABINOIDS ON THE VIABILITY OF CANCER CELL LINES	59
4.4.1 CYTOTOXICITY ASSAY.....	59
4.4.2 HEMOLYSIS ASSAY	59
4.4.3 APOPTOSIS	60
4.4.4 MEMBRANE POTENTIAL	60
4.4.5 WESTERN BLOT	60
4.4.6 STATISTICAL ANALYSIS	61
4.5 RESULTS AND DISCUSSION.....	61

4.5.1 FULL-SPECTRUM CANNABIS EXTRACT CHARACTERIZATION.....	61
4.5.2 PREPARATION AND CHARACTERIZATION OF THE NANOPARTICLES	63
4.5.3 CYTOTOXICITY	70
4.5.4 MITOCHONDRIAL MEMBRANE POTENTIAL AND APOPTOSIS.....	72
4.5.5 ANALYSIS OF CELL PROLIFERATION AND AUTOPHAGY MARKERS	74
4.6 CONCLUSIONS	76
<i>Chapter 5</i>	78
5.0 FINAL CONSIDERATIONS	78
5.1 CONCLUSIONS	78
5.2 RECOMMENDATIONS FOR FUTURE WORK	79
<i>Chapter 6</i>	80
6.0 REFERENCES	80
<i>Appendix</i>	103

Chapter 1

1.0 INTRODUCTION

The polymer industry plays a significant role in our society as polymers have become essential materials in modern societies. But, issues with the extensive use of fossil-based raw materials, large amounts of reagents, and the accumulation of polymeric materials in the environment have increased. The necessity of releasing the polymer industry from its dependence on depleting resources represents a major concern, pushing the search for industrially applicable renewable alternatives (MONTERO DE ESPINOSA; MEIER, 2011).

Materials in the environment give scientists and engineers the possibility to change the polymerization process intend to develop a sustainable society. Research has focused mainly on replacing fossil raw materials with renewable alternatives and on developing end-of-life options that generate materials that are suitable for recycling or biodegradation (ZHU; ROMAIN; WILLIAMS, 2016).

The development of sustainable technologies has been dealt with in several ways, one of which is the application of the principles of green chemistry to various processes. The design of chemical products and processes, that reduce or eliminate the use and generation of hazardous substances, is essential to living without having a negative impact to the environment. The sustainability evaluation of a product's manufacture starts from the analysis of the employed feedstock and its extraction. This consideration highlights the importance of the 7th principle of green chemistry: "a raw material or feedstock should be renewable rather than depleting, wherever technically and economically practicable" (LLEVOT; MEIER, 2016).

A collaborative effort by industry, academia, and the government is needed to promote the adoption of the green chemistry technologies necessary to achieve a sustainable civilization. The progress of chemistry research, associated with the industrial revolution, created a new scope for the preparation of novel polymeric materials based on renewable resources.

Biomass-derived chemicals can be converted into monomers with unique structures, leading to materials with novel properties, or modified in order to substitute commercial petroleum-based. Vegetable oils represent one of the most interesting classes of renewables for

the synthesis of sustainable monomers and polymers and it can undergo polymerization by different polymerization processes, as emulsion solvent evaporation and miniemulsion polymerization via thiol-ene. Miniemulsion polymerization is a heterogeneous polymerization process used for the production of polymers in the form of nanoparticles, aiming at different applications of polymeric material. The thiol-ene reactions can be used in polymer and monomer synthesis and modification, side-chain/end-group modification and preparation of various types of branched macromolecules. In the solvent evaporation technique, polymer solutions are prepared in volatile solvent and emulsions are formulated. These kinds of polymeric nanoparticles can be used in biomedical and pharmaceutical applications as antitumor therapy (LOWE, 2014; MACHADO, FABRICIO; LIMA; PINTO, 2007; MONTERO DE ESPINOSA; MEIER, 2011; RAO; GECKELER, 2011).

Nanoparticles have been of significant interest over the last decade as they offer great benefits for drug delivery to overcome limitations in conventional chemotherapy for anticancer treatments for example. Nanoparticles for use as antitumor drug carriers have been in development due to their many advantages as prolonging the biological circulation time, minimizing non-specific uptake, preventing undesirable side effects, improving cellular penetration, and allowing for specific cancer-targeting. (NGUYEN, 2011).

A considerable amount of works has been conducted in search of novel cancer therapies using nanoparticle technology. Combined treatments employ either naturally active ingredients or drugs already intended for other uses, with the aim to increase cell sensitivity to therapy and reduce drug toxicity, using a particular pharmaceutical combination and nanotechnology to develop drug delivery systems for targeting drugs to specific tumors. (PICCOLO; MENALE; CRISPI, 2015).

In this work, different kinds of active pharmaceutical ingredients (APIs) will be investigated to enhance cancer treatments. Zinc phthalocyanine (promising sensitizer for the use in photodynamic therapy for anticancer treatment) and full-spectrum *Cannabis* extract (recently discovered with promising action against cancer) were encapsulated in renewable and biodegradable nanoparticles synthesized by *in situ* miniemulsion via thiol-ene and solvent evaporation technique with a monomer derived from vegetable oil. Given the therapeutic potential of the substances mentioned, it is necessary to obtain rigorous scientific data to evaluate the production of polymeric nanoparticles and the action of the proposed drugs encapsulated.

This document was divided into 6 chapters, as described next.

Chapter 1 → In this Chapter, the motivation, aims and overview of the work are given.

Chapter 2 → A theoretical background information and basic principles are presented to facilitate the understanding of the following chapters.

Chapter 3 → First step of the research project is presented as publication-style chapter: Zinc phthalocyanine encapsulation via thiol-ene miniemulsion polymerization and *in vitro* phototoxicity studies.

Chapter 4 → Second step of the research project is presented as publication-style chapter: Preparation and characterization of full-spectrum *Cannabis* extract loaded Poly(thioether-ester) nanoparticles: *in vitro* evaluation of their antitumoral efficacy.

Chapter 5 → Conclusions and recommendations for future work.

Chapter 6 → References.

1.1 OBJECTIVES

1.1.1 OBJECTIVE

Study of the synthesis of biobased polymeric nanoparticles containing active pharmaceutical ingredients (APIs) for use as antitumor therapy.

1.1.2 SPECIFIC OBJECTIVES

- Produce renewable monomer by esterification of 10-Undecenoic acid and 1,3-propanediol, derived from castor oil;
- To analyze two different thiols, 1,4-butanedithiol and pentaerythriol tetrakis, as comonomers.
- To develop biobased polymeric nanoparticles by thiol-ene miniemulsion and solvent evaporation;
- Encapsulate zinc phthalocyanine and full-spectrum *Cannabis* extract;
- Evaluate the physicochemical properties of polymeric nanoparticles obtained;
- Evaluate encapsulation efficiency and drug release profile from polymeric nanoparticles;
- Carry out *in vitro* cytotoxicity studies of polymeric nanoparticles;
- Examine the effect of particles produced in tumor cells through *in vitro* analysis.

Chapter 2

2.0 REVIEW

2.1 GREEN CHEMISTRY: MONOMERS AND POLYMERS FROM RENEWABLE RESOURCES

The term green chemistry, as adopted by the IUPAC, is defined as: the invention, design and application of chemical products and processes to reduce or to eliminate the use and generation of hazardous substances. Since their initial appearance in the scientific literature, the terms "green" and "sustainable" have been increasingly used and are nowadays present in several research areas. Green chemistry may be considered in the scientific and economical context in which academia, industry and government are attempting to converge their efforts for the development of a sustainable civilization (VACCARO, 2016).

Green chemistry, also called sustainable chemistry, dates from 1991 when the U.S. Environmental Protection Agency (EPA) launched the Alternative Synthetic Pathways for Pollution Prevention research program under the auspices of the Pollution Prevention Act of 1990. But the name green chemistry was officially adopted in 1996. American chemistry Paul Anastas, one of the principal founders of green chemistry, claimed that by improving how chemicals are synthesized, it might be possible to prevent the production of pollutants. Also helped, together with John Warner in 1998, to create green chemistry's 12 principles: as prevent waste wherever possible; design chemicals that break down into harmless products after they are used; or; use renewable feedstocks (BRITANNICA, [S.d.]).

Fossil oil is consumed both in supplying energy as well as in the production of chemicals and polymers. Its extensive exploitation over the last 60 years has led to the cost-effective easy manufacture of daily life products. The increase in the world population and economic development, along with the decrease of the economically available amount of fossil oil, highlights the issue of its finite availability. With a regeneration time of several million years, fossil resources are faster extracted and consumed than they are produced and are thus considered as non-renewable. Furthermore, environmental concerns related to their production and use, such as greenhouse gas emission and the disposal of these non-degradable materials

that led to serious environmental pollution, motivate researchers to develop sustainable solutions (LLEVOT; MEIER, 2016; TSCHAN *et al.*, 2012).

The progress of chemistry research, associated with the industrial revolution, created a new scope for the preparation of novel polymeric materials based on renewable resources, first through the chemical modification of natural polymers from the mid-nineteenth century, which gave rise to the first commercial thermoplastic materials, like cellulose acetate and nitrate and the first elastomers, through the vulcanization of natural rubber. Later, these processes were complemented by approaches based on the controlled polymerization of a variety of natural monomers and oligomers (BELGACEM; GANDINI, 2008).

The utilization of renewable raw materials, taking advantage of the synthetic potential of nature, can meet other principles of green chemistry, such as a built-in design for degradation or an expected lower toxicity of the resulting products (MEIER; METZGER; SCHUBERT, 2007).

Biomass-derived chemicals can be either converted into monomers with unique structures, leading to materials with novel properties, or modified in order to mimic commercial petroleum-based key molecules and monomers. Some of the most widely applied renewable raw materials in the chemical include plant oils, polysaccharides, sugars, wood, and others. For instance carbon dioxide is copolymerized with propylene oxide to generate propylene carbonate polyols; Terpenes, such as limonene, are chemically transformed to limonene oxide and copolymerized with carbon dioxide to generate poly(limonene carbonate); Triglycerides, from vegetable oils, are transformed into long chain aliphatic polyesters; Natural carbohydrate polymers, such as starch, are broken down to glucose, which is subsequently transformed to polymers such as poly(ethylene furoate), polylactide, bio-derived poly(ethylene terephthalate) or bio-derived polyethylene. Products obtained from these renewables are as diverse as pharmaceuticals, coatings, packaging materials or fine chemicals (LLEVOT; MEIER, 2016; MEIER; METZGER; SCHUBERT, 2007; ZHU; ROMAIN; WILLIAMS, 2016).

Vegetable oils represent one of the most interesting classes of renewables for the synthesis of sustainable monomers and polymers, as they are available in high amounts, and relatively low prices make them industrially attractive. Their long aliphatic chain contributes as a major element to the polymer backbone (LLEVOT *et al.*, 2016; MEIER; METZGER;

SCHUBERT, 2007). Besides, their biodegradability, biocompatibility, and low cytotoxicity offered many advantages. (MONTERO DE ESPINOSA; MEIER, 2011).

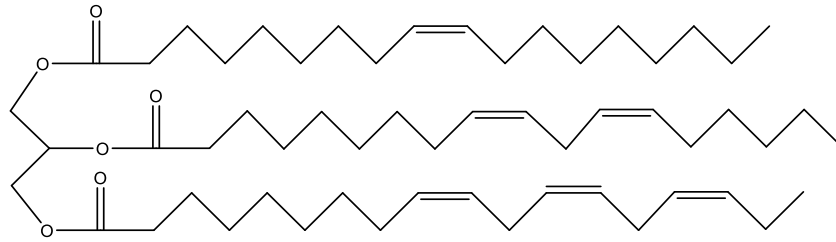
Biodegradable polymers are defined as polymers that are degraded and catabolized, eventually to carbon dioxide and water, by naturally occurring microorganisms such as bacteria, fungi or algae. In addition, when they are degraded, these polymers should not generate any substances that are harmful to the natural environment. Generally, natural materials or synthetic polymers which contain hydrolysable bonds in the backbone, such as polyamides, polyesters and, polyethers, are interesting candidates for biodegradation. Several parameters have been reported to influence the degradation behavior of biodegradable polymers as the chemical composition, the molecular weight and the crystallinity of the polymer. Although the biodegradability of a material is independent of the origin of the starting raw materials used, biomass represents an abundant renewable resource for the production of biodegradable materials (TSCHAN *et al.*, 2012).

2.2 SYNTHESIS OF MONOMERS FROM VEGETABLE OILS

Oils of vegetable origin are historically and currently the most important renewable feedstock of the chemical industry (BIERMANN *et al.*, 2011). Due to their universal availability, inherent biodegradability and low price, vegetable oils have become an area of intensive interest for both academic and industrial research as platform chemicals for polymeric materials (MIAO, SHIDA *et al.*, 2014).

The major components of vegetable oils are triglycerides (tri-esters of glycerol with long-chain fatty acids) with varying composition of fatty acids depending on the plant, the crop, the season, and the growing conditions (MEIER; METZGER; SCHUBERT, 2007). Vegetable triglycerides are among the most renewable resources exploited in science, in addition to other reasons, because of their unsaturated varieties (BELGACEM; GANDINI, 2008). A general molecular structure of triglycerides is demonstrated in **Figure 1**.

Figure 1- Demonstration of an example structure of polyunsaturated triglyceride.



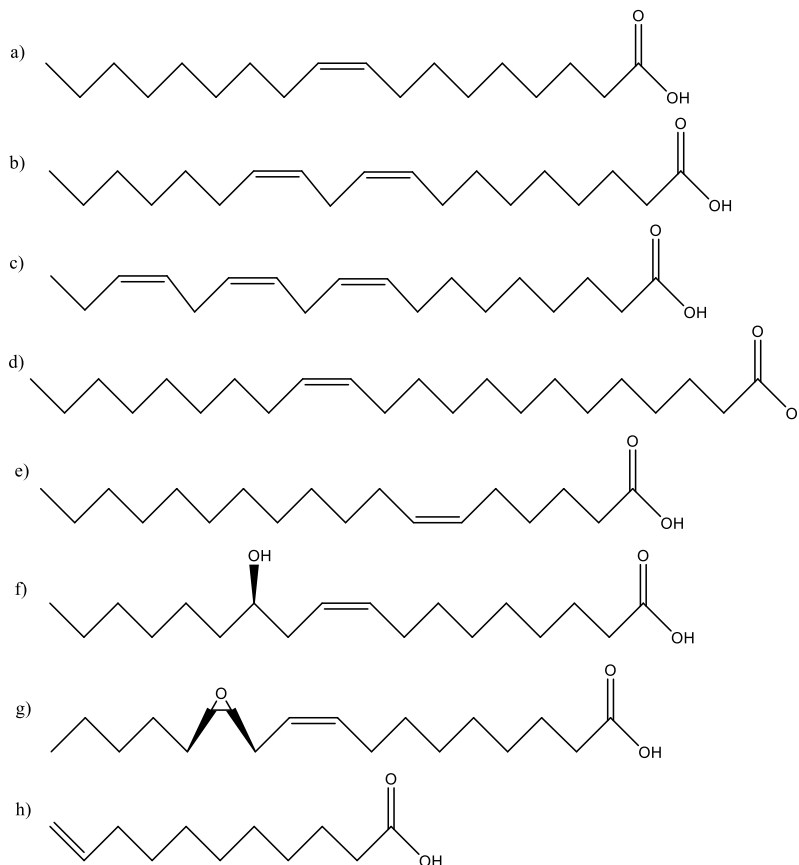
Source: Adapted from MIAO *et al.*, 2014.

Although triglycerides are found in almost all plants, the quantity that is available varies, and even common crops such as soybeans are estimated to yield only 20 wt% of triglycerides. Another challenge is that the chemical compositions of triglycerides vary both between and within a particular crop (ZHU; ROMAIN; WILLIAMS, 2016).

The physical and chemical properties of vegetable oils are mainly determined by the fatty acid chain length and the numbers and locations of double bonds in the fatty acid chains. Usually, the length of the fatty chain is between C12 and C20, with oleic acid (C18:1), linoleic acid (C18:2) and linolenic acid (C18:3) being the most common (MIAO, SHIDA *et al.*, 2014).

The fatty acids account for 95% of the total weight of triglycerides and their content is characteristic for each plant oil (MONTERO DE ESPINOSA; MEIER, 2011). The structures of some frequently studied fatty acids are depicted in **Figure 2**.

Figure 2-Fatty acids commonly used in polymer chemistry: a) oleic acid, b) linoleic acid, c) linolenic acid, d) erucic acid, e) petroselinic acid, f) ricinoleic acid, g) vernolic acid, h) 10-undecenoic acid.



Source: Adapted from MONTERO DE ESPINOSA; MEIER, 2011.

Fatty acids and esters can be easily obtained either by simple hydrolysis or alcoholysis of triglycerides. They are valuable renewable building blocks for the synthesis of designed monomers in the search for specific polymer properties that do not require extensive chemical modification prior to their application (MONTERO DE ESPINOSA; MEIER, 2011).

There is a growing interest in the use of fatty acids as precursors of monomers, not only because of their renewability, but also because of the properties they can provide to the final molecule (MONTERO DE ESPINOSA; MEIER, 2011). The most common oils used in this kind of studies are castor oil, due to the hydroxyl group presence, and soybean oil, due to the low cost and high availability. Castor oil is a very versatile renewable feedstock for all kinds of polymeric materials, including polyesters, polyamides, polyurethanes, and many others (TÜRÜNÇ, OĞUZ; MEIER, 2010).

A process that has considerable potential is reacting the alkene groups found in unsaturated fatty esters to produce α,ω -diene or α,ω -diols. Methyl 10-undecenoic acid, a castor oil derived, was shown to be a suitable starting material for the preparation of esters with alkene groups that can be lead in biodegradable polymers (TÜRÜNÇ, OĞUZ; MEIER, 2010; ZHU; ROMAIN; WILLIAMS, 2016).

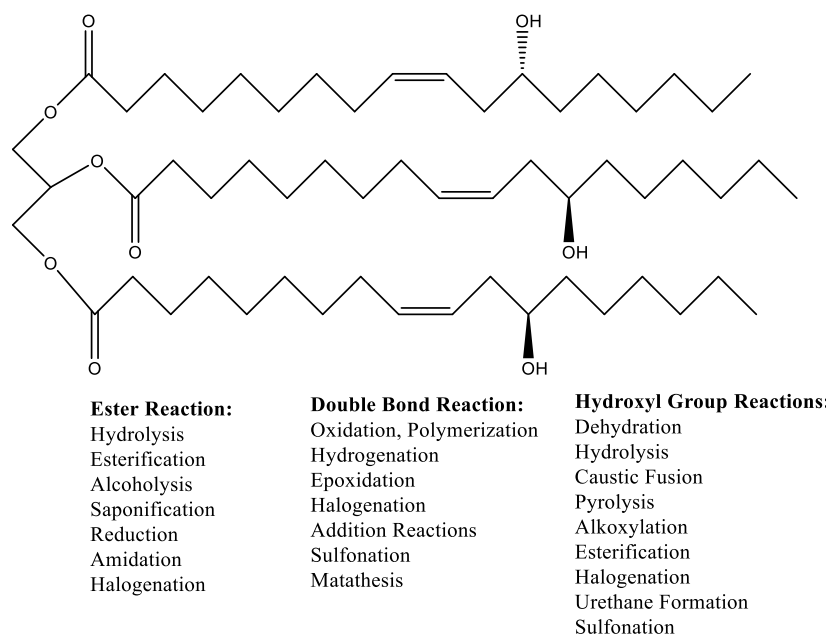
2.3 CASTOR OIL AS RENEWABLE RAW MATERIAL

Castor oil, from castor plant (*Ricinus communis*), a native of tropical Asia and Africa, is one of the most exploited vegetable oil as raw material for the chemical industry. It is naturalized and cultivated on commercial scale all around the world in temperate zones. Like other plant oils, castor oil has to be extracted by a variety of processes or a combination of processes, such as different pressures and solvent extraction followed by a refining process.

The fatty acids of castor oil consist of up to 90% ricinoleic acid and varying small amounts of saturated and unsaturated fatty acids as oleic acid, linoleic acid and, linolenic acid. The high content of ricinoleic acid is the reason for the high value of castor oil and its versatile application possibilities in the chemical industry. From castor oil processing, like from other applications of vegetable oils, glycerol is obtained as a byproduct, being a platform chemical with widespread application possibilities in cosmetics, pharmaceuticals, detergents, the manufacture of resins and additives, and also in the food industry (DEL RIO *et al.*, 2011; MUTLU; MEIER, 2010).

As mentioned, castor oil is a very useful renewable resource and finds a wide range of applications for material synthesis in industry. For instance, certain characteristics of castor oil, like high lubricity, high viscosity over a wide range of temperatures, and insolubility in aliphatic petrochemical fuels and solvents, make it directly applicable as lubricant; coatings and inks, polymers and foam. Biotechnology offers ways to alter the composition of castor oil fatty acids with a focus on processes in the chemical industry with emphasis on development and application in polymer science. **Figure 3** summarizes the possible chemical transformations of castor oil depending on the reacting functional group (MUTLU; MEIER, 2010).

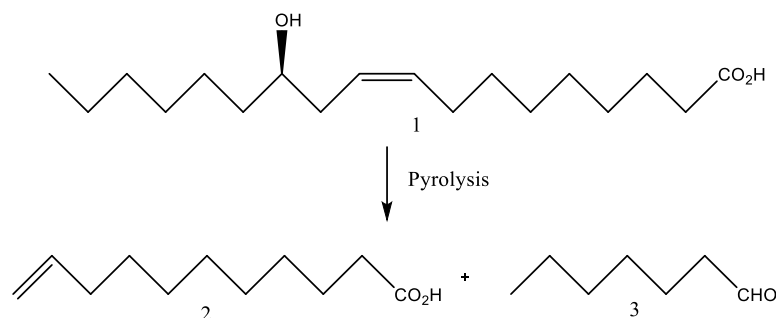
Figure 3-Chemical reactions for the preparation of a variety of derivatives of castor oil.



Source: Adapted from MUTLU; MEIER, 2010.

The pyrolysis of ricinoleic acid at high temperatures (>350 °C) splits the ricinoleate molecule at the hydroxyl group to form heptaldehyde and undecenoic acid (**Figure 4**) which is a platform chemical that can be used to synthesize a large variety of renewable monomers and polymers (FIRDAUS *et al.*, 2014; KREYE; TÓTH; MEIER, 2011; MUTLU; MEIER, 2010).

Figure 4- Products of the thermal fragmentation of ricinoleic acid. 1) Ricinoleic Acid, 2) 10-undecenoic acid, 3) Heptanal.



Source: Adapted from KREYE; TÓTH; MEIER, 2011.

The use of castor oils as a raw material in the synthesis of polymeric materials is very well established. Polymers of castor oil are applied in various fields such as wound dressing,

drug delivery, bone tissue engineering and membranes for fuel cell fabrication (MENSAH; AWUDZA; O'BRIEN, 2018).

A vast array of copolymers is viable when castor oil (or ricinoleic acid) is combined with other monomers. Materials with varied properties could be obtained by tweaking the chemistry of these copolymers. Altering of comonomer compositions leads to polyesters with controlled mechanical, thermal, viscoelastic properties, as well as degradation profiles. (RAJALAKSHMI; MARIE; MARIA XAVIER, 2019).

Laurentino *et al.* (2018) synthesized a biobased monomer acrylated ricinoleic acid from castor oil and copolymerized with methyl methacrylate in miniemulsion forming polymeric nanoparticles. The addition of the biobased monomer led to a decrease in the glass transition temperature of the copolymer and to the formation of a small fraction of gel, resulting in materials with interesting properties for future applications as pressure sensitive adhesives (LAURENTINO *et al.*, 2018).

In the medical field, biodegradable aliphatic polyesters are the preferred materials as biomaterials because of their biodegradation and biocompatibility. Cardoso *et al.* (2018) obtained biocompatible polymeric nanoparticles via thiol-ene polymerization in miniemulsion using a fully renewable α,ω -diene monomer obtained from 10-undecenoic acid and 1,3-propanediol, both derived from castor oil.

Also in the biomedical application of polymers nanoparticles, MACHADO *et al.* (2017) synthesized a poly(thioether-ester) nanoparticles via thiol-ene miniemulsion polymerization using a biobased α,ω -diene monomer, namely dianhydro-d-glucityl diundec-10-enoate, synthesized from 10-undecenoic acid (derived from castor oil) and isosorbide (derived from starch) (MACHADO, THIAGO O. *et al.*, 2017). These kinds of polymers nanoparticles have tremendous scope for further fabrications for the biomedical application area, including studies for anticancer treatments.

2.4 NANOPARTICLES POLYMERIZATION TECHNIQUES

Nanoparticles are frequently defined as solid, colloidal particles in the range 10-1000 nm. This is a collective term given for any type of polymer nanoparticle, but specifically for nanospheres and nanocapsules. Nanocapsules act as drug reservoirs, due to their vesicular structure, in which the retained active pharmaceutical ingredients are reserved in an aqueous or

non-aqueous liquid core placed in the vesicle cavity and enclosed by the solidified polymeric shell. On the other hand, nanospheres are matrix particles, particles whose entire mass is solid and molecules may be adsorbed at the sphere surface or encapsulated within the particle (EL-SAY; EL-SAWY, 2017; RAO; GECKELER, 2011).

The field of polymer nanoparticles plays an important role in a wide spectrum of areas ranging from electronics (CHAUHAN *et al.*, 2017), conducting materials (ZHANG, JIAN *et al.*, 2017), medicine (KLEPAC *et al.*, 2018; TALIANOV *et al.*, 2021) and biotechnology (KHAN *et al.*, 2020).

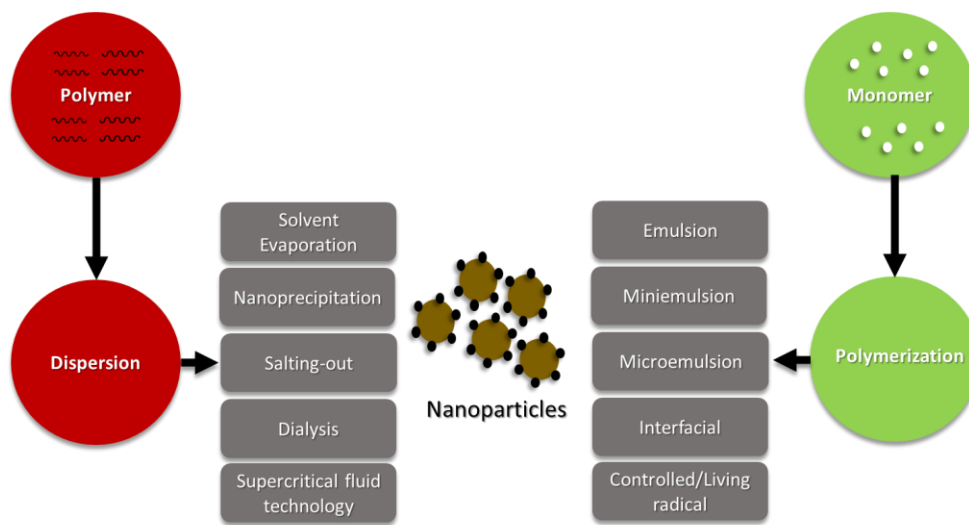
The polymeric nanoparticles are promising vehicles for drug delivery by easy manipulation to prepare carriers with the objective of delivering the drugs to a specific target and has advantages such as increases the stability of any volatile pharmaceutical agents; offer a significant improvement over traditional oral and intravenous methods of administration in terms of efficiency and effectiveness and delivers a higher concentration of pharmaceutical agent to the desired location. The choice of polymer and the ability to modify drug release from polymeric nanoparticles have made them great candidates for cancer therapy, delivery of vaccines, contraceptives, and delivery of targeted antibiotics (NAGAVARMA *et al.*, 2012).

Polymers are very convenient materials for the manufacture of nanoparticles with many potential medical applications. The polymers used in preparation of nanoparticles should be compatible with the body in the terms of adaptability and biodegradable. The most commonly used natural polymers in preparation of polymeric nanoparticles are chitosan, gelatin, sodium alginate and albumin. The synthetic polymers are mostly represented by Polylactides(PLA), Polyglycolides(PGA), Poly(lactide co-glycolides) (PLGA), Polyanhydrides, Polyorthoesters, Polycyanoacrylates, Polycaprolactone, Poly glutamic acid, Poly malic acid, Poly(N-vinyl pyrrolidone), Poly(methyl methacrylate), Poly(vinyl alcohol), Poly(acrylic acid), Poly acrylamide, Poly(ethylene glycol) and Poly(methacrylic acid). Although there are many possibilities of polymers, the application of derivatives of castor oil, as 10-undecenoic acid, for preparation of monomers used on production of polymer nanoparticles has been increased (EL-SAY; EL-SAWY, 2017; NAGAVARMA *et al.*, 2012).

Polymers nanoparticles can be conveniently prepared either from preformed polymers or by direct polymerization of monomers using classical mechanisms. Methods like solvent evaporation (SANTOS, PAULA CHRISTINA MATTOS DOS *et al.*, 2019), salting-out

(ZHANG, ZHENG; GRIJPMAN; FEIJEN, 2006), dialysis (SHEIKH *et al.*, 2009), and supercritical fluid technology (MISHIMA, 2008), can be utilized for the preparation of polymer nanoparticles from preformed polymers. On the other hand, polymer nanoparticles can be directly synthesized by the polymerization of monomers using various polymerization techniques such as microemulsion, miniemulsion, and interfacial polymerization (**Figure 5**) (RAO; GECKELER, 2011).

Figure 5- Schematic representation of various techniques for the preparation of polymer nanoparticles.



Source: Adapted from (RAO; GECKELER, 2011).

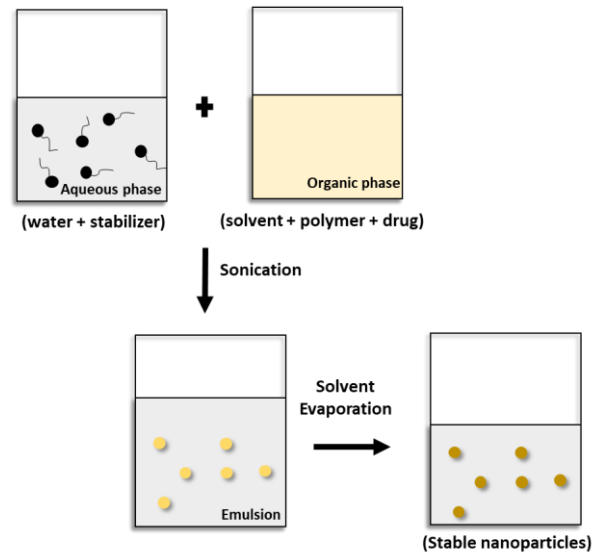
Although there are a lot of heterogeneous polymerization processes for the production of polymers in the form of particles, in this study the solvent evaporation technique and miniemulsion polymerization *in situ* by thiol-eno will be used.

2.4.1 SOLVENT EVAPORATION TECHNIQUE

The emulsification solvent evaporation technique was first reported by Gurny *et al.* (1981). Hydrophobic polymer (synthetic, semi-synthetic or natural) and drug (usually lipophilic) are dissolved in an organic solvent (e.g chloroform, dichloromethane, ethyl acetate) which is volatile and water-immiscible. This solution is then emulsified in an aqueous stabilizer solution. Emulsification is carried out by sonication or under high-energy homogenization to reduce the size of the emulsion droplets and an emulsion is formed. The organic solvent is then removed by evaporation at room temperature under stirring or under reduced pressure. Afterward, the solidified nanoparticles can be collected by ultracentrifugation and washed with

distilled water to remove additives such as surfactants (**Figure 6**) (AHLIN GRABNAR; KRISTL, 2011; GURNY R, PEPPAS NA, HARRINGTON DD, 1981; MASOOD, FARHA, 2016; QUINTANAR-GUERRERO *et al.*, 1998; RAO; GECKELER, 2011).

Figure 6- Scheme of the emulsification-solvent evaporation.



Source: Adapted from (AHLIN GRABNAR; KRISTL, 2011).

Solvent evaporation is the most employed technique to prepare nanoparticles of polymers in the current literature on techniques using a dispersion of preformed polymers (BAGHERZADEH-KHAJEHMARJAN *et al.*, 2023; MA *et al.*, 2020; NIYOM; CRESPIY; FLOOD, 2021). In the polymerization of monomers, the publications on the miniemulsion polymerization and the development of a wide range of renewable polymer materials have recently increased substantially (RAO; GECKELER, 2011).

2.4.2 MINIEMULSION POLYMERIZATION

The miniemulsion is part of the emulsified polymerization systems and has as main characteristic the size of the drops and the stability of the final emulsion. A nanoemulsion can be considered as a conventional emulsion containing very small particles (size ranging from 50 to 500 nm) (ANTONIETTI; LANDFESTER, 2002; MCCLEMENTS, 2012).

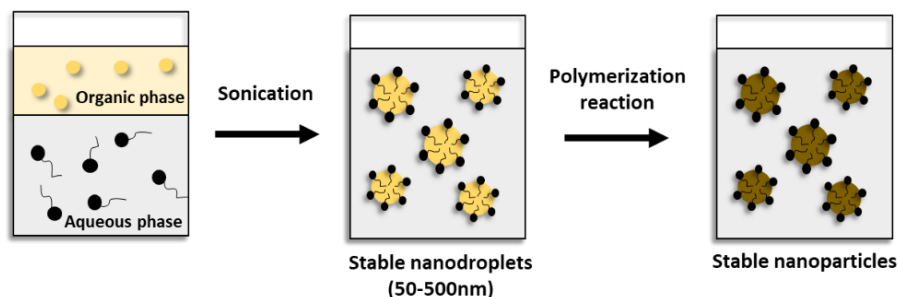
Ugelstad *et al.* (1973) were pioneers in the study of polymerizations in miniemulsions describing the polymerization process in monomer drops. Their discussions led to speculation about the possibility of nucleation and polymerization in very small monomer droplets during emulsion polymerization.

Asua (2002) defined miniemulsions as dispersions of small monomer drops in water, stabilized by a surfactant against the coalescence of the drops by the action of the Brownian motion (union of two or more drops, occurring the rupture of the interface and resulting in a larger drop) and a co-stabilizer, to minimize diffusional degradation (Ostwald Ripening, a process in which small drops are grouped by the difference of pressure, leading to an increase in the average size of droplets). A typical formulation includes water, monomer, co-stabilizing (when used), surfactant and initiator (which can be soluble in the aqueous or organic phase). The surfactant is dissolved in water, the active to be encapsulated is dissolved in the monomer and both are mixed under agitation. A shear mechanism (homogenization) is required to ensure the submicrometric size of the drops (LANDFESTER, KATHARINA *et al.*, 1999).

The mechanical homogenization of miniemulsions can be obtained by different methods. Initially, simple agitation was used as the main means of homogenization. Subsequently the use of omni-mixers and ultra-turrax was cataloged. However, the energy transferred by these techniques is not enough to obtain small drops distributed homogeneously. A much higher energy for fragmentation of large drops into small ones is required. Currently, ultrasonication is used especially for homogenization of small quantities. While micro-corrugators or high-pressure homogenizers are favorable for large quantities of emulsion (ANTONIETTI; LANDFESTER, 2002).

In the first stage of the miniemulsion polymerization process, small drops are formed by a system containing the dispersed phase (monomer, active to be encapsulated and co-stabilizer) and continuous phase (aqueous phase with a surfactant). The initiator can be added in the dispersed phase or continuous phase, depending on whether it is hydro or organic soluble. The surface area of droplets in these systems is very large, and most surfactant is adsorbed on the surface of the droplets (FONSECA *et al.*, 2013). In the second step the drops are nucleated and polymerized (LANDFESTER, K., 2006; SCHORK *et al.*, 1999). In **Figure 7**, the scheme of the miniemulsion polymerization process is demonstrated.

Figure 7- Scheme of the miniemulsion process.



Source: Adapted from LANDFESTER, 2006.

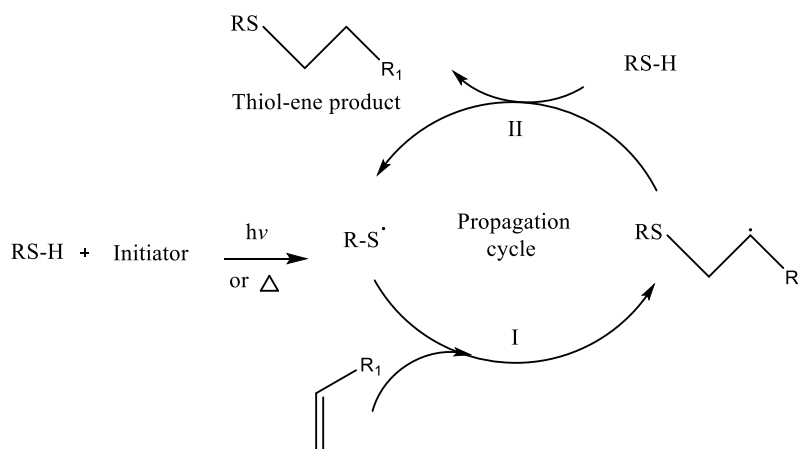
2.4.3 THIOL-ENE POLYMERIZATION

Thiol chemistry, a versatile tool, was first described in 1905 by Posner (POSNER, 1905). The author reports the thiol coupling to different types of mono and bi unsaturated compounds such as aliphatics, aromatics, terpenes, and hydroaromatics. The thiol-ene free radical addition draws special interest due to its application range and simplicity. Early work on this field has appeared in late 1930s to early 1950s (MACHADO, THIAGO O.; SAYER; ARAUJO, 2017).

A patent concerning the polymerization of dithiols and dialkenes via radical additions dates back to 1941. The reaction is well known to proceed via free-radical mechanism. Generally, radical reactions are known to be quite fast reactions, and thiol-ene additions offer some additional features such as robustness and efficiency, which have made this reaction to be considered as one of the click reactions and very popular during the last years (TÜRÜNÇ, OĞUZ; MEIER, 2012).

Like a traditional free-radical polymerization, thiol-ene polymerization reaction proceeds divided into three stages: initiation, propagation and termination, plus a chain transfer step. At initiation, the formation of thiol groups occurs by removing hydrogen. During propagation, the thiol radical is added to the unsaturated moiety (ene) group of the olefin, which generates an unpaired electron in the central carbon of the chain. Chain transfer occurs when the central carbon donates the electron to the thiol group, producing another thiol group, thereby restoring the mechanism (**Figure 8**). Termination occurs through radical-radical coupling (LOWE, 2010).

Figure 8- The mechanism for the hydrothiolation of a C=C bond in the presence of an initiator.



Source: Adapted from LOWE, 2010.

The efficiency of this reaction, therefore, requires the unsaturation in terminal position and strongly depends on the thiol compound used. As mentioned above, the propagation step of this reaction is the addition of a thiyl radical to a C=C double bond and the subsequent abstraction of a hydrogen atom by the formed carbon radical from another thiol compound, forming a new thiyl radical. The formation of the carbon radical is reversible and a rate-determining step, which explains the low reactivity of internal alkenes (TÜRÜNÇ, OĞUZ; MEIER, 2012).

There has been impressive growth in the use of the thiol-ene reaction in polymer synthesis and modification as the use in monomer synthesis and side-chain/end-group modification, preparation of various types of branched macromolecules, the preparation of inorganic-organic composites, nanoparticle modification, surface modification, bio-related applications, and crosslinked polymers (LOWE, 2014).

Cases of reactions between vegetable oils or derivatives and thiols are found in the scientific literature, such as the work made by Turunç *et al.* (2010) that described the use of methyl-10-undecenoate, a castor oil derived, in thiol-ene reactions. A variety of renewable monomers was obtained in high yields. Their polymerization was also studied and the material properties of the resulting polyesters were investigated revealing good thermal properties, making them possible candidates for the substitution of petroleum-based materials. Lluch *et al.* (2010) developed a methodology that was applied in a biomass-derived monomer of 10-undecenoic acid. Thiol-ene click step growth polymerization was used to prepare alkene-functionalized linear polymers with variable molar mass.

Hu *et al.*, (2017) developed a multi-responsive crosslinked-core poly(thioether ester) micelles. Firstly, a poly (thioether ester) was synthesized by the thiol-ene polymerization using ethanedithiol and glycidyl methacrylate as monomers. The resultant poly (thioether ester) was then coupled with carboxyl terminated poly (ethylene glycol) (PEG) and lipoic acid to give a graft copolymer that could self-assemble into micelles in the aqueous media and turn into crosslinked-core nanoparticles in the presence of dithiothreitol. The crosslinked-core micelles showed a more compact structure and higher drug loading efficiency as compared with non-crosslinked micelles. These results indicate that the cross-linked micelles may provide huge potential for controlled drug delivery in cancer therapy.

In the work of Chen *et al.* (2014), cationic polymeric nanocapsules were generated as potentially therapeutic nanocarriers. These nanocapsules were synthesized from allyl-functionalized cationic polylactide (CPLA) by efficient UV-induced thiol-ene interfacial cross-linking in transparent miniemulsions. These nanocapsules can effectively bypass the multidrug resistance of cancer cells, thereby resulting in increased intracellular drug concentration and reduced cell viability.

In virtue of some already mentioned advantages of thiol-ene reactions, as the possibility that be carried out under mild conditions, the possibility of producing cross-linked and functionalized structures and improvement of degradability, this kind of reaction is considered a great environmentally friendly candidate for synthesizing biocompatible and biodegradable polymers for biomedical application as cancer therapy (CARDOSO *et al.*, 2018; HOYLE; BOWMAN, 2010; VANDENBERGH *et al.*, 2014; VANDENBERGH; RANIERI; JUNKERS, 2012).

The use of *in situ* miniemulsion polymerization (polymerization of monomer and encapsulation of active at the same time) by thiol-ene have been evidenced. The nanoparticles have several applications: pharmaceutical, biomedical, and cosmetic. These can be administered in different routes such as intravenous, ocular, oral, intramuscular, subcutaneous and cutaneous. The development of polymeric nanoparticle formulations containing anticancer-like actives, for example, is a relevant strategy. This kind of system can increase the bioavailability of encapsulated substances and reduce problems related to early degradation. In addition, it's possible to functionalize the surface of the nanoparticles, with a coupling of proteins, for example, focusing on increased circulation in the biological environment and the possibility of targeted site delivery.

2.5 APPLICATION OF POLYMERIC NANOPARTICLES IN CANCER THERAPY

Nanoparticles have been of significant interest over the last decade as they offer great benefits for drug delivery system. In recent times, nanoparticles are extensively employed as biomaterials because of their favorable characteristics in terms of simple elaboration and design, good biocompatibility, and a broad structure variety (NGUYEN, 2011). Nanoparticles can be considered ideal candidates for cancer therapy in comparison with other possibilities as chemotherapy (EL-SAY; EL-SAWY, 2017).

Chemotherapy is a predominant treatment strategy against cancer wherein anticancer drugs are used to induce cell death in cancer cells. However, it has several limitations such as the requirement of high drug dose, adverse effects, and multidrug resistance that reduce the efficacy of the therapy. To overcome the limitations associated with chemotherapy, nanomedicine strategies employing the formulations of anticancer drugs in various nanocarriers forms have been reported (VIVEK *et al.*, 2014).

Nanoparticles for anticancer drug delivery had reached the first clinical trial in the mid-1980s, and the first nanoparticles (e.g., liposomal with encapsulated doxorubicin) had entered the pharmaceutical market in 1995. Since then, numerous new nanoparticles for cancer drug delivery are under development due to their many advantages as enhancing solubility of hydrophobic drugs, prolonging circulation time, preventing side effects, improving intracellular penetration, and allowing for specific cancer-targeting (NGUYEN, 2011).

In **Table 1** recent uses of nanoparticles for cancer therapy are given. The Polyhydroxyalkanoates (PHAs) are natural, non-toxic, biodegradable and biocompatible polyesters. The Cyclodextrin (CDs) and its derivatives are natural cyclic oligosaccharides and Poly(lactic-co-glycolic acid) (PLGA) is a copolymer of lactic acid and glycolic acid. These polymers have been studied for biomedical application and in this project another alternative polymer system will be described, synthesized and analyzed. The 1,3-propylene diundec-10-enoate (PTEe) polymer has some benefits such as renewable source, biodegradability, biocompatibility, low cytotoxicity, and can develop nanoparticles by different technics as *in situ* polymerization, that can be performed in only one step with the possibility of use water as a continuous phase, and the absence of organic solvents.

Table 1- Examples of currently developed nanoparticles as drug delivery systems for the treatment of cancer.

Polymeric nanoparticles	Anticancer agents	Method used for nanoparticle preparation	Study design	References
Polyhydroxyalkanoates (PHAs) nanoparticles	Ellipticine	Emulsification/Solvent evaporation method	<i>in vitro</i>	(F, 2013; MASOOD, F. ET AL., 2013)
	Cisplatin	Emulsification/Solvent evaporation method	<i>in vitro</i>	(SHAH, M., ULLAH, N., CHOI, M. H., KIM, M. O. & YOON, 2012)
	Thymoquinone	Emulsification/Solvent evaporation method	<i>in vitro</i>	(SHAH, M., IMRAN, M., HWAN, M., OK, M. & CHUL, 2010)
	Paclitaxel	Double emulsification/Solvent evaporation	<i>in vitro</i>	(VILOS, 2013)
	5-Fluorouracil	Double emulsification/Solvent evaporation	<i>in vitro</i>	(LU, X. Y., ZHANG, Y. & WANG, 2010)
	Etoposide	Solvent evaporation	<i>in vitro</i>	(KILIÇAY, 2011)
	Doxorubicin	Double emulsification/Solvent evaporation	<i>in vitro</i>	(CHAN, ZHANG <i>et al.</i> , 2010)
Rhodamine B isothiocyanate (RBITC)	Emulsification/Solvent evaporation method	<i>in vitro</i>	(YAO, 2008)	
Poly (lactic-co-glycolic acid) (PLGA) nanoparticles	Paclitaxel	Emulsification and Nanoprecipitation	Pre clinical (mice)	(DANHIER, FABIENNE <i>et al.</i> , 2009)
	Topotecan-tamoxifen	Double emulsification/Solvent evaporation	<i>in vitro</i>	(KHUROO, 2014)
	Lupeol	Emulsification/Solvent evaporation method	<i>in vitro</i>	(CHÁIREZ-RAMÍREZ, 2015)
	Gemcitabine	Emulsification/Solvent evaporation method	<i>in vitro</i>	(JAIDEV, L. R., KRISHNAN, U. M. & SETHURAMAN, 2015)
	9-nitro-camptothecin	Nanoprecipitation	<i>in vitro</i>	(DERAKHSHANDEH, K., ERFAN, M. & DADASHZADEH, 2007)
	Paclitaxel, Doxorubicin	Double emulsification/Solvent evaporation	<i>in vitro</i>	(WANG, 2011)
	Paclitaxel	Nanoprecipitation	<i>in vitro</i>	(LE BROEC-RYCKEWAERT, 2013)
Cisplatin	Emulsification/Solvent evaporation method	<i>in vitro</i>	(MATTHEOLABAKIS, G., TAOUFIK, E., HARALAMBOUS, S., ROBERTS, M. L. & AVGOUSTAKIS, 2009)	

Polymeric nanoparticles	Anticancer agents Ellipticine	Method used for nanoparticle preparation	Study design	References
Poly (lactic-co-glycolic acid) (PLGA) nanoparticles	Paclitaxel/superparamagnetic iron oxide	Emulsification/Solvent evaporation method	<i>in vitro</i>	(SCHLEICH, 2013)
	Tamoxifen, Quercetin	Emulsification/Solvent evaporation method	<i>in vitro</i>	(JAIN, A. K., THANKI, K. & JAIN, 2013)
	Docetaxel	Nanoprecipitation	<i>in vitro</i>	(CHAN, J. M. ET AL., 2009)
	Δ^9 -Tetrahydrocannabinol	Nanoprecipitation	<i>in vitro</i>	(MARTÍN-BANDERAS, L. <i>et al.</i> , 2015)
	Doxorubicin	Solvent displacement	<i>in vitro</i>	(CHITTASUPHO, 2009)
	Paclitaxel	Nanoprecipitation	Pre clinical	(LIANG, 2011)
	Bicalutamide	Nanoprecipitation	<i>in vitro</i>	(DHAS, N. L., IGE, P. P. & KUDARHA, 2015)
	siRNA, Paclitaxel	Emulsification/Solvent evaporation method	<i>in vitro</i>	(SU, W.-C., SU, W.-P., CHENG, 2012)
	Paclitaxel, Doxorubicin	Double emulsification/Solvent evaporation	<i>in vivo</i>	(CUI, Y., XU, Q., CHOW, P. K.-H., WANG, D. & WANG, 2013)
	Methotrexate	Emulsification and diffusion	<i>in vivo</i>	(JAIN, 2015)
	Cisplatin	Nanoprecipitation	Pre clinical	(DHAR, S., GU, F. X., LANGER, R., FAROKHZAD, O. C. & LIPPARD, 2008)
	Doxorubicin	Solvent displacement	<i>in vitro</i>	(CHITTASUPHO, C., LIRDPRAPAMONGKOL, K., KEWSUWAN, P. & SARISUTA, 2014)
	Paclitaxel	Nanoprecipitation	Pre clinical (mice)	(DANHIER, F. ET AL., 2012)
	Curcumin	Nanoprecipitation	<i>in vivo</i>	(LI, L. ET AL., 2014)
	PE38KDL	Double emulsification/Solvent evaporation	Pre clinical (mice)	(CHEN, H. ET AL., 2008)
Paclitaxel and magnetic fluid	Emulsification/Solvent evaporation method	<i>in vitro</i>	(ARAVIND, 2013)	
Gemcitabine	Double emulsification/Solvent evaporation	<i>in vitro</i>	(AGGARWAL, S., YADAV, S. & GUPTA, 2011)	
Paclitaxel	Emulsification/ Precipitation	<i>in vitro</i>	(NARAYANAN, 2015)	

Polymeric nanoparticles	Anticancer agents Ellipticine	Method used for nanoparticle preparation	Study design	References
	Capecitabine	Emulsification/Solvent evaporation method	<i>in vitro</i>	(WEI, K., PENG, X. & ZOU, 2014)
Poly-(lactic-co-glycolic acid) (PLGA) nanoparticles	SN-38	Emulsification/Solvent evaporation method	<i>in vitro</i>	(VANGARA, K. K., LIU, J. L. & PALAKURTHI, 2013)
	BSA	Double emulsification/Solvent evaporation	<i>in vitro</i>	(KOCBEK, P., OBERMAJER, N., CEGNAR, M., KOS, J. & KRISTL, 2007)
Cyclodextrin (CDs) nanoparticles	Docetaxel	Nanoprecipitation	<i>in vitro</i>	(VARAN, C. & BILENSOY, 2014)
	Camptothecin	Nanoprecipitation	<i>in vitro</i>	(CIRPANLI, Y., BILENSOY, E., LALE DOĞAN, A & CALIŞ, 2009)
	Acyclovir	Nanoprecipitation	<i>in vitro</i>	(PERRET, F., DUFFOUR, M., CHEVALIER, Y. & PARROT-LOPEZ, 2013)
	Paclitaxel	Emulsification/Solvent evaporation method	<i>in vivo</i>	(MIAO, Q. ET AL., 2012)

Source: Adapted from (MASOOD, FARHA, 2016).

Nanoparticles utilization in conventional chemotherapy is recognized and have been accepted by the FDA (Food and Drug Administration) for broader usage. Anticancer drugs entrapment within nanoparticles guards them against efflux transporters and the nano-sized range accelerates its entrance through biological membranes. Besides, the polymer shell affords protects the drug against the body enzymes. Current developments in nanotechnology have revealed many types of targeting strategies for augmenting drug accumulation into the tumor while restricting the undesirable toxicity to normal cells. As the nanoparticles designed for targeted drug delivery systems, that increase the anticancer active ingredients delivered in tumors and no affecting non-cancerous regions (EL-SAY; EL-SAWY, 2017).

Some of the applications of nanoparticles in cancer therapy can be seen in the work of Vivek *et al.* (2014) that developed a novel biodegradable antibody conjugated polymeric nanoparticles designated for targeted delivery in breast cancer receptors. The formulated nanoparticles were capable of sustained pH depended drug release. The results indicated that the formulated nanoparticles were found to provide better anticancer and inhibitory activity against breast cancer cells than the free anticancer agent by *in vitro* and *in vivo* evaluations.

Han *et al.* (2012) evaluated the inhibition of glioma growth *in vivo* by combining the interstitial chemotherapy and the targeting drug delivery strategy. They developed 3-bis(2-chloroethyl)-1-nitrosourea-loaded wafers that were implanted in the tumor and 3-bis(2-chloroethyl)-1-nitrosourea-loaded poly(lactic acid) nanoparticles decorated with transferrin that were administrated by intracarotid perfusion. The results showed that the combined therapy significantly prolonged the survival time of glioma-bearing rats in comparison with either treatment alone.

Feuser *et al.* (2016a) synthesized and characterized Zinc (II) phthalocyanine loaded poly(methyl methacrylate) obtained by miniemulsion polymerization for photodynamic therapy in leukemic cells. The cytotoxicity and phototoxicity studies indicated that the nanoparticles improving the photobiological activity of zinc phthalocyanine on leukemic cells. Although good results of Zinc (II) phthalocyanine loaded poly(methyl methacrylate) were obtained for photodynamic therapy, the poly(methyl methacrylate) is not a biodegradable polymer. Boosting other works with new kinds of renewable and biodegradable polymer as poly(thioether-ester).

Due to reasons exploited, nanoparticles present many applications in cancer remediation. There are a lot of possibilities of nanoparticle technology that need to be explored to harness their remarkable perspective as a new class of targeted remediation for cancer therapy.

2.6 ANTICANCER ACTIVE PHARMACEUTICAL INGREDIENTS (APIs)

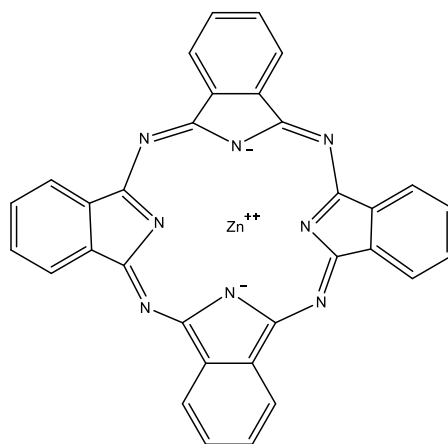
According to the World Health Organization (WHO), an active pharmaceutical ingredient (API) is any substance or combination of substances used in a finished pharmaceutical product, intended to furnish pharmacological activity or to otherwise have a direct effect in the diagnosis, cure, mitigation, treatment or prevention of disease, or to have direct effect in restoring, correcting or modifying physiological functions in human beings (WORLD HEALTH ORGANIZATION, 2011). Anticancer APIs also called antineoplastic drugs are effective in the treatment of malignant, or cancerous, disease. There are several major classes of anticancer APIs. These include alkylating agents, antimetabolites, natural products, hormones, and a great number of assets that demonstrate anticancer activity and are used in the treatment of malignant diseases (BRITANNICA, [S.d.]).

2.6.1 ZINC PHTHALOCYANINE

Phthalocyanines form a class of aromatic compounds traditionally used as dyes due to their intense absorption in the visible region. They are synthetic dyes classified as second-generation photosensitizers. They have had applications in areas such as photodynamic therapy, corrosion inhibitors, antimycotic material, sensors, among others (UENO; MACHADO; MACHADO, 2009).

The molecular structure of a phthalocyanine is formed by alternating carbon and nitrogen atoms by conjugated bonds, in addition to four pyrrole groups linked to the macrocycle. Phthalocyanines are planar molecules whose aromatic character is ensured by eighteen relocated electrons (**Figure 9**). Due to this, they present high absorption capacity in the ultraviolet and visible regions of the electromagnetic spectrum. The higher intensity absorption bands are located in the visible zone, where nitrogen atoms, which are more electronegative than carbon atoms, attract around them a high electronic density. The central metal has considerable influence on its photosensitizing property. Zinc phthalocyanines are among the most promising sensitizers of this group for the use in photodynamic therapy for anticancer treatment (TOMAZINI *et al.*, 2007).

Figure 9- Molecular structure of zinc phthalocyanine.



Source: Author.

Photodynamic therapy is a therapeutic modality that involves the activation of photosensitive substances, light source and the generation of cytotoxic oxygen and free radical species to promote selective destruction of target tissues or cancerous tumors. In this type of treatment, a drug is administered and accumulates in neoplastic tissues. When these tissues are irradiated with a light at visible wavelength, it occurs to the eradication of the tumor. The

absorption of light by the dye, in the presence of oxygen, starts photophysical and biological processes that result in the formation of reactive oxygen species capable of harming cellular constituents and causing cell death by apoptosis or necrosis (FEUSER, PAULO EMILIO, 2012; TOMAZINI *et al.*, 2007).

Moon *et al.* (2012) have developed studies applying zinc phthalocyanine in photodynamic treatment against cancer. *In vitro* and *in vivo* experiments have proven increased cytotoxic efficiency, reducing tumor growth and leading to their apoptosis.

De Oliveira *et al.* (2017) developed and evaluated zinc phthalocyanine nanoemulsions for use in photodynamic therapy for *Leishmania ssp.* The encapsulation of zinc phthalocyanine in nanoemulsions was positive because it has improved the stability in aqueous medium and the photobiological activity, compared to free zinc phthalocyanine, against the promastigote stage of *L. infantum* and *L. amazonensis* and amastigote stage of *L. amazonensis*.

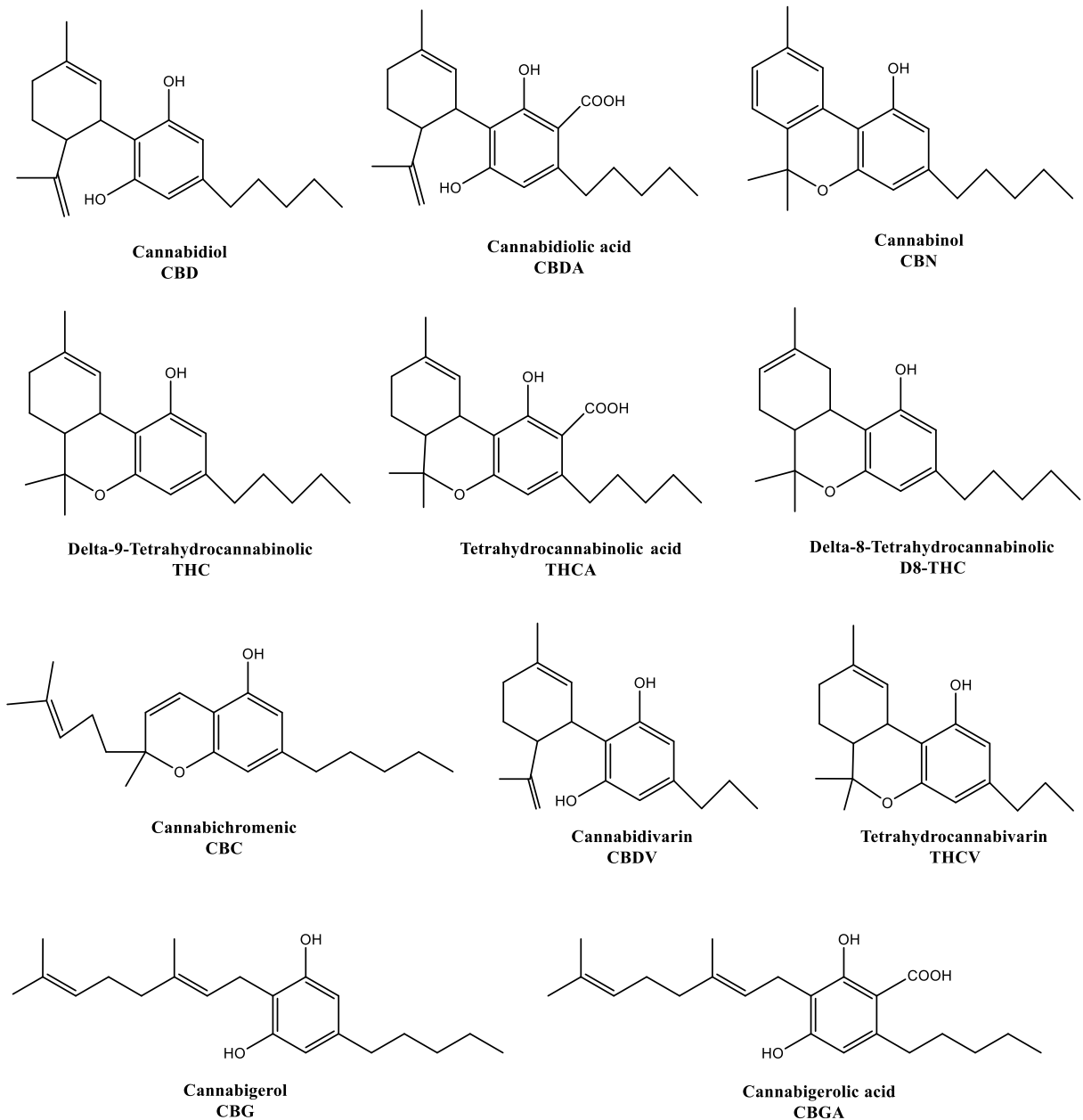
2.6.2 CANNABIS EXTRACT

The Swedish botanist Carolus Linnaeus presented the scientific term *Cannabis Sativa* to one of the oldest plants in mankind. *Cannabis* is classified into the family *Cannabaceae* and comprises three main species: a fiber-type one, named *C. sativa L.*, a drug-type one, containing high levels of the psychoactive compound delta-9-tetrahydrocannabinol (THC), named *C. indica Lam.*, and another one with intermediate characteristics, named *C. ruderalis Janisch.* However, the continuous crossbreeding of these species to generate hybrids has led to the use of a monotypic classification, in which all plants are classified as belonging to *C. sativa* species and subdivided into chemotypes. Before the Christian Era, *Cannabis* was used in Asia and India as a medicine, but the first medicinal report of the plant was attributed to the Chinese, who described them in documents written more than 2000 years ago (BRIGHENTI *et al.*, 2017; ZUARDI, 2006).

Cannabis is a complex plant with about 426 chemicals, of which more than 60 are cannabinoid compounds. Cannabinoids belong to terpenophenolic compounds and are the main constituents of the Cannabis plant (**Figure 10**). The four major compounds are delta-9-THC, cannabidiol (CBD), delta-8-THC and cannabinol (CBN). Even though the chemical structures of these four compounds are similar, their pharmacological effects can be very different. In the plant, cannabinoids are synthesized and accumulated as cannabinoid acids, but when the herbal product is dried, stored and heated, the acids decarboxylate gradually into their proper forms.

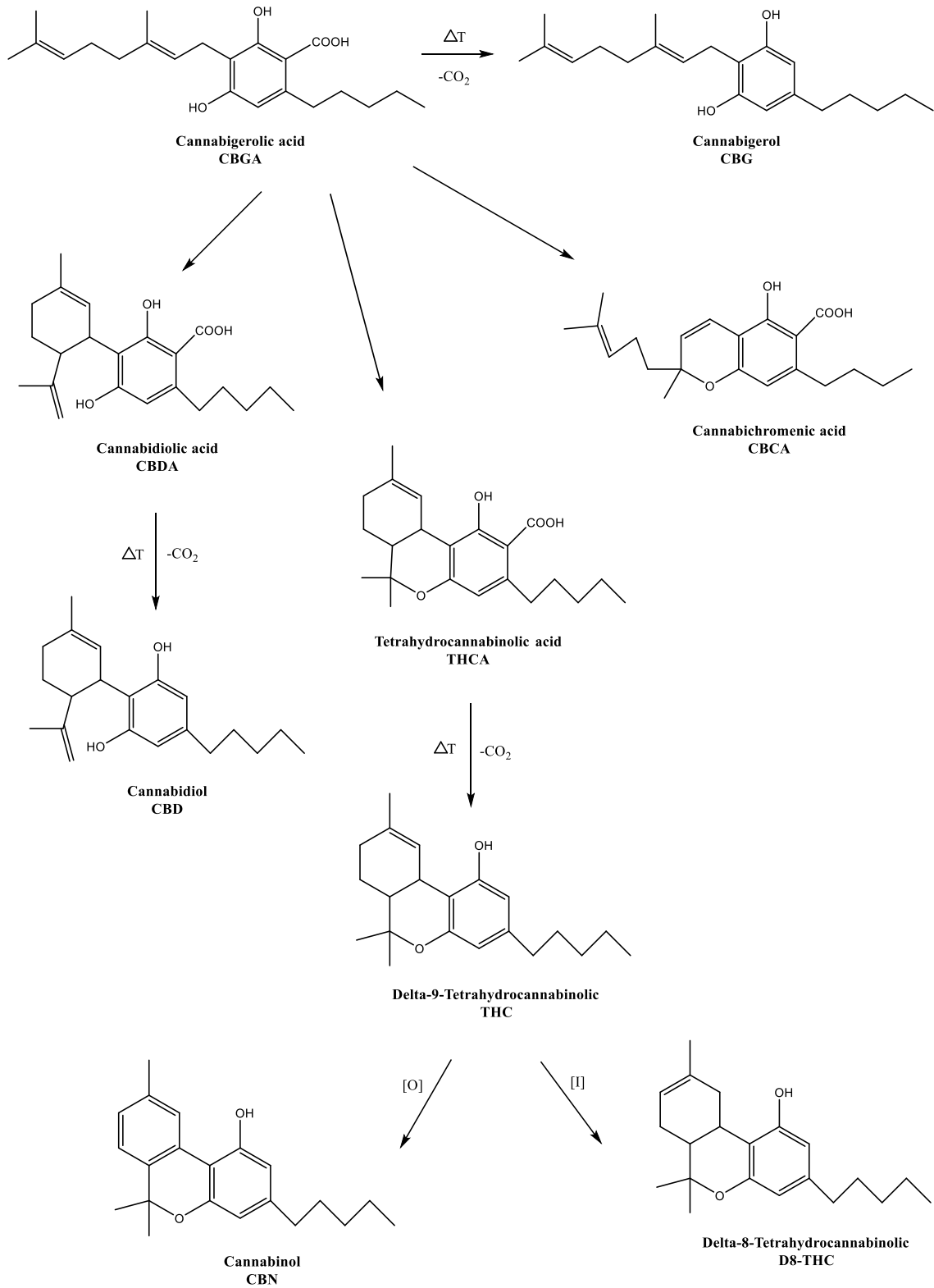
Cannabigerolic acid (CBGA) is the starting point in the biosynthetic pathway of all cannabinoids, which are synthesized *in vivo* in a carboxylated form. In the plant, CBDA and THCA are synthesized by enzymatic catalyzed reactions. *Ex vivo* stress conditions, like heat and UV light, decompose these precursors to their decarboxylated form: CBGA → Cannabigerol (CBG), CBDA → CBD and THCA → THC, respectively (**Figure 11**) (ATAKAN, 2012; ZIVOVINOVIC *et al.*, 2018).

Figure 10- Main cannabinoids present in *Cannabis Sativa*.



Source: Adapted from CIOLINO; RANIERI; TAYLOR, 2018.

Figure 11- Biosynthetic pathway for the production of cannabinoids and main breakdown products of THC.



ΔT = heating, $[\text{O}]$ = oxidation, $[\text{I}]$ = isomerization

Source: Adapted from DE BACKER *et al.*, 2009.

The systematic study of *Cannabis sativa* and its main components started in the 1960s. Isolation, elucidation of structures, stereochemistry, synthesis, metabolism, pharmacology and the physiological effects of cannabinoids extended during the 1980s and 1990s. The stereoselectivity of cannabinoid analogue action at rat brain membranes suggested the existence of a cannabinoid receptor. The receptors were named according to their order of discovery as CB₁ and CB₂. Both are G-protein coupled receptors. Within the central nervous systems, CB₁ is primarily localized at presynaptic nerve terminals and accounts for the majority of neurobehavioral effects of cannabinoids. CB₂, in contrast, is the major cannabinoid receptor in the immune system, but may also be expressed in neurons. The endocannabinoid system comprises these cannabinoid receptors, the endogenous agonists and the related biochemical machinery responsible for synthesizing *Cannabis* substances and terminating their actions (enzymes that generate and degrade or transform them) (ALEXANDER, 2016; SAITO; WOTJAK; MOREIRA, 2010).

The endocannabinoid system is a molecular system responsible for regulating and balancing many processes in the body, including immune response, communication between cells, appetite and metabolism, memory, and more. Despite the integral role the endocannabinoid system has in human body function, it was discovered relatively recently and much of its importance is only just becoming understood by scientists and the medical community at large. However, the discovery of the endocannabinoid system has given that opportunity to understand *Cannabis* potentialities for treatments of many diseases (MECHOULAM; PARKER, 2013).

Atakan (2012) and Alexander (2016) in their studies systematically summarized the potential of *Cannabis* and its extracts in treatments of diseases such as chronic pain, nausea, eating disorders, glaucoma, neurodegeneration, multiple sclerosis, schizophrenia, lung cancer, glioma, glioblastoma multiforme, epilepsy, stress, and anxiety.

Velasco *et al.* (2016) developed a work about the use of cannabinoids as anticancer agents. They affirm that exist solid scientific evidence supporting that cannabinoids exhibit a remarkable anticancer activity in preclinical models of cancer such as glioma and melanoma. Due to this, clinical studies aimed at testing them as single agents or in combination therapies are urgently needed.

Scientists have also been developing works focusing on the encapsulation of isolated cannabinoids from *Cannabis* in an attempt to improve the administration of these compounds, reduce problems related to degradation and oxidation, and the possibility of increasing their bioavailability. Hernan *et al.* (2012) produced microspheres containing CBD, using polycaprolactone as a coating substance, through the emulsion technique with solvent evaporation for potential application as pathological in cancer cells. In another study, the group tested the encapsulation of THC using the same technique also for the anticancer applications. The results obtained are positive for the use of these actives in alternative treatments. The results obtained are positive for the use of these actives in alternative treatments on leukemia, and carcinoma (DE LA OSSA *et al.*, 2013).

Martín-Banderas *et al.* (2014) used poly(d,l-lactide-co-glycolide)-PLGA to produce nanoparticles containing THC. The nanoprecipitation technique was used to produce particles between 59-434 nm in an attempt to apply antitumor activity. It was assumed that the intense cytotoxic activity of delta-9-THC-loaded PLGA nanoparticles may be indicative of promising antitumor activity. Still in the line of antitumor activities, Durán-Lobato *et al.* (2015) encapsulated the CB13 cannabinoid using the O/W emulsion technique with solvent evaporation. The particles were also functionalized with chitosan in an attempt to increase the internationalization of the active in cancer cells. The formulations have the potential of carriers as oral delivery systems of CB13 for cancer therapy.

The vast majority of the studies, using cannabinoids for cancer therapy, have been performed with pure compounds, mainly THC or CBD. The *Cannabis* plant, however, produces hundreds of additional compounds (other cannabinoids, terpenoids, flavonoids, and polyphenols) that together show promising therapeutic properties and/or the potential capability of enhancing some cannabinoids actions, this is the entourage effect. (BLASCO-BENITO *et al.*, 2018). The entourage effect relates with the synergism of cannabinoids compounds. That is, combinations of the *Cannabis* plant components can in certain circumstances be more effective than these compounds alone (NAMDAR *et al.*, 2019; SANCHEZ-RAMOS, 2015). Therefore, there is great potential in studying the synergistic effect of a mix of cannabinoids, found in full-spectrum *Cannabis* extract, for cancer treatments.

2.7 FINAL CONSIDERATIONS

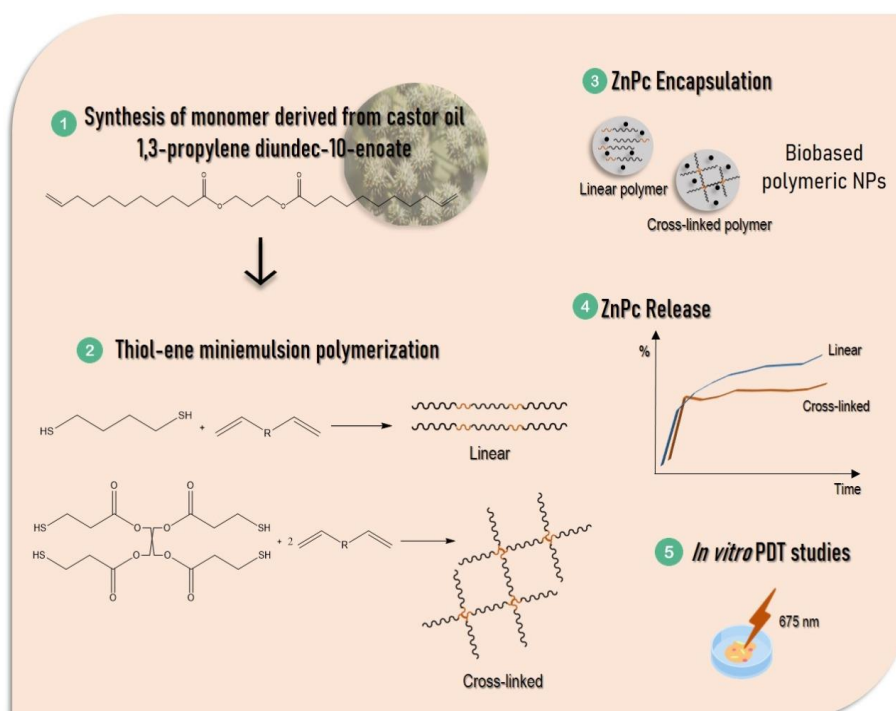
The polymer industry plays a significant role in our society. However, issues with the extensive use of fossil-based raw materials in the environment have increased. Materials in the environment enables to change the polymerization process intending to develop a sustainable society. The synthesis of sustainable chemical products and processes is essential to healthy of the planet. In this context, plant oils offer many advantages apart from their reliability for the preparation of novel polymeric materials based on renewable resources. Thus, the use of an esterification of 10-undecenoic acid with 1,3-propanediol to produce a renewable diene-diester monomer, followed by a copolymerization of the produced monomer with a dithiol appears as an excellent opportunity for the production of nanoparticles biobased as an alternative for biomedical applications. The use of the thiol-ene polymerization technique to obtain a polymer of adequate molar mass and, consequently, nanoparticles with encapsulation of active substances, brings even more advantages, related to the simpler polymerization technique, which can be performed *in situ*, with the absence of organic solvents, since water is used as a solvent in the process of producing particles and processes under mild temperature conditions.

There is an increasing demand for biocompatible and biodegradable materials for specific applications in biomedical as cancer therapy, encouraging scientists in working on researches towards designing polymers, with enhanced properties and clean processes, containing antineoplastic APIs. About the APIs investigated in this research project, zinc phthalocyanine has been studied for photodynamic therapy application in anticancer treatment, and full-spectrum *Cannabis* extract, recently discovered with promising action against cancer, has the entourage effect potentiality. The nanoencapsulation of these APIs in biobased polymeric nanoparticles can control the release of the substances, increase bioavailability, reduce problems with volatility and degradation, reduce side effects and, increase treatment efficiency.

The purpose of the present study is to synthesize a monomer derived from vegetable oil by esterification of 10-Undecenoic acid (obtained by pyrolysis of castor oil) and 1-3-propanediol (also derived from castor oil). Subsequently, use thiol-ene miniemulsion and solvent evaporation techniques to obtain biodegradable nanoparticles loaded with anticancer APIs for biomedical applications in cancer therapy.

Chapter 3

This chapter is part of a publication entitled “Zinc phthalocyanine encapsulation via thiol-ene miniemulsion polymerization and *in vitro* phototoxicity studies” published in the **Journal of Polymeric Materials and Polymeric Biomaterials** (<https://doi.org/10.1080/00914037.2020.1838517>).



3.0 ZINZ PHTHALOCYANINE ENCAPSULATION VIA THIOL-ENE MINIEMULSION POLYMERIZATION AND IN VITRO PHOTOTOXICITY STUDIES

3.1 INTRODUCTION

Thiol-ene addition reactions are known for more than a century. Yet, only recently thiol-ene polymerization has gained noticeable attention as a technique to synthesize polymers from non-depleting sources with some unique features and several advantages over traditional free-radical polymerization (CARDOSO *et al.*, 2018). In these reactions, diene and dithiol monomers are copolymerized by a combination of step-growth and chain-growth polymerization mechanisms leading to linear polymer chains. If one of these monomers possesses 3 or more of these functionalities (double bonds or thiol groups) crosslinked polymers could be obtained. One of the advantages of the thiol-ene polymerization mechanism over conventional free-radical

polymerization is the easiness of adding different functional groups, such as ester linkages, in the main polymer chain to tune some of the properties of the polymer such as degradability and other physical features (HOELSCHER *et al.*, 2018).

Thiol-ene polymerization is a versatile method that can be carried out by thermal or photoinitiation and normally yields high conversion and possess rapid kinetics. It proceeds as the traditional free-radical polymerization, featuring three steps: initiation, propagation, and termination, plus a chain transfer step. The polymerization can be carried out under mild conditions and normally generate inoffensive by-products. Besides, some additional features such as robustness have made this reaction very popular during the last years (MACHADO, THIAGO O.; SAYER; ARAUJO, 2017; TÜRÜNÇ, OĞUZ; MEIER, 2012).

The use of renewable raw materials can significantly contribute to sustainable development. Biomass-derived chemicals can be either converted into monomers with unique structures, leading to materials with novel properties or modified to mimic commercial petroleum-based key molecules and monomers (MEIER; METZGER; SCHUBERT, 2007). Some of the most widely applied renewable raw materials in the chemical industry include plant oils that are transformed into long-chain aliphatic polyesters (LLEVOT; MEIER, 2016; ZHU; ROMAIN; WILLIAMS, 2016). Among them, castor oil stands as a very versatile renewable feedstock for all kinds of polymeric materials. 10-undecenoic acid, a castor oil derived compound, was shown to be a suitable starting material for the preparation of α,ω -diene-diesters monomers prone to thiol-ene polymerization (CARDOSO *et al.*, 2018; LLEVOT; MEIER, 2016; TÜRÜNÇ, OĞUZ; MEIER, 2010). Recent *in vitro* cytotoxicity studies demonstrated that poly(thioether-ester) nanoparticles could be used as drug carriers for applications in the medical field due to its biodegradability, biocompatibility, and antioxidant activity (CARDOSO *et al.*, 2018; MACHADO, THIAGO O. *et al.*, 2017).

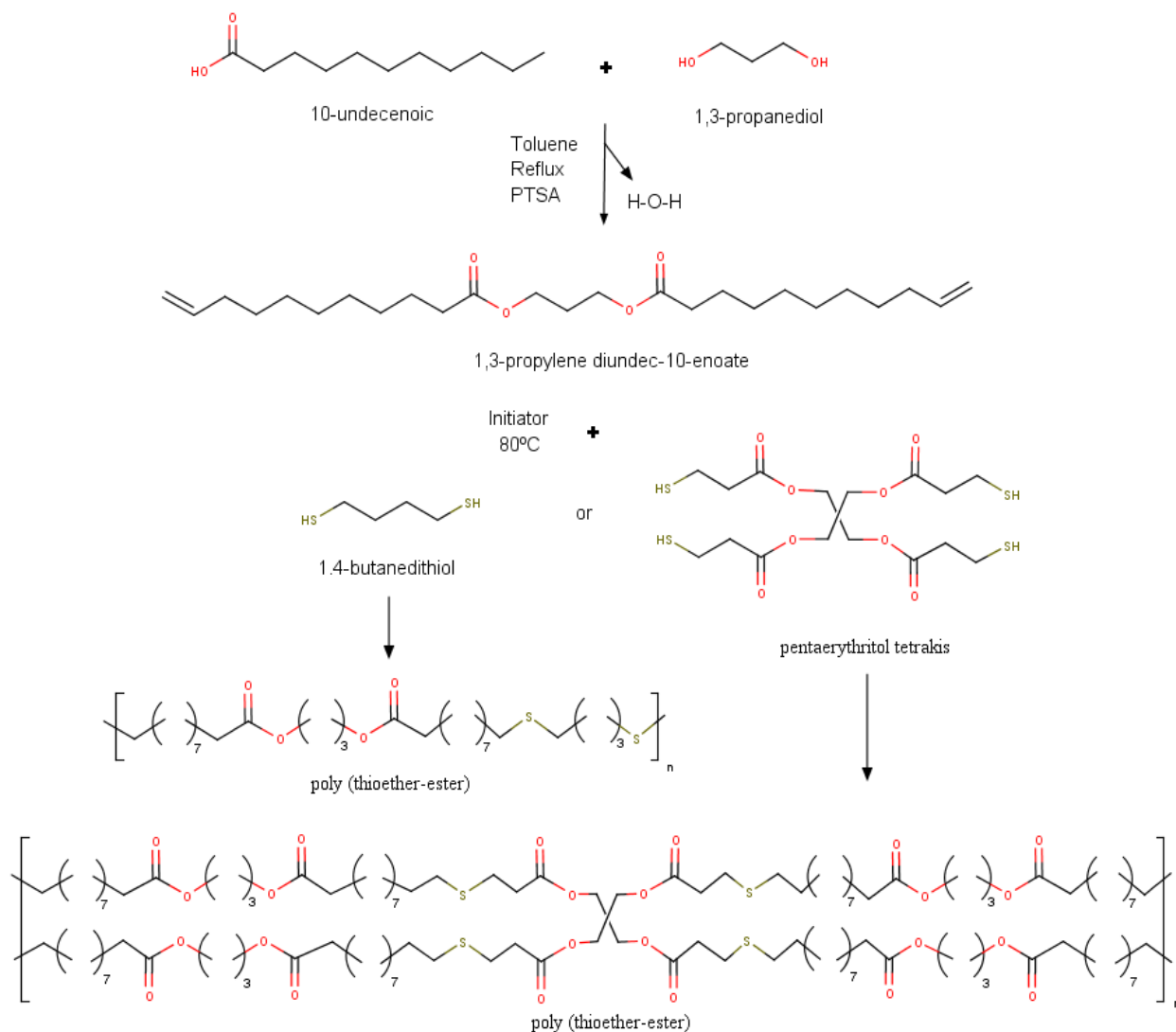
Polythioether nanoparticles can be obtained by thiol-ene miniemulsion polymerization or by the use of preformed polymer in a miniemulsification / solvent evaporation method. The main advantage of *in situ* encapsulation technique as miniemulsion polymerization is the ability to produce complex nanostructures in a single reaction step with high polymerization rates (ASUA, 2002; LANDFESTER, KATHARINA *et al.*, 1999). In general, miniemulsions consist of submicrometric (50–500 nm) and colloidally stable monomer droplets dispersed in an aqueous phase. The monomer droplets are the major polymerization locus allowing the performance of different polymerization mechanisms such as step-growth (VALÉRIO;

ARAÚJO; SAYER, 2013) and chain-growth, either cationic (ALVES *et al.*, 2018) or free-radical (COSTA, CRISTIANE *et al.*, 2013; ROMIO, ANA P. *et al.*, 2009) and the encapsulation of different substances (BERNARDY *et al.*, 2010; STAUDT *et al.*, 2013).

Photodynamic therapy (PDT) is a promising novel therapeutic method for the treatment of tumors, a clinical modality involving the administration of a photosensitizing agent. PDT is based on selective accumulation of a photosensitizer drug in tumor and activation with visible light to produce cytotoxic reactive oxygen species (ROS) that lead to cell damage (BOLFARINI *et al.*, 2012; CALORI *et al.*, 2019; PRIMO; TEDESCO, 2013; ROGUIN *et al.*, 2019). Zinc phthalocyanine (ZnPc) is a second-generation photosensitizer for photodynamic therapy. It belongs to a class of lipophilic phthalocyanines and has a high optical absorbance coefficient within the 600–800 nm range (CALORI *et al.*, 2019; FEUSER, PAULO EMILIO; GASPAR; *et al.*, 2016). However, the low solubility in water and the possibility of aggregation in aqueous solution tends to drastically decrease its therapeutic efficacy. Therefore, the development of new drug delivery carriers for photosensitizer encapsulation tends to ensure a higher PDT efficacy when compared with free photosensitizer (DA VOLTA SOARES *et al.*, 2011; FEUSER, PAULO EMILIO; GASPAR; *et al.*, 2016).

The utilization of poly(thioether-ester) nanoparticles as a drug delivery system can be a novel attractive alternative for cancer therapy by PDT. Therefore in the present work, ZnPc was encapsulated *via* thiol-ene miniemulsion polymerization using a biobased α,ω -diene-diester monomer synthesized from a castor oil derivative (**Scheme 1**). Lastly *in vitro* cytotoxicity and phototoxicity assays were carried out in human red blood (RBCs), murine fibroblast (NIH3T3), and human breast cancer (MDA-MB231) cells.

Scheme 1- Schematic representation of the esterification reaction for synthesis of renewable monomer and the studied thiol-ene reaction between 1,3-propylene undec-10-enoate with thiol or tetrathiol.



Source: Author.

3.2 EXPERIMENTAL PROCEDURE

3.2.1 MATERIALS

10-undecenoic acid (Sigma-Aldrich, 98%), 1,3-propanediol (Sigma-Aldrich, 99.6%), p-toluenesulfonic acid monohydrate (PTSA, Sigma-Aldrich, 98.5%), toluene (Sigma-Aldrich, 99.8%), hexane (Sigma-Aldrich, 99.8%), diethyl ether (Sigma-Aldrich, > 99.0%), magnesium sulfate (Sigma-Aldrich, > 99.5%), sodium dodecyl sulfate (SDS, Sigma-Aldrich, 99%), zinc phthalocyanine (ZnPc, Sigma-Aldrich, 98%), azobisisobutyronitrile (AIBN, Vetec, 98%),

butanedithiol (dithiol, Sigma-Aldrich, 97%), pentaerythritol tetrakis (tetrathiol, 3-mercaptopropionate) (Sigma-Aldrich, > 95%), chloroform (Sigma-Aldrich, 99%), dimethyl sulfoxide (DMSO, Sigma-Aldrich, $\geq 99.9\%$), phosphate Buffered Saline solution (PBS, pH 7.4), 3-(4,5-dimethylthiazol-2-yl)-2,5-diphenyltetrazolium bromide (MTT), dulbecco's modified eagle medium (DMEM, Sigma-Aldrich), fetal bovine serum (FBS, Atena biotecnologia), isopropyl alcohol (VETEC) and distilled water.

3.2.2 SYNTHESIS OF THE BIOBASED α,ω -DIENE-DIESTER MONOMER

The synthesis of the α,ω -diene-diester monomer, 1,3-propylene diundec-10-enoate (PTEe), was based on previous work (CARDOSO *et al.*, 2018). The reactants: 10-undecenoic acid (50.0 g, 0.27 mmol), 1,3-propanediol (8.4 g, 0.11 mmol), p-toluenesulfonic acid (3.0 g, 0.0157 mmol), and toluene (200 mL) were added to a round-bottomed flask equipped with a magnetic stirrer and a Dean-Stark apparatus. The mixture was heated to reflux and water was collected during the reaction time. Once the reaction was completed, after 3 hours, the reaction mixture was allowed to cool down. The toluene was removed by reduced pressure and the residue was filtered through a short pad of basic aluminum oxide with hexane as eluent. Hexane was removed, under reduced pressure, and the crude product was dissolved in diethyl ether (200 mL) and washed two times with water (200 mL). The mixture was dried over anhydrous MgSO_4 , filtered and the solvent removed. The product was analyzed by $^1\text{H NMR}$ spectroscopy (Bruker AC 200, frequency 200 MHz).

3.2.3 SYNTHESIS OF ZnPc LOADED IN PTEe NANOPARTICLES VIA THIOL-ENE MINIEMULSION POLYMERIZATION

The organic phase was prepared using the α,ω -diene diester monomer PTEe (1.0 g), and, if used, phthalocyanine (0.01 g) under magnetic stirring until complete drug solubilization. The aqueous phase, composed of distilled water (9.8 g) and sodium dodecyl sulfate (0.0304 g), was added to the organic phase and magnetically agitated (500 rpm) for 10 min. Then, butanedithiol (1:1 dithiol-to-diene molar ratio) or 3-mercaptopropionate (1:2 tetrathiol-to-diene molar ratio) was added to the system and the mixture was let under mild magnetic stirring (250 rpm) for 5 min. In the case of 3-mercaptopropionate, chloroform (1 mL) was added to aid the solubilization of the reactants in the organic phase. The final coarse emulsion was sonicated for 2 min with an amplitude of 60% in pulse mode (10 s of sonication, 2 s of pause) using a Fisher Scientific Sonic Dismembrator model 500. An ice bath was used to prevent heat buildup during the sonication. At the end of the sonication step, the initiator AIBN (0.0066 g) was added

and sonicated for 10 s. After miniemulsification, the reactional mixture was placed in a thermostatic bath at 80°C for 4 h.

3.3 CHARACTERIZATION

3.3.1 PARTICLE SIZE, SURFACE CHARGE, AND MORPHOLOGY

Intensity average diameters of the monomer droplets and polymer particles were measured by dynamic light scattering (DLS—Malvern Instruments, Zeta Sizer Nano-S90). The latex samples were diluted with distilled water before DLS analysis. The surface charge of the nanoparticles was investigated through zeta potential measurements (MALVERN Zetasizer Nanosizer MPT-2 Autotitrator). All samples were analyzed three times at 25°C. The nanoparticles morphology was analyzed using transmission electron microscopy (TEM) model (JEM 2100F 100 kV). The samples were diluted in distilled water down to 0.5% of solids content and one single drop was placed on a carbon-coated copper grid (300 mesh) and dried overnight at room temperature.

3.3.2 FOURIER-TRANSFORM INFRARED SPECTROSCOPY

Chemical characterization was performed by Fourier Transform Infrared Spectroscopy (FTIR) model Shimadzu Spectrometer, model IRPrestige-21. The analysis was performed with a resolution of 4 cm⁻¹, 32 scans in a range of 4000-400 cm⁻¹, using KBr pellets.

3.3.3 THERMAL ANALYSIS

Differential scanning calorimetry (DSC, Perkin Elmer 600) analysis was performed on a nitrogen atmosphere (20 mL/min) at a heating rate of 10°C/min, from -30° to 160°C. The melting temperature, T_m, was recorded from the second heating ramp. The thermal degradation analysis (TGA, Netzch STA 449F3) was carried out from 25°C up to 600°C, at a constant heating rate of 10°C/min under nitrogen atmosphere (60 mL/min).

3.3.4 ENCAPSULATION EFFICIENCY

The encapsulation efficiency (EE%) followed studies described by MACHADO *et al.* (MACHADO, THIAGO O. *et al.*, 2017). An amount of ZnPc nanoparticles (500 µL) was centrifuged (Mini Spin Eppendorf AG) for 30 min using Amicon Ultra 0.5 (Millipore®, 100 kDa) filter at 13,000 rpm. The supernatant (200 µL) was diluted in distilled water (2000 µL) and analyzed by UV-vis spectrophotometry (Hitachi U-1900) at a wavelength of

672 nm. The ZnPc concentration was determined by a calibration model with linearity ($R^2=0.9966$) using different concentrations of ZnPc diluted in DMSO ($0.7-10 \mu\text{g.mL}^{-1}$) (**Figure A.1**). The EE% was calculated through the difference between the total amount of ZnPc added to the miniemulsion (M_t) and the amount found in the permeate (M_p) as shown in Eq. (1).

EE% was calculated from Eq 1:

$$EE (\%) = \frac{M_t - M_p}{M_t} \times 100 \quad (1)$$

The experiments were conducted in duplicate ($n = 2$).

3.4 IN VITRO STUDIES

3.4.1 RELEASE PROFILE STUDIES

The *in vitro* release profile was determined using a methodology described elsewhere (YUAN *et al.*, 2010). PTEe nanoparticles loaded with ZnPc were centrifuged for 10 min (Mini Spin Eppendorf AG). The supernatant was discarded and the nanoparticles were weighed and put in a dialysis bag (INLAB 33 mm of width x 21 mm of diameter) containing a receptor medium contained 10 ml of PBS pH 7.4 (physiological) containing 0.2% SDS. The suspension was continuously stirred and the temperature was maintained at 37°C in a thermostatically controlled water bath. At given time intervals, samples of 2 ml were withdrawn and analyzed using UV–vis spectrophotometry at a wavelength of 672 nm. After each measurement, the medium was returned to the system. All the drug release experiments were performed in duplicate. The release profile was obtained by associating the percentage of the drug released with time. The release data were fit using the mathematical models of zero-order ($Qt = Q_0 + K_0t$), first-order ($\ln Qt = \ln Q_0 + K_1t$), Korsmeyer–Peppas ($\frac{M1}{M_\infty} = Kt^n$), and Higuchi ($Qt = K_H t^{1/2}$) (COSTA, P; SOUSA LOBO, 2001). The linear regression analysis (R^2) and the straight-line equation were determined using the software Excel. The mathematical model with the best fit is the model that provides the highest value of the coefficient of determination.

3.4.2 CYTOTOXICITY ASSAY

Murine fibroblast (NIH3T3) cells were selected to evaluate the cytotoxicity of free ZnPc and ZnPc loaded in PTEe nanoparticles. The cells were cultured in a flask containing DMEM supplemented with 10 wt.% of fetal bovine serum (FBS) and 100 U/mL penicillin-

streptomycin. The cells were maintained at 37°C in a humidified incubator containing 5 wt.% CO₂. After incubation, the cells were seeded at 1x10⁴ cells/well in a 96-well plate. After incubation time (24 h), the cells were treated with ZnPc (diluted in DMSO) and ZnPc-PTEe nanoparticles (diluted in DMEM) at different concentrations: 2, 4, 8, and 12 µg.mL⁻¹ (equivalent at a concentration of ZnPc) and incubated for 24 h. After incubation time, DMEM was removed and the viability of the cells was performed by MTT assay. Briefly, 100 µL of MTT was added to a 96-well plate and incubated for 3 h (5% CO₂, 37°C) to allow the formazan formation reaction. Afterward, MTT was removed and 100 µL of isopropyl alcohol was added to dissolve the formazan crystals and the absorbance was measured at 570 nm (SpectraMax M3, microplate reader).

3.4.3 PHOTOTOXICITY STUDIES

Breast cancer (MDA-MB231) cells were selected to evaluate the phototoxicity of free ZnPc and ZnPc loaded in PTEe nanoparticles. The cells were cultured in a flask containing DMEM supplemented with 10 wt.% of fetal bovine serum (FBS) and 100 U/mL penicillin-streptomycin. The cells were maintained at 37 °C in a humidified incubator containing 5 wt.% CO₂. After incubation, the cells were seeded at 1x10⁴ cells/well in a 96-well plate. After incubation time (24 h), the cells were treated with free ZnPc and ZnPc-PTEe nanoparticles at different concentrations: 1, 2, 4, and 8 µg.mL⁻¹ (equivalent at a concentration of ZnPc) and incubated for 2 h (MDA-MB231) After incubation period for 2 h, MDA-MB231 cells were exposed to visible light (675 nm) with a dose of 6 J/cm² (Photon Lase I, DMC, Brazil) and incubated for more 24 h. After incubation, DMEM was removed and the viability of the cells was analyzed by MTT assay. The experiments were performed in triplicate with three wells for each condition and the results were expressed as the percentage of viable cells in comparison to the control group (only cells). The maximum concentration of DMSO in this experiment was 0.1%.

3.4.4 HEMOLYSIS ASSAY

The hemolysis assay was performed following the methodology described by *Feuser et al.* (2016a). This study was approved by the Human Ethics Committee of Universidade do Extremo Sul Catarinense. The human red blood (RBCs) cells were obtained from three healthy donors. The RBCs were collected in tubes containing 3.2 wt.% of sodium citrate. 4 mL of whole blood was added to 8 mL of a sterile saline solution and the RBCs were isolated from serum by

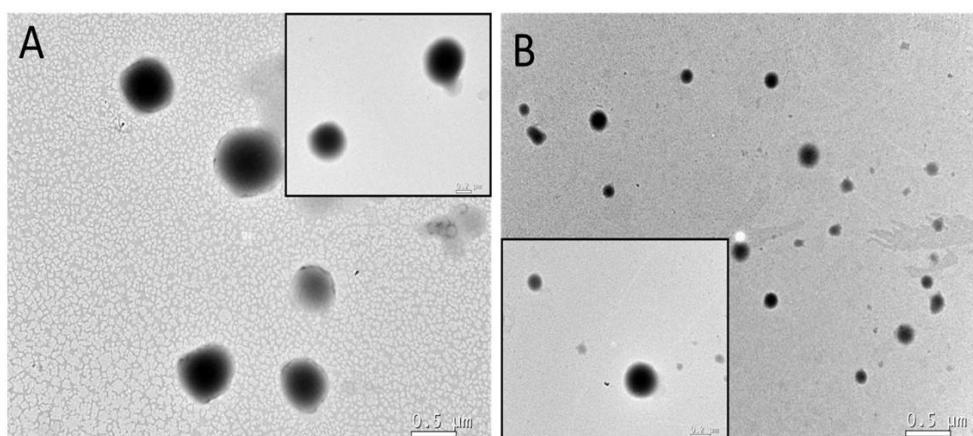
centrifugation at 1500 rpm for 10 min and washed three times with saline solution. Following the last wash, in an Eppendorf, the human erythrocytes were diluted in 2 mL of saline solution and then 80 μL of the diluted was added to 920 μL of saline. RBCs were treated with free ZnPc and ZnPc loaded in PTEe nanoparticles at concentrations of 3, 6, and 12 $\mu\text{g}\cdot\text{mL}^{-1}$ and stirring (350 rpm) at 37°C for 120 min. In sequence, the samples were centrifuged at 10,000 rpm for 5 min and 100 μL of supernatant was transferred to a 96-well plate. The absorbance value was measured at 540 nm (SpectraMax M3). As positive and negative controls, 80 μL of the RBCs suspension was incubated with 920 μL of distilled water and saline, respectively. The analyses were performed in triplicate.

3.5 RESULTS AND DISCUSSION

To prepare the diene monomer 1,3-propylene diundec-10-enoate, an esterification reaction was performed between 1,3-propanediol and 10-undecenoic acid. PTEe nanoparticles were obtained via thiol-ene miniemulsion polymerization using the diene monomer and two different thiols, butanedithiol (BDT) and pentaerythritol tetrakis. The BDT is a dithiol, resulting in a linear polymer, whereas PTT is a tetrathiol resulting in a crosslinked polymer matrix .

The morphology of PTEe nanoparticles was observed by TEM. As can be seen in **Figure 12**. PTEe nanoparticles obtained with dithiol and tetrathiol presented spherical morphology. The particles were effectively visualized when TEM equipment was operated at the lowest current possible, which in turn provides low image resolution. When the current was increased during the microscopic analyses, the polymeric particles were degraded under the strong electron beam.

Figure 12- TEM images of ZnPc-PTEe nanoparticles. A) Dithiol+ZnPc; B)Tetrathiol+ZnPc.



Source: Author.

Table 2 shows the intensity average diameter of monomer droplets and polymer particles, polydispersity index (PdI), and encapsulation efficiency. Droplets with intensity average diameters in the range of 120 - 160 nm and PdI around 0.2 were obtained after miniemulsification. The PTEe nanoparticles obtained with dithiol after polymerization presented a size smaller than PTEe nanoparticles obtained with tetrathiol. The larger particle sizes are related to the higher viscosity of the dispersed phase when tetrathiol was used as a comonomer, as it increased the resistance to droplet breakage during sonication resulting in larger monomer droplets and, consequently, larger polymeric particles. Differently, the addition of ZnPc barely affected the particle size.

Table 2- Intensity mean diameter: droplets (Dp_g) and nanoparticles (Dp); Polydispersity index: droplets (PdI_g), nanoparticles (PdI) obtained by DLS and encapsulation efficiency (EE).

Samples	Dp_g (nm)	PdI_g (nm)	Dp (nm)	PdI	EE (%)	Zeta potential (mV)
Dithiol	123±5	0.19±0.02	122±7	0.20±0.02	-	- 51.4 ± 0.7
Dithiol+ZnPc	131±4	0.15±0.05	119±4	0.18±0.03	99.9 ± 0.1	- 58.9 ± 2.6
Tetrathiol	123±1	0.16±0.02	122±1	0.14±0.0	-	- 48.8 ± 1.5
Tetrathiol+ZnPc	161±9	0.15±0.05	145±2	0.13±0.01	98.1 ± 0.4	- 59.0 ± 1.2

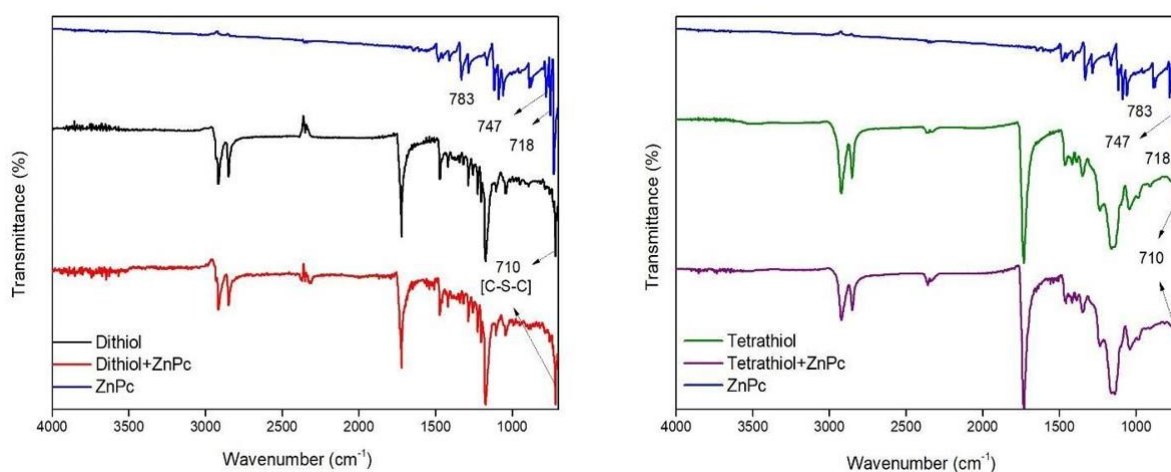
Source: Author.

Another important characterization for the development of new drug nanocarriers is the analysis of the surface charge. The zeta potential analysis can provide important information about the colloidal stability and possible interactions between the nanoparticles and the biological medium (HE *et al.*, 2010; HONARY; ZAHIR, 2013; ZHANG, YU; YANG; PORTNEY, 2008). As observed in **Table 2**, all nanoparticles exhibited a very negative surface charge contributing to higher colloidal stability. The negative surface charge is related to the use of anionic surfactant (SDS) adsorbed on the nanoparticle surface (SANTOS, PAULA CHRISTINA MATTOS DOS *et al.*, 2019). Studies reported in the literature have shown that nanoparticles with negative surface charge did not present cytotoxicity in the blood and can be safely administered into the bloodstream depending on the dose (CHO *et al.*, 2014; FORNAGUERA *et al.*, 2015).

FT-IR spectrum (**Figure 13**) of ZnPc loaded in PTEe polymeric nanoparticles showed that the peak corresponding to double-bond stretching (which typically occurs at 1640 cm^{-1})

disappeared, indicating an absence of residual diene monomer (SANTOS, PAULA CHRISTINA MATTOS DOS *et al.*, 2019). The band related to the C=O group of the esters appears in the range from 1750 cm^{-1} to 1735 cm^{-1} . The presence of C—S—C stretching at 710 cm^{-1} can be observed in both polymers, evidencing the addition of thiol radicals (CARDOSO *et al.*, 2018). The ZnPc presented peak characteristics (718 , 747 , and 783 cm^{-1}) of β -ZnPc (FEUSER, PAULO EMILIO; GASPAR; *et al.*, 2016; HUSSEIN, 2011). After the incorporation of ZnPc in PTEe nanoparticles, with dithiol or tetrathiol, the FTIR spectra were similar to empty PTEe nanoparticles, suggesting that there was no significant interaction between drug and polymer (not chemically bonded), indicating that ZnPc was molecularly dispersed in the polymer matrix (DHANA LEKSHMI *et al.*, 2010; DOS REIS ANTUNES JUNIOR *et al.*, 2017; FEUSER, P.E. PAULO EMILIO *et al.*, 2015).

Figure 13- FTIR spectrum of ZnPc loaded polymeric nanoparticles.



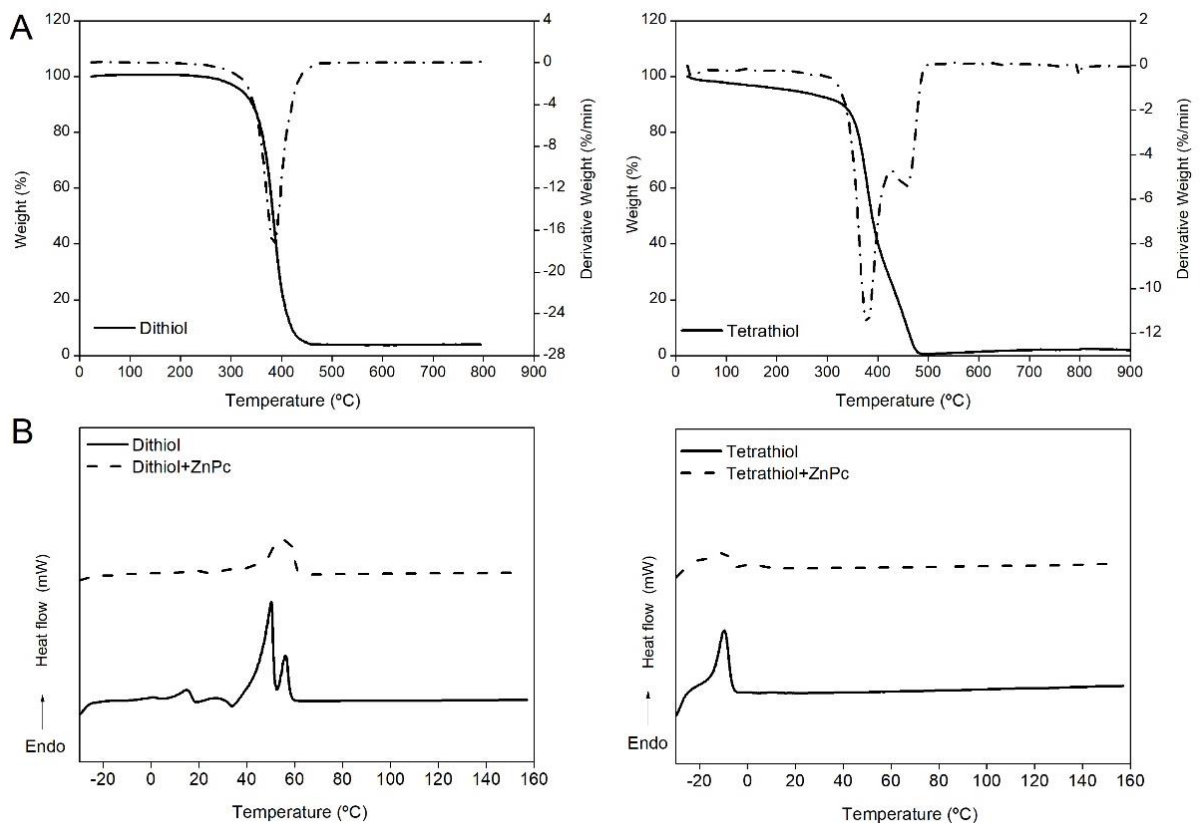
Source: Author.

Nanoparticles were also evaluated by thermal analysis, DSC, and TGA, as presented in **Figure 14**. It was observed, in TGA analysis, only one main degradation stage of PTEe nanoparticles, which occurred between 350 and 400°C , when dithiol was used as the comonomer. Vandenberg *et al.* (2012) observed a similar thermal degradation behavior of poly(β -thioether ester) when 1,6-hexanediol diacrylate was used as the diene monomer and a dithiol as comonomer. The TGA curve for PTEe nanoparticles obtained with tetrathiol presented two degradation stages, probably due to the crosslinking of the polymer matrix.

The glass transition temperature (T_g) and the melting temperature (T_m) of PTEe nanoparticles were investigated by DSC analysis. The T_g of the polymer couldn't be determined at the temperature range of the analysis. Contrarily, the endothermic peak corresponding to T_m

was observed between 40° and 60°C, with two melting peaks, for the PTEe obtained with dithiol. A double-melting point behavior is sometimes observed in semicrystalline polymers. The double melting endotherms reveal that the polymers first undergo a melting process causing an increase in chain mobility and leading to a re-crystallization, which is followed by a second melting. (TÜRÜNÇ, OĞUZ; MEIER, 2010) Analyzing the PTEe nanoparticles obtained with tetrathiol, the T_m was observed between -20° and 0°C. It was also observed that the polymer had a lower degree of crystallinity, this result was expected as the tetrathiol led to a crosslinked polymer and the cross-links hinder the mobility of the chains. The thermal properties of the PTEe nanoparticles didn't change with the incorporation of ZnPc. The thermal analysis did not show any significant interaction between drug and polymer, corroborating with FTIR analyses.

Figure 14- Thermal degradation analysis (TGA) and differential scanning calorimetry (DSC) of nanoparticles samples of dithiol and tetrathiol polymers and ZnPc loaded.



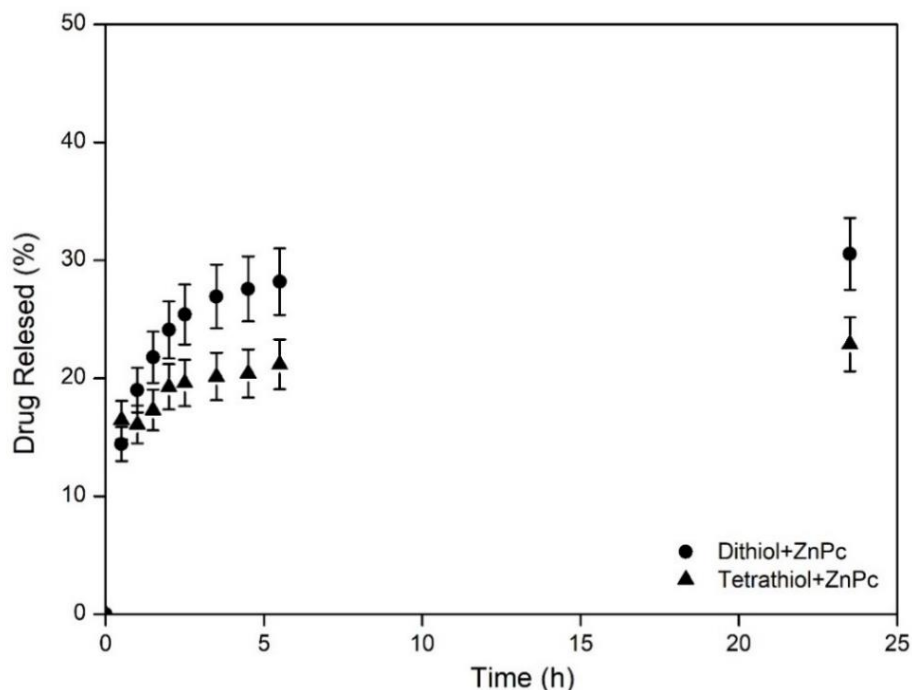
Source: Author.

3.5.1 IN VITRO STUDIES

A release study was performed to evaluate the release profile of ZnPc from PTEe nanoparticles obtained with different thiol comonomers, dithiol and tetrathiol, and polymer matrix structures, linear or crosslinked polymers. In this study, a known amount of ZnPc incorporated into PTEe nanoparticles ($12 \mu\text{g}\cdot\text{mL}^{-1}$) was added to a dialysis bag and immersed in a bath under sink conditions and physiological pH (7.4).

As can be seen in **Figure 15**, the release profiles exhibited an initial burst release 25% (dithiol) and 20% (tetrathiol) in the first hours, followed by a slow release rate that is characteristic of a biphasic release (DOS REIS ANTUNES JUNIOR *et al.*, 2017; FEUSER, P.E. PAULO EMILIO *et al.*, 2016; LI, CHEN *et al.*, 2014). The burst effect observed in the first hours can be attributed to the rapid dissolution of drugs located close to nanoparticles surface (SIAFAKA *et al.*, 2015). After 24 h, the amount of ZnPc released from PTEe nanoparticles reached 33% for dithiol polymer and about 27% for PTEe nanoparticles obtained with tetrathiol. The slower release rate of ZnPc incorporated in PTEe nanoparticles obtained with tetrathiol could be explained by the crosslinked structure of the polymer matrix that can reduce the mobility of ZnPc inside the particles and thus, its diffusion in the polymer matrix, decreasing the release rate of ZnPc.

Figure 15- The release profile of ZnPc-PTEe nanoparticles obtained with dithiol and tetrathiol in pH 7.4. Data refer to the mean \pm standard deviation ($n = 2$) with an experimental error of $\pm 10\%$.



Source: Author.

Mathematical models were applied for different time intervals (first 6 h and after 6 h), to verify the release mechanism of ZnPc from PTEe nanoparticles. In this study, the zero-order, first-order, Korsmeyer–Peppas, and Higuchi model were used. In the first hours, the release kinetics of PTEe nanoparticles obtained with dithiol was best explained by the Korsmeyer–Peppas (**Table 3**). Similarly, after 6 h, the release kinetics was best explained by the same Korsmeyer–Peppas model. For the PTEe nanoparticles obtained with tetrathiol, the release profile was best explained by Higuchi followed by Korsmeyer–Peppas model in the first time interval. In the second time interval (after 6 h), the model that best explains is Higuchi followed by a zero-order model.

The Higuchi model is based on the Fick's Law in which the release occurs by the diffusion mechanism. The zero-order model describes the release of compounds with low solubility in the continuous medium where the drug release of the compound is slow and proportional to its concentration with significant contribution of erosion (BARAKAT; ELBAGORY; ALMURSHEDI, 2009; COSTA, P; SOUSA LOBO, 2001; DE MELLO; RICCI-JÚNIOR, 2011). The Korsmeyer–Peppas model with release exponent n could predict the

mechanism of drug release (HAZRA *et al.*, 2014). The Korsmeyer–Peppas model showed that the ZnPc release from PTEe nanoparticles obtained with dithiol and tetrathiol was controlled by Fickian diffusion in both time intervals ($n > 0.5$, upper limit), suggesting a release of the ZnPc from PTEe nanoparticles by diffusion mechanism through the polymer matrix (COSTA, P; SOUSA LOBO, 2001; DOS REIS ANTUNES JUNIOR *et al.*, 2017; HAZRA *et al.*, 2014). When the model is controlled by non-Fickian diffusion ($n < 0.5$) it's suggested a release by a combination of diffusion and erosion. The values of "n" less than 0.5 indicate a pseudo-Fickian process. The diffusion curves are very similar to a Fickian process, however, it reaches the release equilibrium more quickly (COSTA, P; SOUSA LOBO, 2001; HAZRA *et al.*, 2014).

Table 3- Mathematical models and kinetic parameters.

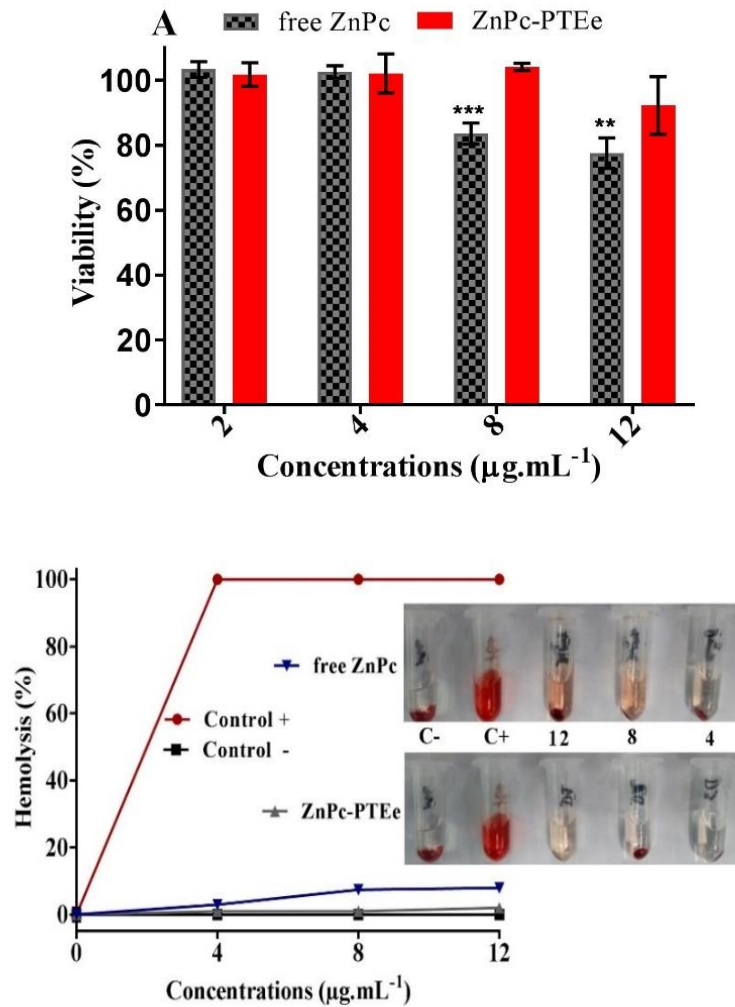
Mathematical models	Dithiol						Tetrathiol					
	0 - 6h			6 – 24h			0 - 6h			6 – 24h		
	R ²	k	n	R ²	k	n	R ²	k	n	R ²	k	n
Zero order	0.792	0.417	-	0.934	0.002	-	0.847	0.018	-	0.999	0.002	-
First order	0.727	0.103	-	0.935	0.004	-	0.828	0.050	-	0.998	0.004	-
Higuchi	0.903	8.102	-	0.954	0.809	-	0.896	3.258	-	1.000	0.688	-
Korsmeyer Peppas	0.954	1.047	0.592	0.970	0.748	0.108	0.880	1.123	0.257	0.998	1.016	0.118

Source: Author.

The cytotoxicity studies of ZnPc loaded in PTEe nanoparticles were performed with PTEe nanoparticles obtained with dithiol. The particles obtained with tetrathiol were difficult to re-disperse after lyophilization, perhaps due to the low T_m . Therefore, the cytotoxicity analyses were not performed for these particles. For the PTEe nanoparticles obtained with dithiol, the cytotoxicity assays were evaluated in two non-tumor cells, NIH3T3 and RBCs. As can be seen in **Figure 16A**, free ZnPc, and ZnPc loaded in PTEe nanoparticles at different concentrations did not present any cytotoxic effect when exposed to the NIH3T3 cells. Free ZnPc presented hemolysis at concentrations of 8 (7.4 %) and 12 (8.2 %) $\mu\text{g.mL}^{-1}$ (**Figure 16B**). On the other hand, the incorporation of ZnPc in PTEe nanoparticles prevented any hemolytic damage. According to the criterion of Standard Test Method for analysis of hemolytic properties of nanoparticles (ASTM E2524-08), percentage hemolysis $> 5\%$ indicates that the tested material did not cause damage. These results indicate that PTEe nanoparticles prevent

the possible cytotoxic effect of ZnPc, proving a drug protection (DANHIER, FABIENNE; FERON; PRÉAT, 2010; FEUSER, P.E. PAULO EMILIO *et al.*, 2016).

Figure 16- (A) Cytotoxic effect of free ZnPc and ZnPc-PTEe nanoparticles at different concentrations in NIH3T3 cells (B) Hemolysis assay. Relative rate of hemolysis in RBCs upon incubation (2h) with free ZnPc and ZnPc-PTEe nanoparticles at different concentrations. Data represent mean \pm SD (n = 3). (* p< 0.05) one-way ANOVA followed by Tukey's test.

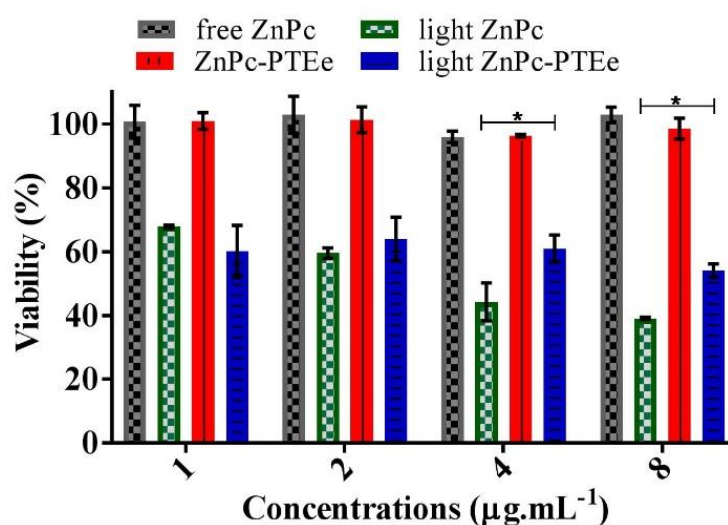


Source: Author.

The phototoxicity assay was performed in MDA-MB231 cells using different concentrations (1, 2, 4, and 8 $\mu\text{g.mL}^{-1}$) without exposition to visible light and irradiated with red light (675 nm, 12 J/cm² of light dose). Free ZnPc and ZnPc loaded in PTEe nanoparticles without exposition to visible light did not show a reduction in MDA-MB231 cell viability

(**Figure 17**). In contrast, when MDA-MB231 cells were irradiated with red light a significant decrease in cellular viability was observed. The cytotoxic effect was more pronounced in free ZnPc, promoting a significant reduction in cell viability at concentrations of 1 (45%), 2 (50%), 4 (58%), and 8 (64%) $\mu\text{g.mL}^{-1}$. ZnPc loaded in PTEe nanoparticles presented similar phototoxicity to free ZnPc at concentrations of 1 and 2 $\mu\text{g.mL}^{-1}$. At concentrations of 4 and 8 $\mu\text{g.mL}^{-1}$, the cytotoxic effect was higher for free ZnPc than ZnPc loaded in PTEe nanoparticles. The lowest phototoxicity of ZnPc loaded in PTEe nanoparticles can be related to the slow release of ZnPc from PTEe nanoparticles, in which the incubation time did not ensure the total drug release. However, even with lower cytotoxic effect at higher concentrations, the ZnPc loaded in PTEe nanoparticles enhanced the cytotoxic efficiency due to singlet oxygen photogeneration, which can damage cellular constituents, culminating in cell death and tissue destruction (KUMAR; SHAN; ZHANG, 2008; SIQUEIRA-MOURA *et al.*, 2013). As can be observed in **Figure 17**, the cell death was not in a dose-dependent manner after the treatment with free ZnPc and ZnPc loaded in PTEe nanoparticles. Besides, several other factors, such as light dose, affinity with the cell membrane, and intracellular localization of the photosensitizer can influence the phototoxicity (DA VOLTA SOARES *et al.*, 2011; DEDA *et al.*, 2009; FEUSER, PAULO EMILIO; GASPAR; *et al.*, 2016; SIQUEIRA-MOURA *et al.*, 2013).

Figure 17- Phototoxicity assay at different concentrations of free ZnPc and ZnPc-PTEe nanoparticles on MDA-MB231 cell. Data represent the mean \pm SD (n = 3). (* p < 0.05) two way ANOVA followed by Tukey's test.



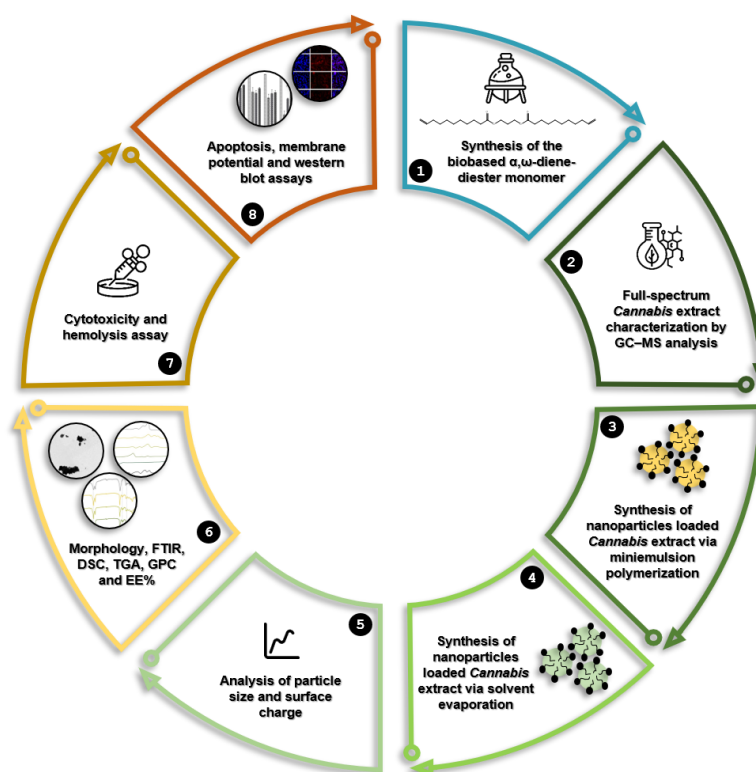
Source: Author.

3.6 CONCLUSIONS

Thiol-ene polymerization reactions were successfully performed to encapsulate a hydrophobic drug (ZnPc) in poly(thioether-ester) nanoparticles through a miniemulsion technique using a biobased α - ω -diene diester monomer derived from castor oil (1,3-propylene diundec-10-enoate). Two different thiols containing two and four thiols groups per molecule were employed as comonomers. Nanoparticles obtained with dithiol and tetrathiol presented an intensity average diameter of around 120 - 160 nm with a high encapsulation efficiency of ZnPc. The FTIR and thermal analysis showed that the ZnPc did not change the characteristics of the nanoparticles, suggesting that ZnPc is molecularly dispersed in the polymeric matrix. The release profile of ZnPc from PTEe nanoparticles presented an initial burst effect followed by a slow-release rate. Studies of cytotoxicity showed that the PTEe nanoparticles protect blood cells against ZnPc decreasing hemolytic damages. Moreover, a low concentration of ZnPc loaded in PTEe nanoparticles ensured the phototoxic effect on the MDA-MB231, confirming PTEe nanoparticles as an effective drug carrier system for application in PDT. These results encourage further studies with these nanoparticles with the incorporation of other photosensitizers and *in vitro* studies.

Chapter 4

4.0 This chapter is part of a publication entitled “Preparation and Characterization of full-spectrum *Cannabis* extract loaded Poly(thioether-ester) nanoparticles: *in vitro* evaluation of their antitumoral efficacy” published in the **Journal of Colloids and Surfaces A: Physicochemical and Engineering Aspects** (<https://doi.org/10.1016/j.colsurfa.2022.130676>).



4.0 PREPARATION AND CHARACTERIZATION OF FULL-SPECTRUM CANNABIS EXTRACT LOADED POLY(THIOETHER-ESTER) NANOPARTICLES: IN VITRO EVALUATION OF THEIR ANTITUMORAL EFFICACY

4.1 INTRODUCTION

Cannabis Sativa L. is a complex plant containing about 426 chemicals, of which more than 60 are cannabinoid compounds, in addition to terpenes, sugars, alkaloids, and quinones (BRIGHENTI *et al.*, 2017; MECHOULAM; PARKER, 2013).

In the plant, cannabinoids are synthesized and accumulated as cannabinoid acids, but when dried, stored and heated, the acids decarboxylate gradually into their proper forms. A

considerable number of these compounds have double bond connections in their constitution (ATAKAN, 2012; ZIVOVINOVIC *et al.*, 2018).

Despite the use of *Cannabis* in medicine having been documented for millennia, only recently has the therapeutic importance of *Cannabis* and cannabinoids receptors as well as chemically related compounds been accepted (DE LA OSSA *et al.*, 2013). The receptors were named according to their order of discovery as CB₁ and CB₂. CB₁ is primarily located at presynaptic nerve terminals and accounts for the majority of the neurobehavioral effects of cannabinoids. CB₂, in contrast, is the major cannabinoid receptor in the immune system, but may also be expressed in neurons (ALEXANDER, 2016; SAITO; WOTJAK; MOREIRA, 2010).

The revelations of the endocannabinoid system have provided the opportunity to understand *Cannabis* potentialities for the treatment of many diseases (MECHOULAM; PARKER, 2013) such as chronic pain, nausea, eating disorders, glaucoma, neurodegeneration, multiple sclerosis, cancer, Alzheimer's disease, epilepsy, stress, and anxiety (ALEXANDER, 2016; ATAKAN, 2012; MAAYAH *et al.*, 2020; PETERS; MURILLO-RODRIGUEZ; HANUS, 2007; SAVAGE *et al.*, 2016; ŚLEDZIŃSKI *et al.*, 2018; TORRES *et al.*, 2011; VELASCO, G.; SÁNCHEZ; GUZMÁN, 2016). In fact, delta-9-tetrahydrocannabinol (THC) is supposed to have the capacity to inhibit angiogenesis and consequently cell growth of tumor cells leading to their death (MARTÍN-BANDERAS, L. *et al.*, 2015). Interestingly, THC has been shown to exert antitumoral activity through tribbles homolog 3-dependent (TRB3-dependent) inhibition of the Akt/mammalian target of rapamycin complex 1 (mTORC1) axis and the subsequent stimulation of autophagy-mediated cancer cell death (HERNÁNDEZ-TIEDRA *et al.*, 2016; SALAZAR *et al.*, 2009).

The anticancer activity of cannabidiol (CBD) has been established in numerous types of tumors, including glioma, breast cancer, prostate cancer, leukemia and cervical carcinomas, among others (ABRAMS, DONALD I. *et al.*, 2021; FRAGUAS-SÁNCHEZ *et al.*, 2020; VELASCO, G.; SÁNCHEZ; GUZMÁN, 2015; VELASCO, GUILLERMO; SÁNCHEZ; GUZMÁN, 2012). Despite the medicinal potential of cannabinoids, they are poorly water-soluble, susceptibility to degradation and oily-resin nature, and it can be difficult to limit its administration (DE LA OSSA *et al.*, 2013; HERNAN PEREZ DE LA OSSA *et al.*, 2012). Currently, the administration of whole-plant *Cannabis* is mainly through inhalation pathways or by oral ingestion (HAZEKAMP *et al.*, 2013). Such consumption increases the therapeutic

ingredient levels in the bloodstream and is followed by a short therapeutic action period (MACCALLUM; RUSSO, 2018). Furthermore, absorption of phytocannabinoids is highly dependent on various factors, such as recent patient feeding, the cannabinoids instability in acidic gastric pH, and the low systemic bioavailability (DE LA OSSA *et al.*, 2013; UZIEL *et al.*, 2020).

Nanoparticles as a drug delivery system can be used here to administer full-spectrum *Cannabis* extract. The nanoparticles can extend the stability of the extract, reducing the degradation and oxidation process, change the drug biodistribution, increase their availability and offer a significant improvement over traditional oral methods of administration in terms of efficiency and effectiveness. It can also deliver a higher concentration of the drug to a convenient spot (NAGAVARMA *et al.*, 2012). Biobased polymer nanoparticles, such as a poly(thioether-ester) nanoparticles, are great candidates for biomedical applications by virtue of their biocompatibility, biodegradability, and also antioxidant activity (CARDOSO *et al.*, 2018; MACHADO, THIAGO O. *et al.*, 2017). Poly(thioether-ester) nanoparticles can be manufactured by using a preformed polymer in a miniemulsification using a solvent evaporation method or by thiol-ene miniemulsion polymerization. The *in situ* encapsulation technique, such as miniemulsion polymerization, has the ability to develop complex molecular nanoparticles in a single-step reaction (ASUA, 2002; LANDFESTER, KATHARINA *et al.*, 1999). Miniemulsions can be described as stable colloidal monomer droplets, in a range of 50–500 nm, dispersed in an aqueous system.

The monomer droplets use to be the polymerization location leading to different kinds of polymerization mechanisms such as step-growth (VALÉRIO; ARAÚJO; SAYER, 2013) and chain-growth, either cationic (ALVES *et al.*, 2018) or free-radical (COSTA, CRISTIANE *et al.*, 2013; ROMIO, ANA PAULA *et al.*, 2009), and also the encapsulation of diverse drugs and actives (BERNARDY *et al.*, 2010; STAUDT *et al.*, 2013).

The thiol-ene polymerization mechanism has many advantages over traditional free-radical polymerization, such as the ability to add different functional groups, for example ester linkages in the main chain of the polymer. These kinds of linkages can add some properties to the polymer, such as biodegradability or even mechanical characteristics (HOELSCHER *et al.*, 2018). The polymerization can be carried out in moderate conditions and normally generates inoffensive by-products (MACHADO, THIAGO O.; SAYER; ARAUJO, 2017; TÜRÜNÇ, OĞUZ; MEIER, 2012). The use of renewable raw materials can make the process more

sustainable. Biomass-derived chemicals can be used to develop monomers with particular structures, with innovative properties or modified to have characteristics close to those of petroleum-based monomers (MEIER; METZGER; SCHUBERT, 2007).

Plant oils, such as castor oil, are the most widely applied renewable raw materials in the chemical industry. They are used to forming long-chain aliphatic polyesters.

Recent research in the field of micro or nanoparticles for phytocannabinoid delivery systems involve individual constituents, such as CBD (APARICIO-BLANCO *et al.*, 2019; BERROCOSO *et al.*, 2017; FRAGUAS-SÁNCHEZ *et al.*, 2020; HERNAN PEREZ DE LA OSSA *et al.*, 2012; KAMALI *et al.*, 2019), Δ^9 -THC (DE LA OSSA *et al.*, 2013; HERNÁN PÉREZ DE LA OSSA *et al.*, 2013; HOMMOSS; PYO; MÜLLER, 2017; MARTÍN-BANDERAS, L. *et al.*, 2015; MARTÍN-BANDERAS, LUCÍA *et al.*, 2014), CB13 (BERROCOSO *et al.*, 2017; DURÁN-LOBATO *et al.*, 2014, 2015) or a mixture of THC and CBD (CHERNIAKOV *et al.*, 2017; HERNÁN PÉREZ DE LA OSSA *et al.*, 2013).

Uziel *et al.* 2020 developed full-spectrum *Cannabis* extract microdepots to control the release of cannabinoids for continued therapeutic effect (UZIEL *et al.*, 2020). Nevertheless, there is a need to describe and analyze the encapsulation of the full-spectrum of *Cannabis* also in nanoparticles. In fact, there are relevant studies indicating THC as an antineoplastic agent (TOMKO *et al.*, 2020). The purpose of the present study was to encapsulate THC-enriched full-spectrum *Cannabis* extract-CN via thiol-ene miniemulsion polymerization-Me and thiol-ene miniemulsification/solvent evaporation method-Se using a biobased α,ω -diene-diester monomer synthesized from a castor oil derivative and the *in vitro* studies. The novelty of the study is to encapsulate the complete extract by *in-situ* polymerization. Few studies have reported the encapsulation of the complete extract, and none with *in situ* polymerization.

4.2 MATERIAL AND METHODS

4.2.1 MATERIALS

10-undecenoic acid (Sigma-Aldrich, 98%), 1,3-propanediol (Sigma-Aldrich, 99.6%), p-toluenesulfonic acid monohydrate (PTSA, Sigma-Aldrich, 98.5%), toluene (Sigma-Aldrich, 99.8%), hexane (Sigma-Aldrich, 99.8%), diethyl ether (Sigma-Aldrich, > 99.0%), magnesium sulfate (Sigma-Aldrich, > 99.5%), sodium dodecyl sulfate (SDS, Sigma-Aldrich, 99%), full-spectrum *Cannabis Sativa* ethanol extract (CN, donated by Brazilian Association of Medicinal Cannabis Patients, CNPJ: 34.532.173/0001-19), delta9-tetrahydrocannabinol (THC, LGC

Standards, 1mg/mL in methanol), (-)-cannabidiol (CBD, LGC Standards, 1mg/mL in methanol), cannabinol (CBN, LGC Standards, 1mg/mL in methanol), azobisisobutyronitrile (AIBN, Vetec, 98%), butanedithiol (dithiol, Sigma-Aldrich, 97%), tetrahydrofuran (THF, Neon, P.A), dichloromethane (Neon, P.A), methanol (Neon, P.A), phosphate Buffered Saline solution (PBS, pH 7.4), 3-(4,5-dimethylthiazol-2-yl)-2,5-diphenyltetrazolium bromide (MTT, Sigma-Aldrich), dulbecco's modified eagle medium (DMEM, Sigma-Aldrich), fetal bovine serum (FBS, Atena biotecnologia), isopropyl alcohol (VETEC) and distilled water.

4.2.2 SYNTHESIS OF THE BIOBASED α,ω -DIENE-DIESTER MONOMER

The synthesis of the α,ω -diene-diester monomer, 1,3-propylene diundec-10-enoate (PDE), was based on a previous work (CARDOSO *et al.*, 2018). The reagents: 10-undecenoic acid (50.0 g, 0.27 mmol), 1,3-propanediol (8.4 g, 0.11 mmol), p-toluenesulfonic acid (3.0 g, 0.0157 mmol), and toluene (200 mL) were combined in a round-bottomed flask equipped with a Dean-Stark apparatus coupled. A magnetic stirrer was used to homogenize the mixture. The mixture was heated and during the reaction time, 3 h, water was collected (reflux system). Once the reaction was completed, the toluene was removed under reduced pressure. The residue was filtered through a short pad of basic aluminum oxide with hexane as eluent. Then the hexane was removed, and the final product was dissolved in diethyl ether (200 mL) and washed twice with water (200 mL). The mixture was dried over anhydrous $MgSO_4$, filtered and the solvent removed. The product was analyzed by HNMR spectroscopy (Bruker AC 200, frequency 200 MHz).

4.2.3 SYNTHESIS OF PTE_e NANOPARTICLES CONTAINING FULL-SPECTRUM CANNABIS EXTRACT VIA THIOL-ENE MINIEMULSION POLYMERIZATION (Me-PTE_e)

The organic phase was prepared using the α,ω -diene diester monomer PDE (1.0 g) and full-spectrum *Cannabis* extract about 10% (Me1), 30% (Me2), or 50% (Me3) in relation to the monomer (0.10g; 0.30g; 0.50g respectively) under magnetic stirring until complete drug solubilization. To the aqueous phase, distilled water (9.8 g) and sodium dodecyl sulfate (0.0304 g) were added to the organic phase and stirred (500 rpm) for 10 min. Next, butanedithiol (1:1 dithiol-to-diene molar ratio) was added to the system and stirred (250 rpm) for 5 min. Subsequently, the emulsion was sonicated for 2 min (amplitude of 60% in pulse mode, 10s of sonication, 2s of pause) using a Fisher Scientific Sonic Dismembrator model 500. At the end

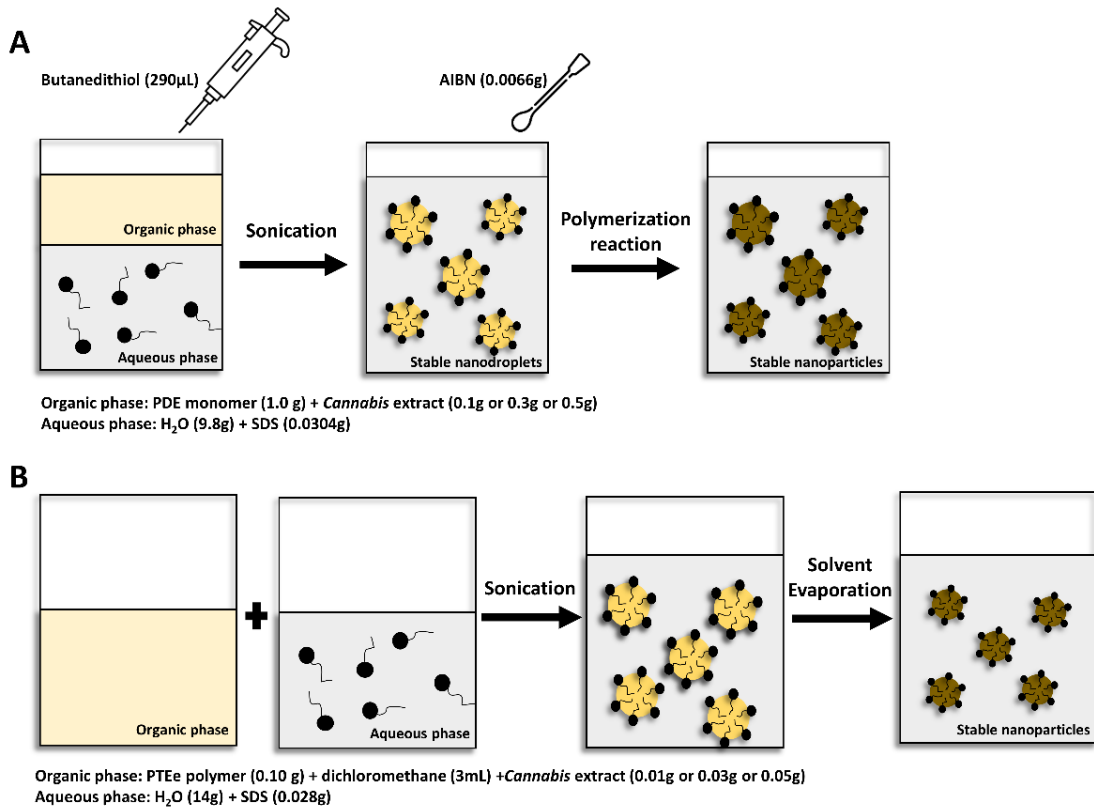
of the sonication step, the initiator AIBN (0.0066 g) was added and sonicated for 10s. After miniemulsification, the thiol-ene polymerization was performed in a thermostatic bath at 80°C for 4 h. **Figure 18A** shows the schematic representation of the synthesis of nanoparticles and encapsulation of *Cannabis* extract by Me-PTEe.

4.2.4 SYNTHESIS OF PTEe NANOPARTICLES CONTAINING FULL-SPECTRUM CANNABIS EXTRACT VIA MINIEMULSIFICATION AND SOLVENT EVAPORATION (Se-PTEe)

In the case of miniemulsification and solvent evaporation it is necessary to first prepare the PTEe via thiol-ene polymerization in bulk. The diene monomer (1g) and the organic-soluble initiator, AIBN (0.0066g), were mixed at room temperature. After complete initiator solubilization, dithiol was added to the system (1:1 dithiol-to-diene molar ratio). The reaction mixture was placed on a hot plate magnetic stirrer at 80°C for 4 h. The final product of the bulk polymerization reaction was solubilized in THF and the polymer was precipitated into cold methanol for isolation by filtration and drying. Subsequently, the nanoparticle production by miniemulsification and solvent evaporation was performed.

The organic phase was prepared using the dried polymer from bulk polymerization (0.10 g), dichloromethane as solvent (3mL, 3.99g) and full-spectrum *Cannabis* extract about 10% (Se1), 30% (Se2), or 50% (Se3) in relation to the polymer (0.010g; 0.030g; 0.050g respectively) under magnetic stirring until complete drug solubilization. The aqueous phase, composed of distilled water (14 g) and sodium dodecyl sulfate (0.028 g), was added to the organic phase and magnetically stirred (500 rpm) for 10 min. The final coarse emulsion was sonicated for 2 min with an amplitude of 60% in pulse mode (10s of sonication, 2s of pause) using a Fisher Scientific Sonic Dismembrator model 500. An ice bath was used to prevent heat buildup during the sonication. At the end of the sonication step, the solvent (dichloromethane) was removed using a hot plate magnetic stirrer at 50°C for 3h. **Figure 18B** shows the schematic representation of the synthesis of nanoparticles and encapsulation of *Cannabis* extract by Se-PTEe.

Figure 18- Synthesis of nanoparticles and encapsulation of *Cannabis* extract by Me-PTEe and Se-PTEe.



Source: Author.

4.3 CHARACTERIZATION

4.3.1 FULL-SPECTRUM CANNABIS EXTRACT CHARACTERIZATION, QUALITATIVE AND QUANTITATIVE

GC-MS analysis

To characterize the full-spectrum *Cannabis* extract qualitatively a Gas Chromatograph coupled with mass spectrometer (GC/MS) was used. The GC/MS analysis was performed using an instrument Agilent GC 7890A coupled with MS detector Agilent 5975C. The column, a HP-5MS (Agilent) fused silica capillary column (30 m length x 250 µm i.d. x 0.25 µm film thickness composed of 5% phenyl-95% methylpolysiloxane) was connected to a quadrupole detector operating in EI mode at 70 eV and the mass scan ranged from 50 to 400 m/z. Helium was used as the carrier gas at a flow rate of 1.0 mL min⁻¹. The injector and interface temperatures were 250 °C with a split ratio of 30:1. The solvent delay was 4.0 min and the injection volume was 1.0 µL with auto sampler Agilent GC Sampler 80 equipped with a 10 µL

syringe. The oven temperature program consisted of 120 °C for 2 min, then 8°C/min to 270 °C and remaining at this temperature for 5 min with a total run time of 25.75 min. To identify the compounds, their mass spectra were compared with those from the National Institute of Standards and Technology. The calculation of linear retention indices (*LRI*) was made using the approximation by Van den Dool and Kratz according to equation (1) (BIZZO *et al.*, 2020; KRATZ, [S.d.]).

The compounds were identified by comparing their mass spectra with those from the National Institute of Standards and Technology and a comparison of the retention rates calculated with those of the literature (ADAMS, 2007).

GC–FID analysis

The *Cannabis* extract was quantitatively analyzed on Agilent GC 7890A instrument and with the same column as for the GC/MS analysis, but this time coupled with FID (Flame ionization detector). Analysis conditions were the same as those described for the GC/MS analysis, except for the injector and detector temperatures, which were 270 °C and the splitless injection mode. The concentration was determined based on a linear calibration curve using different concentrations of CBD ($y=181645x-186489$, $r^2=0.9958$, RT=19.24 min); THC ($y=180591x-166939$, $r^2=0.9958$, RT=20.19 min) and CBN ($y=163943x-215013$, $r^2=0.9917$, RT=20.84 min) diluted in methanol (0.5-25 $\mu\text{g}\cdot\text{mL}^{-1}$) (**Figure A.2, A.3 and A.4**).

4.3.2 PARTICLE SIZE, SURFACE CHARGE, AND MORPHOLOGY

Dynamic light scattering (DLS—Malvern Instruments, Zeta Sizer Nano-S90) was used to measure the intensity average diameters of the polymer droplets and particles. Diluted latex samples (1:15) were used for DLS analysis. The surface charge of the nanoparticles was analyzed using zeta potential measurements MALVERN Zetasizer Nanosizer (dilution of 1:10). The morphology of the nanoparticles was analyzed by transmission electron microscopy (TEM) model JEM 2100F 100 kV (dilution of 0.5% solids, carbon-coated copper grid of 300 mesh).

4.3.3 FOURIER-TRANSFORM INFRARED SPECTROSCOPY

The Fourier Transform Infrared Spectroscopy (FTIR) analysis was performed with a resolution of 4 cm^{-1} , 32 scans in a range of 4000-400 cm^{-1} , using KBr pellet by Shimadzu Spectrometer, model IRPrestige-21.

4.3.4 THERMAL ANALYSIS

Differential scanning calorimetry (DSC, Perkin Elmer 600) was performed under a nitrogen atmosphere (20 mL/min) at a heating rate of 10°C/min. From -30° to 90°C, held for 2min at 90°C, cooled down from 90°C to -30°C, held for 1min at -30°C and heated from -30.00°C to 120°C. The melting temperature, T_m , was recorded from the second heating ramp. The thermogravimetric analysis (TGA, STA 449F3 Jupiter) was carried out from 30°C up to 800°C, at a constant heating rate of 10°C/min under nitrogen atmosphere (60 mL/min) in samples of approximately 10 mg.

4.3.5 GEL PERMEATION CHROMATOGRAPHY

Molecular weight distributions were determined by Gel Permeation Chromatography, using a high-performance liquid chromatograph (HPLC, model LC 20-A, Shimadzu) equipped with a PL gel MiniMIX precolumn (5 μm , 50x4 mm), two PL gel MiniMIX columns (5 μm , 250x4.6 mm) in series, and a RID-10A refractive index detector. THF was used as eluent with a flow rate of 0.3 mL min⁻¹ at 40 °C. For the calibration curve of the equipment, polystyrene standards with molar masses ranging from 580 to 9.835x10⁶ g mol⁻¹ were used.

4.3.6 ENCAPSULATION EFFICIENCY

The encapsulation efficiency (EE%) was determined as described by Machado *et al.* 2017 (MACHADO, THIAGO O. *et al.*, 2017). An amount of CN nanoparticles (500 μL) was centrifuged (Mini Spin Eppendorf AG) for 30 min using an Amicon Ultra 0.5 (Millipore®, 100 kDa) filter at 13,000 rpm. The permeate (200 μL) was diluted with distilled water (2000 μL) and analyzed by Gas Chromatography with Flame-Ionization Detection (GC-FID) (7890A) using the same column, analytical conditions and calibration curves as those described in section 2.5.1.

The EE was calculated by the difference between the total amount of CN added to the miniemulsion (M_t) and the amount in the permeate (M_p) as shown in Eq. (1). The measures were conducted in duplicate (n = 2).

$$EE (\%) = \frac{M_t - M_p}{M_t} \times 100 \quad (1)$$

4.4 IN VITRO STUDIES: ANALYSIS OF THE EFFECT OF THE ENCAPSULATED CANNABINOIDS ON THE VIABILITY OF CANCER CELL LINES

4.4.1 CYTOTOXICITY ASSAY

B16F10, NIH3T3, T98 and U87 cells were used to evaluate the cytotoxicity of free CN and CN loaded PTEe nanoparticles obtained by miniemulsion polymerization and miniemulsification/solvent evaporation. All cell lines were cultured in DMEM supplemented with 10% wt fetal bovine serum, 1% antibiotic and maintained under culture conditions (37°C in a humidified atmosphere with 5% wt CO₂). The cells were seeded at a density of 1×10^4 cells/well in 96-well plates and incubated under culture conditions for 24 h. Subsequently, B16F10 and NIH3T3 cells were treated with DMEM containing different concentrations of free CN, Me-PTEe and Se-PTEe nanoparticles and incubated for 24h. T98 and U87 were treated with DMEM containing different concentrations of free CN, and Se-PTEe nanoparticles and incubated for 24h. After incubation time, the DMEM was removed, and the cellular viability was determined by the MTT method. A colorimetric assay was used to measure cell metabolic activity to determine the cytotoxic activity. Briefly, 100 μ L of a MTT solution (0.5 mg/mL) was added in each well and incubated for 3 h under culture condition to allow the formation of formazan. In sequence, 100 μ L of isopropyl alcohol was added in each well to dissolve the formazan crystals. Subsequently, absorbance was measured at 570 nm using a SpectraMax[®] M3 microplate reader. All experiments were performed in triplicate and the results were expressed as the percentage of viable cells compared to the control group (only cells). The maximum concentration of DMSO used in this experiment was of 0.2 %.

4.4.2 HEMOLYSIS ASSAY

The hemolysis assay was performed following the method described by Feuser *et al.* (2015). Human red blood cells (erythrocytes) were obtained from three healthy donors. This study was approved by the Ethics Committee of the Universidade do Extremo Sul Catarinense (Criciúma, Brazil). Human blood was collected in tubes containing 3.2 wt% sodium citrate. Human blood (4 mL) was added to 8 mL of sterile saline solution, and the erythrocytes were isolated by centrifugation at $1,500 \times g / 10$ min. The erythrocytes were washed three times with saline solution. Following the last wash, the erythrocytes were diluted in saline solution (2mL), and 70 μ L of the diluted solution was added to 930 μ L of saline solution. The erythrocytes were treated with different concentrations and stirred at 200 rpm and maintained at 37°C for 2 h. Subsequently, the erythrocytes with different treatments were centrifuged at $10,000 \times g$ for 5

min, and the supernatant was analyzed in 96-well plate at 540 nm (SpectraMax[®] M3). As positive and negative controls, 70 μ L of the erythrocytes was incubated with 930 μ L of distilled water and saline, respectively.

4.4.3 APOPTOSIS

Cell death mechanism was determined using flow cytometry using Annexin V Apoptosis Kit from BD Biosciences. B16F10 cells were seeded at a density of 2×10^5 cells/well in a 12-well microtiter plate and incubated for 24 h under culture conditions. After the incubation time, both cells were treated with CN and CN loaded PTEe nanoparticles at concentrations near the inhibitory concentration (IC_{50}) and incubated for 24 h under culture conditions. Subsequently, the cells were collected by trypsinization, centrifugated (1000 rpm for 1 min), and resuspended in 300 μ L of $1 \times$ Annexin V Binding Buffer. Apoptosis was determined following the manufacturer's protocol.

4.4.4 MEMBRANE POTENTIAL

Mitochondrial membrane potential was assessed to evaluate the influence of free CN and CN loaded PTEe nanoparticles on B16F10 cells. B16F10 cells were treated with CN and CN loaded PTEe nanoparticles at concentrations near the inhibitory concentration (IC_{50}). Then the cells were washed three times (PBS) and cell nuclei were stained with Hoechst 33342 (blue fluorescence, excitation 405 nm/emission 470) and mitochondrial membrane potential was determined using Mitoprobe (TMRM), ThermoFisher. The images were obtained under a fluorescence microscope, model Nikon Eclipse Ti-U.

4.4.5 WESTERN BLOT

Western blot analysis was performed following standard procedures. Briefly, proteins were extracted using RIPA buffer [150 mM NaCl, 1% (v/v) NP40, 50 mM Tris-HCl pH 8.0, 0.1% (v/v) SDS, 1 mM EDTA, 0.5% (w/v) deoxycholate]. The total protein was quantified by using the Bradford method, revealed by SDS-PAGE on 12% acrylamide gels (Bio-Rad, Hercules, CA, USA) and transferred to polyvinylidene difluoride membranes and blocked in a 5% skim milk solution or 5% BSA (Sigma) and incubated at 4 °C overnight with a primary antibody. The membranes were then probed with the following primary antibodies: anti-pAKT S473 (1:1000; Cell signaling, #9271, Danvers, MA, USA), anti-AKT (1:1000; Cell signaling, #9272, Danvers, MA, USA), anti-LC-3 (1:2000; Sigma-Aldrich; #L7543), anti-actin (1:4000; Sigma; A5441, St. Louis, MO, USA). Antibody binding was detected with horseradish

peroxidase (HRP)-conjugated anti-mouse or anti-rabbit secondary antibodies (1:5000; GE Healthcare, Chicago, IL, USA) and visualized by enhanced chemiluminescence (Bio-Rad, Hercules, CA, USA). The images were obtained with the ImageQuant LAS 500 chemiluminescence CCD camera (GE Healthcare Life Sciences, Chicago, IL, USA). ECL results were scanned and the amount of each protein band was quantified using NIH Image J software (NIH Image, Bethesda, MD, USA, <http://rsb.info.nih.gov/nih-image/>).

4.4.6 STATISTICAL ANALYSIS

Statistical significance was assessed using two-way analysis, Tukey's test ($p < 0.05$) using Prism software version 8.0, GraphPad. All experiments were carried out in triplicate ($n = 3$) and the results were calculated as mean \pm standard deviation.

4.5 RESULTS AND DISCUSSION

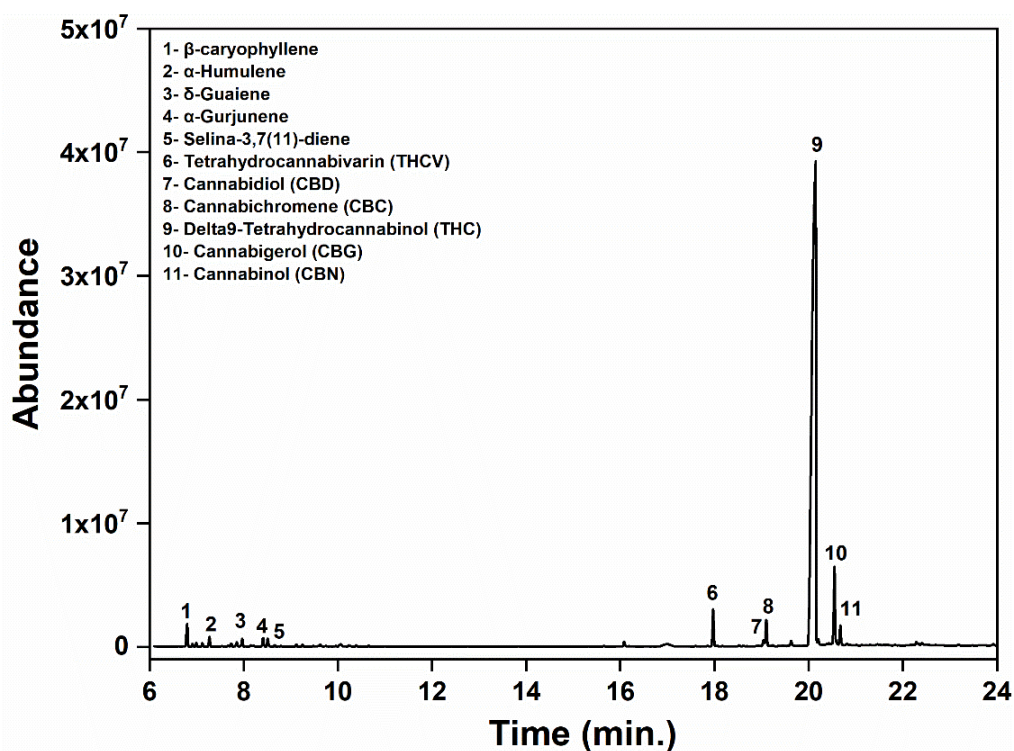
4.5.1 FULL-SPECTRUM CANNABIS EXTRACT CHARACTERIZATION

The full-spectrum *Cannabis* extract was characterized qualitatively using a Gas Chromatograph with MS detector (GC/MS). Using this procedure, the efficient separation of cannabinoids, terpenes, and other compounds was achieved (**Figure 19**). **Table 4** lists the linear retention indices calculated (LRI), the majority ions (m/z) and the retention time of each compound identified. There are a vast number of chemical substances found in the samples of *Cannabis* extracts including cannabinoids, sugars, fats/oils components, and terpenes (CIOLINO; RANIERI; TAYLOR, 2018a).

The terpenes and cannabinoids found in the *Cannabis* samples differ in terms of concentrations, volatility, and polarity. Terpene levels are lower than cannabinoids.

The separation of these two groups of compounds can be obtained by GC, using a wide temperature gradient program (ZEKIČ; KRIŽMAN, 2020). The chemical structures of the cannabinoids generally contain aromatic, alkyl, and alcohol moieties, with the acidic cannabinoids (CBDA, THCA, CBGA) also containing carboxylic acid groups (CIOLINO; RANIERI; TAYLOR, 2018b).

Figure 19- Chromatogram of the full-spectrum *Cannabis* extract at a concentration of 25mg mL⁻¹.



Source: Author.

Table 4- Retention time, linear retention indices calculated (LRI), the majority ions (m/z), chemical function, and a molecular formula of each identified compound.

Compound	LRI	m/z	Retention Time	Chemical function	Molecular formula	Molecular Weight (g/mol)
β -caryophyllene	1461	93, 133, 91, 79, 69	6.80	Sesquiterpene	C ₁₅ H ₂₄	204.4
α -Humulene	1495	93, 80, 121, 91, 79	7.27	Sesquiterpene	C ₁₅ H ₂₄	204.4
δ -Guaiene	1544	107, 93, 108, 91, 105	7.97	Sesquiterpene	C ₁₅ H ₂₄	204.4
α -Gurjunene	1576	204, 161, 91, 105, 133	8.41	Sesquiterpene	C ₁₅ H ₂₄	204.4
Selina-3,7(11)-diene	1583	161, 122, 107, 204, 91	8.51	Sesquiterpene	C ₁₅ H ₂₄	204.4
Tetrahydrocannabivarin (THCV)	2370	271, 203, 286, 243, 272	17.97	Cannabinoid	C ₁₉ H ₂₆ O ₂	286.4
Cannabidiol (CBD)	2477	231, 285, 300, 217, 257	19.04	Cannabinoid	C ₂₁ H ₃₀ O ₂	314.5
Cannabichromene (CBC)	2483	231, 232, 174, 314, 299	19.10	Cannabinoid	C ₂₁ H ₃₀ O ₂	314.5
Delta9-Tetrahydrocannabinol (THC)	2592	299, 314, 231, 271, 243	20.15	Cannabinoid	C ₂₁ H ₃₀ O ₂	314.5
Cannabigerol (CBG)	2635	193, 231, 123, 194, 69	20.55	Cannabinoid	C ₂₁ H ₃₂ O ₂	316.5
Cannabinol (CBN)	2649	295, 238, 310, 223	20.67	Cannabinoid	C ₂₁ H ₂₆ O ₂	310.4

Source: Author.

In the second step of this research work, the concentrations of the main components present in the *Cannabis* extract were determined by Gas Chromatography coupled to the conventional Flame Ionization Detector (GC/FID) based on calibration curves. Results from this analysis showed that the 63.3% of the full-spectrum *Cannabis* extract analyzed corresponds to cannabinoids. More specifically, THC (59.1%, 591.2 mg/g), CBD (1.5%, 14.5 mg/g), and CBN (26.9%, 2.7 mg/g) were the major cannabinoids. The other 36.7% corresponded to other cannabinoids and terpenoids.

In a previous study conducted by Ciolino *et al.* 2018, the mean concentration of THC found in a CBD-enriched *Cannabis* extract designed as an oral supplement ranged between 5.0 and 8.5 mg/g whereas the mean concentration of CBD and CBN varied between 144 and 350 mg/g, and 0.39 and 1.9 mg/g, respectively. In commercial tetrahydrocannabinolic acid (THCA)-rich *Cannabis* plant buds and plant preparations, the concentration of THC varies between 4.4 and 172mg/g, and the CBN concentration between 0.016 and 9.4 mg/g (CIOLINO; RANIERI; TAYLOR, 2018b).

In the work of Citti *et al.* 2018, the mean concentrations of CBD found in commercial hemp oils was 1056 mg/kg, the concentrations of THC was below 1.80 mg/kg and CBN also showed significant variability with mean concentrations around 12.41 mg/kg (CITTI *et al.*, 2018).

This diversity can also be found in other works that analyzed the concentration of cannabinoids in *Cannabis* extracts and products (BORGES *et al.*, 2020; CARVALHO *et al.*, 2020; DEIDDA *et al.*, 2019; PAVLOVIC *et al.*, 2018). These observations reflect the diversity of cannabinoid concentrations found in *Cannabis* extracts. This can be related to the genetics of the *Cannabis* plant, the kind of cultivation, the preparation of the extract, the decarboxylation process, and the oxidation of the samples. The existence CBN in the samples, for example, can be considered a degradation indicator given the fact that CBN originates from the THC oxidation process (BORGES *et al.*, 2020). The highest cannabinoid concentrations can be found in the flowers (HAZEKAMP, 2007).

4.5.2 PREPARATION AND CHARACTERIZATION OF THE NANOPARTICLES

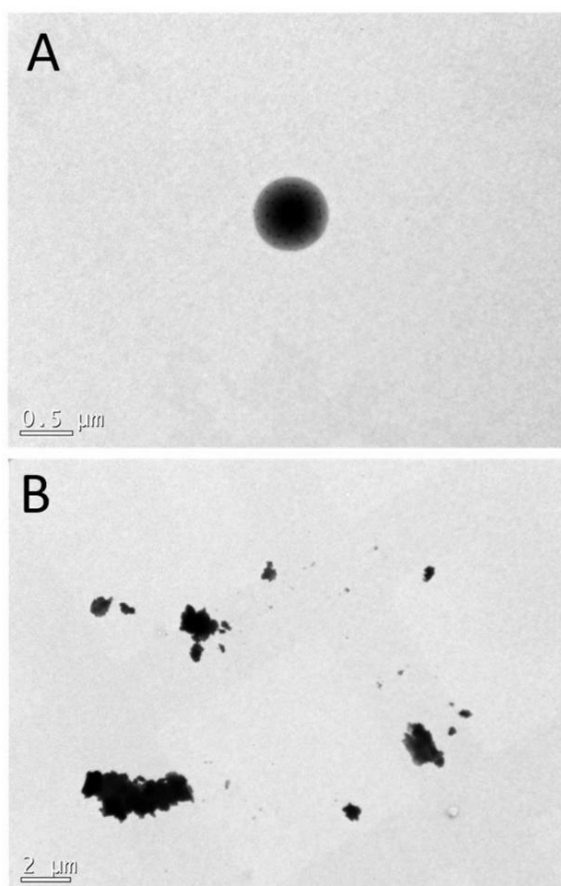
PTEe nanoparticles were obtained via either thiol-ene miniemulsion polymerization-Me of the diene monomer 1,3-propylene diundec-10-enoate and butanedithiol (BDT), or via

miniemulsification with solvent evaporation-Se using PTEe synthesized by thiol-ene bulk polymerization.

As can be seen in the TEM images displayed in **Figure 20**, PTEe nanoparticles prepared by both techniques presented spherical morphology. PTEe nanoparticles degrade under the electron beam and in order to minimize degradation the microscope was operated at the lowest viable current, providing low image resolution.

In **Table 5**, the physical chemical characterizations of the intensity average diameters of monomer droplets and polymer nanoparticles, polydispersity index (PdI), zeta potential and weight average (Mw) are shown. PTEe nanoparticles obtained by the *in situ* thiol-ene miniemulsion polymerization (Me-PTEe) droplets with intensity average diameters in the range of 106 - 229 nm and PdI around 0.17 were obtained. The Se-PTEe nanoparticles obtained by the miniemulsification and solvent evaporation technique exhibited droplets with intensity average diameters in the range of 91 - 146 nm and PdI around 0.15.

Figure 20- Transmission electron microscopy (TEM) images of CN-PTEe nanoparticles. (A) Me1; (B) Se1.



Source: Author.

Table 5- Intensity mean diameter: droplets (D_{pg}) and nanoparticles (D_p); Polydispersity index: droplets (PdI_g), nanoparticles (PdI) obtained by DLS, and weight average by GPC.

Samples	D_{pg} (nm)	PdI_g	D_{pm} (nm)	PdI_m	M_w ($g \cdot mol^{-1}$)
Me0	104 ± 4	0.16	106 ± 5	0.17	2625
Me1	172 ± 20	0.16	175 ± 20	0.08	1449
Me2	202 ± 1	0.25	199 ± 5	0.08	1234
Me3	199 ± 14	0.17	229 ± 26	0.17	1064
Se0	-	-	146 ± 1	0.15	5313
Se1	-	-	95 ± 13	0.23	-
Se2	-	-	97 ± 3	0.11	-
Se3	-	-	91 ± 6	0.12	-

Source: Author.

The average diameter of the monomer droplets and Me-PTEe nanoparticles showed excellent agreement and both increased when CN was used due to the higher viscosity of the dispersed phase. This increases the resistance to produce droplets during sonication, ensuing in bigger monomer droplets and therefore larger polymeric particle sizes. In contrast, the increase in CN in the Se-PTEe formulation scarcely affected the particle size. Indeed, the formulation without *Cannabis* extract had a larger particle size. Some components of *Cannabis* extract can be acting as co-stabilizer of the miniemulsion, minimizing diffusional degradation. The surface charge relation is an important analysis for the formulation and development of new drug nanocarriers. Information about the interactions between the nanoparticles and the biological medium can be found with zeta potential values (FEUSER, PAULO EMILIO; BUBNIAK; *et al.*, 2016; HE *et al.*, 2010). The colloidal stability of a dispersion is related to the strength of repulsion between the particles. In systems where attractive forces dominate, the system becomes unstable, and the particles settle, increasing viscosity. In cases where repulsive forces are strong, a relatively stable colloidal dispersion is obtained (HE *et al.*, 2010; HONARY; ZAHIR, 2013; ZHANG, YU; YANG; PORTNEY, 2008). In this work, all nanoparticle formulations exhibited a negative surface charge between $-38 \pm 6mV$ and $-43 \pm 6mV$ (Me-PTEe) and $-38 \pm 1mV$ to $-48 \pm 1mV$ (Se-PTEe) contributing to higher colloidal stability. The negative surface charge of formulations is related to the use of anionic surfactant (SDS) adsorbed on the nanoparticle surface (DOS SANTOS, PAULA C. M. *et al.*, 2019). Studies have shown that nanoparticles with negative surfaces do not present cytotoxicity in the blood and,

consequently, can be safely applied depending on the dose (CHO *et al.*, 2014; FORNAGUERA *et al.*, 2015).

In GPC analysis, for Me-PTEe formulations, a decrease in the molecular weight when increasing the CN concentration in the miniemulsion is evidenced. CN has different constituents, including cannabinoids and terpenes, and most of them have double bonds in their constitution which could react with thiol acting as chain terminators and thus leading to lower molecular weights (HAO; GU; XIAO, 2015; HAZEKAMP, 2007). As expected, in the case of miniemulsification and solvent evaporation technique-Se-PTEe, the molecular weight did not exhibit effective modifications. In this technique, the polymer is synthesized in a previous step therefore restricting the possibility of reaction between double bond components and the polymer chains.

The encapsulation efficiency could be analyzed for each cannabinoid standard constituent (THC, CBD, and CBN). All formulations (Me-PTEe and Se-PTEe) have high encapsulation efficiency values (> 97%) with the amount of cannabinoids standard for 100 mg of polymer at around 0.1 (Me1 and Se1), 0.3 (Me2 and Se2), or 0.6 mg (Me3 and Se3) of CBD; 5 (Me1 and Se1), 14 (Me2 and Se2), or 23 mg (Me3 and Se3) of THC; and 0.2 (Me1 and Se1), 0.6 (Me2 and Se2), or 1 mg (Me3 and Se3) of CBN. This means that the full spectrum of *Cannabis* extract was perfectly encapsulated into biobased polymeric nanoparticles. This high encapsulation efficiency is possible due to the apolar character and low solubility of *Cannabis* extract in the outer aqueous (DE LA OSSA *et al.*, 2013; MARTÍN-BANDERAS, L. *et al.*, 2015).

In the works of La Ossa *et al.* 2013, CBD and THC were encapsulated in PLC microparticles with high efficiency (> 98%). The amount of CBD for 100 mg of the polymer was around 3 to 26 mg. For THC it was about 8 to 33 mg. These cannabinoid concentrations in microparticles were able to inhibit the growth of cancer cell lines (DE LA OSSA *et al.*, 2013; HERNAN PEREZ DE LA OSSA *et al.*, 2012).

Martín-Banderas *et al.* 2015 also worked with encapsulated THC in PLGA nanoparticles. The encapsulation efficiency values (> 95%) enabled a significant selective cytotoxic effect on lung cancer cell lines (MARTÍN-BANDERAS, L. *et al.*, 2015).

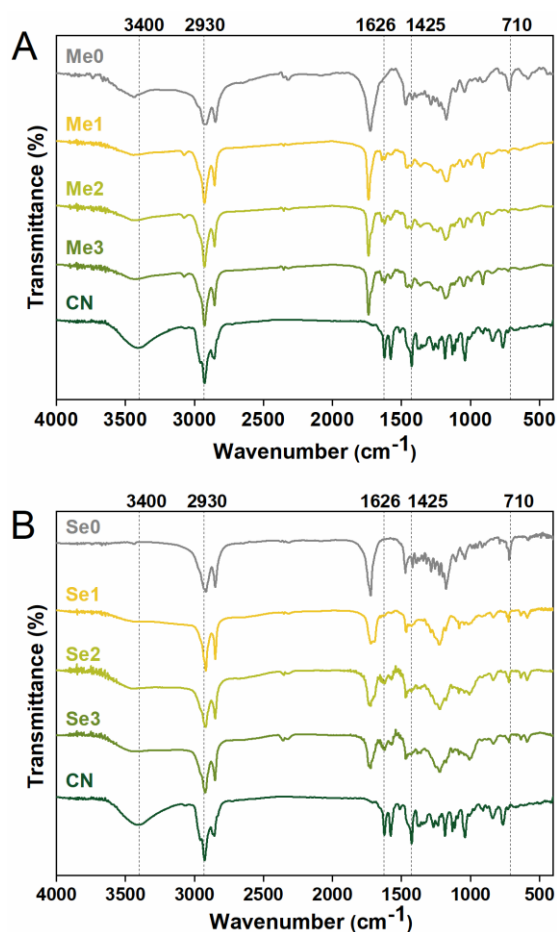
The FTIR spectra of Me-PTEe, Se-PTEe and CN are shown in **Figure 21**. The peak related to double-bond stretching occurs in general at 1640 cm^{-1} , and that peak disappeared indicating the

consumption of the diene monomer (DOS SANTOS, PAULA C. M. *et al.*, 2019). The band related to the C=O group of the esters appears in the range from 1750 cm^{-1} to 1735 cm^{-1} . The addition of thiol radicals at 710 cm^{-1} (C-S-C stretching) could be observed, demonstrating that the thiol-ene reaction occurred in both polymerization techniques (CARDOSO *et al.*, 2018).

The full-spectrum *Cannabis* extract presented characteristic peaks of the O-H groups (3400 cm^{-1}) and alkyl C-H groups (2926 cm^{-1}). In addition, the spectral region showed C-H bending (scissoring) in alkyl groups (1425 cm^{-1}) and C=C stretching in alkene (1626 cm^{-1}) (DORADO *et al.*, 2001; HAZEKAMP, 2007).

After the incorporation of CN in PTEe nanoparticles, in both techniques, the FTIR spectra had a small variation. The C=C (1626 cm^{-1}) band appeared suggesting that there was an interaction between the CN and the polymer, indicating that CN probably was not molecularly dispersed in the polymer matrix.

Figure 21- FTIR spectrum of CN and CN loaded (A)Me-PTEe and (B)Se-PTEe polymeric nanoparticles.



Source: Author.

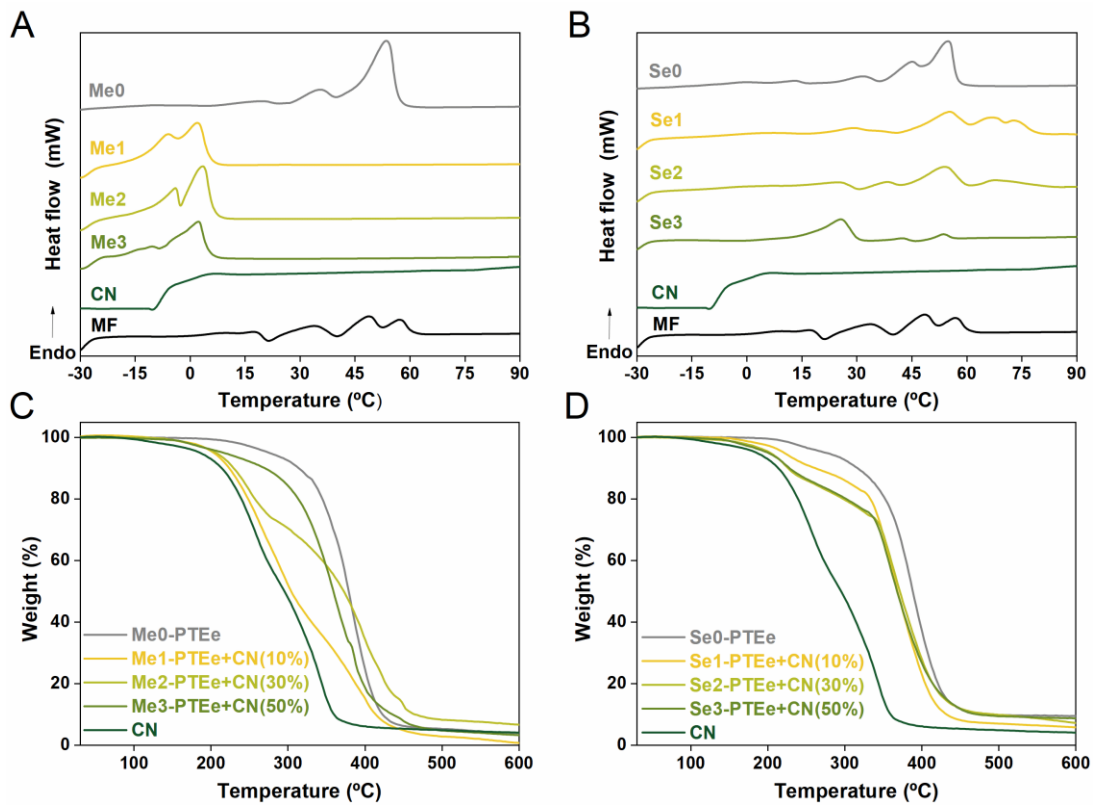
Nanoparticles were also evaluated by thermal analysis, DSC and TGA (**Figure 22**). For Se-PTEe DSC analysis the endothermic peak corresponding to T_m was observed between 40° and 60°C, with a double-melting point behavior. In general, a double-melting point behavior reveals that the polymers first undergo a melting process (increasing chain mobility) and leading to a re-crystallization, followed by a second melting point. This is a feature of semicrystalline polymers (TÜRÜNÇ, OĞUZ; MEIER, 2010). The same behavior of T_m was also observed in a previous work by Freire *et al.*, 2020 with the same polymer (FREIRE *et al.*, 2020).

In the case of Me-PTEe, when CN was added to the formulation, the T_m value of the polymer changed. The T_m decreased for the same value of the first thermal event that occurs in the pure full-spectrum *Cannabis* extract. Apparently, the *Cannabis* extract is acting as a plasticizer of the polymer. This plasticizer effect of *Cannabis* has been previously detected in PLGA (poly-lactic-co-glycolic acid) and PCL (poly- ϵ -caprolactone) microparticles loaded with CBD (FRAGUAS-SÁNCHEZ *et al.*, 2020; HERNAN PEREZ DE LA OSSA *et al.*, 2012). Munjal *et al.* 2006 revealed that the T_g of THC is approximately 7.6°C. The absence of any melting peak suggests that the substance is not crystalline. Low T_g is indicative of the large mobility of a molecule which can undergo chemical interactions or reactions leading to degradation (MANISH MUNJAL, STEVEN P. STODGHILL, MAHMOUD A. ELSOHLY, 2006).

The plasticizers usually improve the flexibility and processability of polymers. They reduce polymer-polymer chain secondary bonding and provide more mobility for the macromolecules (RAHMAN; BRAZEL, 2004).

The plasticizer effect of CN is probably occurring during the *in situ* miniemulsion polymerization. Here the monomer undergoes polymerization at the same time as the drug is encapsulated, in a single step (ASUA, 2002; LANDFESTER, KATHARINA *et al.*, 1999). A physical mixture of the dried polymer and CN (1:1) was analyzed. In this case, the value of T_m does not undergo variation.

Figure 22- Differential Scanning Calorimetry-DSC: (A) Me-PTEe and (B) Se-PTEe. Thermogravimetry analysis-TGA: (C) Me-PTEe and (D) Se-PTEe. Physical mix (1:1) of PTEe and CN.



Source: Author.

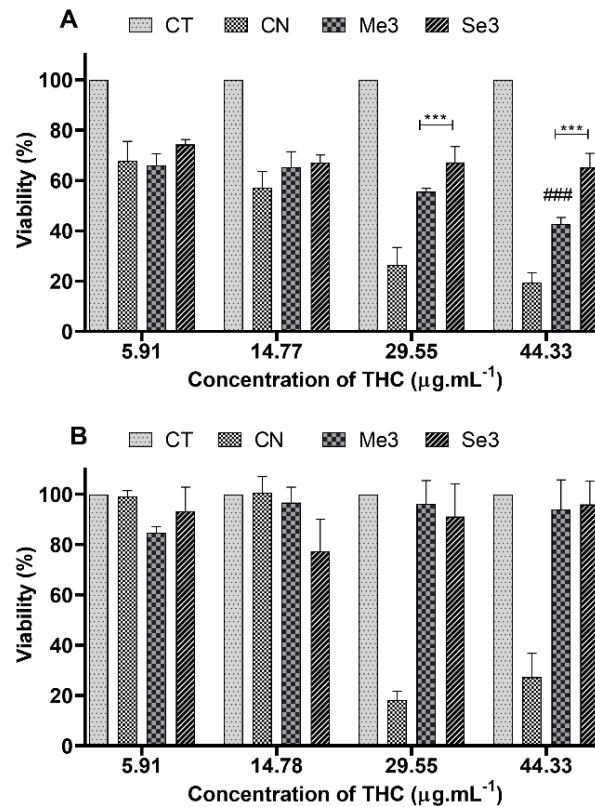
Only one main degradation stage was observed in the TGA analyses of the PTEe nanoparticles without *Cannabis* extract, which occurred between 350 and 400 °C, for both nanoparticle preparation approaches. Vandenberg *et al.*, 2012 observed a similar thermal degradation behavior of poly(β -thioether ester) when 1,6-hexanediol diacrylate was used as the diene monomer and a dithiol as comonomer (VANDENBERGH; RANIERI; JUNKERS, 2012).

For pure CN, the degradation temperature started around 200°C, as observed by Munjal *et al.* 2006 for THC (begins to decompose at 170°C and that the onset for rapid degradation is 200°C) (MANISH MUNJAL, STEVEN P. STODGHILL, MAHMOUD A. ELSOHLY, 2006). When CN was added to the formulations, the polymer thermal properties changed. The CN is acting as a plasticizer of the polymer, changing the thermal properties, as can be seen in DSC analysis. The temperature of degradation decreased because of the bond ruptures of *Cannabis* constituents, which break up with lower thermal energies. The thermal energy absorbed by the cannabis molecules increases their kinetic motion and vibration.

4.5.3 CYTOTOXICITY

After completing the characterization of CN nanoparticles described in the previous section, the effect of free and encapsulated (in PTEe nanoparticles) CN on the viability of three different cancer cell lines (B16F10, T98, U87) and one non-transformed (NIH3T3) cell line was analyzed. As shown in **Figure 22A**, treatment with free and encapsulated CN reduced the viability of B16F10 cells. Of note, the free CN extract induced cell death in a concentration-dependent-manner and presented a more pronounced cytotoxic effect than the encapsulated CN for both PTEe nanoparticles. In NIH3T3 cells (**Figure 22B**) free CN presented a significant cytotoxic effect at concentration of 29.55 and 44.33 $\mu\text{g}\cdot\text{ml}^{-1}$ of THC. On the other hand, CN encapsulated in both PTEe nanoparticles did not induce any cytotoxic effect on the NIH3T3 cells (chosen as no tumor model). The cytotoxic experiment has also been carried out equivalent to THC concentration in B16F10, T98 and U87 cells. Notably, CN encapsulated in Se3 PTEe nanoparticles shows cytotoxic activity in a concentration-dependent-manner (**Figure A.5 A-C**). As control, we observed that empty PTEe nanoparticles did not induce any cytotoxic effect. These results indicate that CN encapsulated in PTEe nanoparticles produced a cytotoxic effect in different cancer cell lines, but not in no transform cells. The study of the cytotoxicity profile of the novel drug nanocarriers using different cell lines is extremely important for the development of a new drug platform (KUCUKSAYAN *et al.*, 2021).

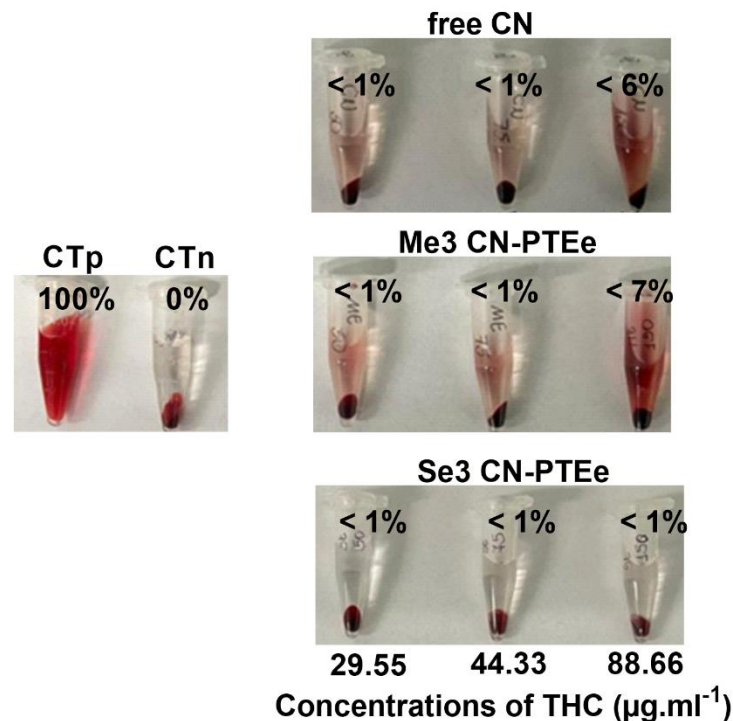
Figure 23- B16F10 (A) and NIH3T3 (B) cells. In vitro cytotoxicity assay of free CN and CN encapsulated in PTEe nanoparticles, Se3 and Me3. Significant differences are shown *** $p < 0.0001$; **** $p < 0.00001$ - compared to the CN group and # $p < 0.01$; ##### $p < 0.00001$ - compared to the CT group - Two-way ANOVA followed by Tukey test).



Source: Author.

The cytotoxic activity of free CN and CN encapsulated in PTEe nanoparticles was also evaluated in human red blood cells (erythrocytes). As shown in **Figure 24**, free CN and PTEe nanoparticles did not present significant damage ($< 1\%$) to the human erythrocytes. Considering that the nanoparticles can have long circulation times in the bloodstream, hemocompatibility studies are extremely important to evaluate any damage to the human erythrocytes (FEUSER, PAULO EMILIO; BUBNIAK; *et al.*, 2016; PLENAGL *et al.*, 2019). The non-cytotoxicity of nanoparticles, when exposed to non-tumor cells, is a strong indication of obtaining a biocompatible and effective nanocarrier for the CN delivery to target cells with minimal toxic effect.

Figure 24- Hemolysis assay on human erythrocytes upon incubation with 10, 20 and 30 nm GNPs solutions at different concentrations. Data represent mean \pm SD (n = 3).

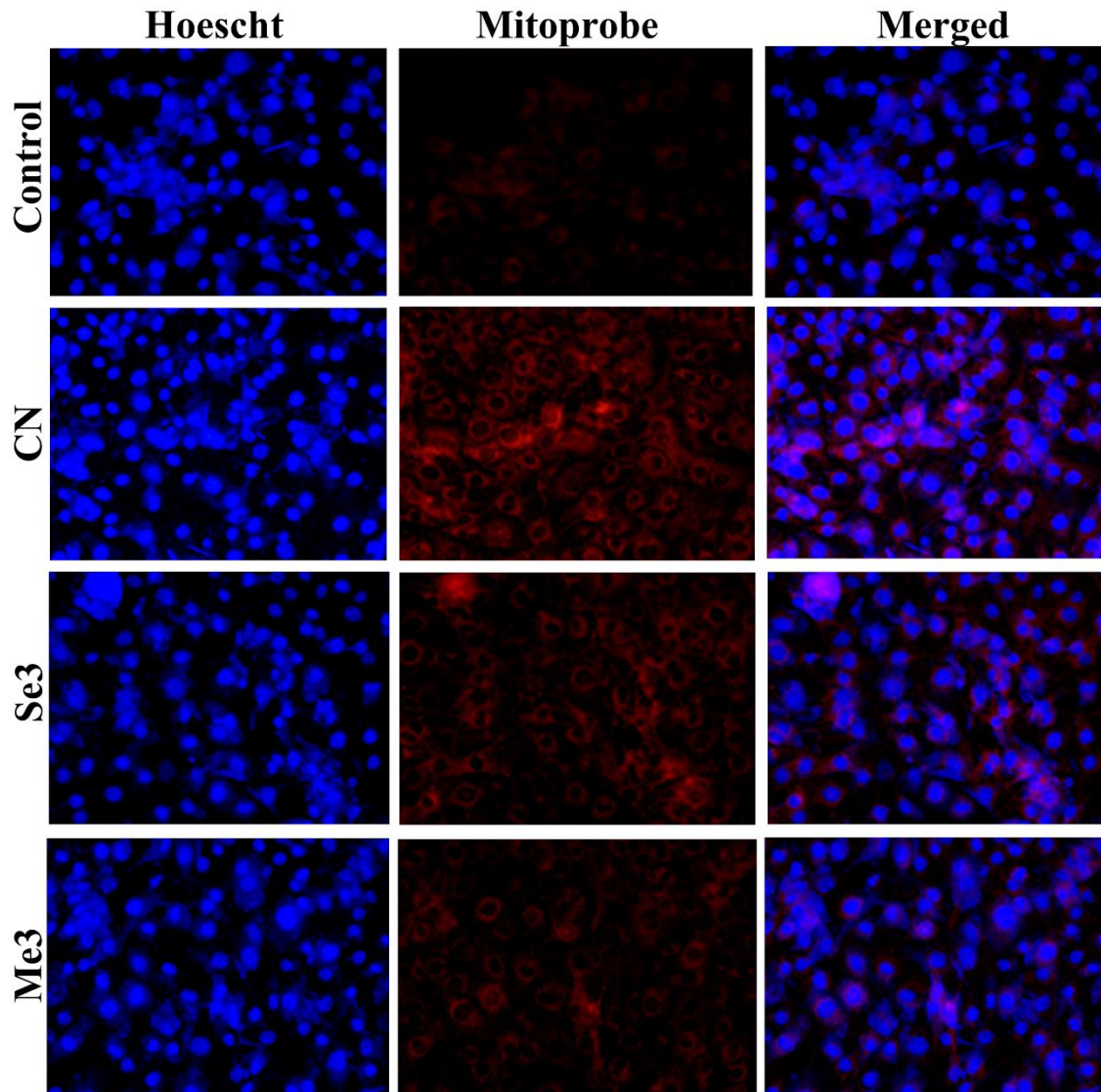


Source: Author.

4.5.4 MITOCHONDRIAL MEMBRANE POTENTIAL AND APOPTOSIS

The mitochondrial membrane potential was determined to evaluate the state of mitochondrial health when B16F10 cells were exposed for 24h with free CN and CN encapsulated in PTEe nanoparticles (Me3 and Se3). As can be observed in **Figure 25**, all treatments led to membrane hyperpolarization, triggering B16F10 cell death *via* apoptosis. The correct regulation of the mitochondrial membrane potential is related to the proper functioning of cells (MATO; VICTORIA SÁNCHEZ-GÓMEZ; MATUTE, 2010). Studies show that *Cannabis* extract is able to change the voltage of channels for calcium, consequently, deregulate intracellular calcium levels and membrane electrical potential (CHAN, JOHN ZEWEN; DUNCAN, 2021). Because of this, there is a higher incidence of calcium in the cell environment, causing hyperpolarization in the mitochondrial plasma membrane and this dysregulation causes cell death by apoptosis (MATO; VICTORIA SÁNCHEZ-GÓMEZ; MATUTE, 2010; OLIVAS-AGUIRRE *et al.*, 2021).

Figure 25- Effects of free CN and CN encapsulated in PTEe nanoparticles (Se3 and Me3) on the mitochondrial membrane potential of B16F10 cells. Cells were stained with TMRM and Hoescht and analyzed by fluorescence microscopy.

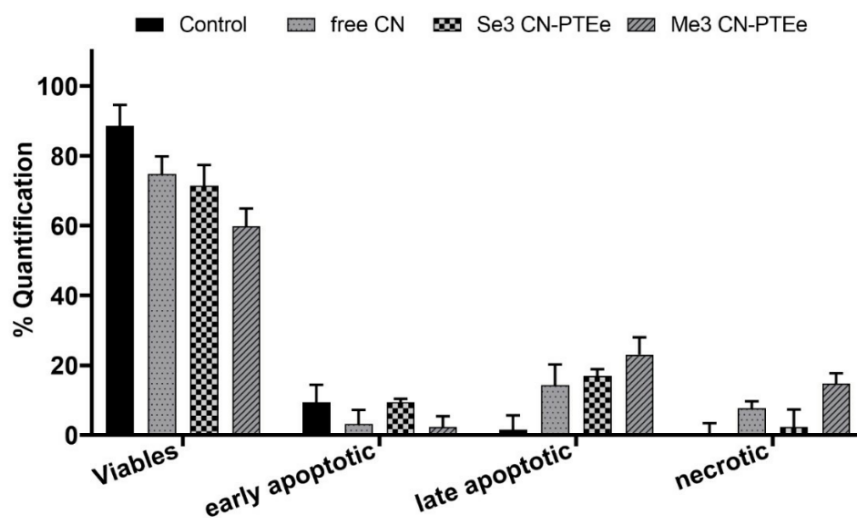


Source: Author.

Apoptosis induced by the free CN and CN encapsulated in PTEe nanoparticles was confirmed by flow cytometry analysis (**Figure 25 and A.6**). As can be seen in **Figure 25**, there was no statistical difference between free CN and CN encapsulate in PTEe nanoparticles (Se3 and Me3). The B16F10 cell death after treatment with free CN and CN encapsulate in PTEe nanoparticles was preferably induced by apoptosis. Other studies have also shown that *Cannabis* extracts used in different tumor cell lines induced apoptotic cell death (ABRAMS, D. I.; GUZMAN, 2014; NUGENT *et al.*, 2020). The melanoma cell line B16 has been shown

to express endocannabinoid receptors which, when active Δ^9 -THC tend to inhibit the cellular growth (BLÁZQUEZ *et al.*, 2006; SELTZER *et al.*, 2020). *Cannabis* selectively acts on tumor cells inducing apoptosis. Thus, treatment with these compounds does not lead to the activation of apoptosis in non-tumor cells (CHAN, JOHN ZEWEN; DUNCAN, 2021; MCALLISTER *et al.*, 2011).

Figure 26- Flow cytometry analysis. B16F10 cells were stained with an Annexin V-FITC and propidium iodide (PI) at different incubation times after treatment with MEL-B at nearly the IC50 concentration. Data are average value \pm standard deviation (n=3).



Source: Author.

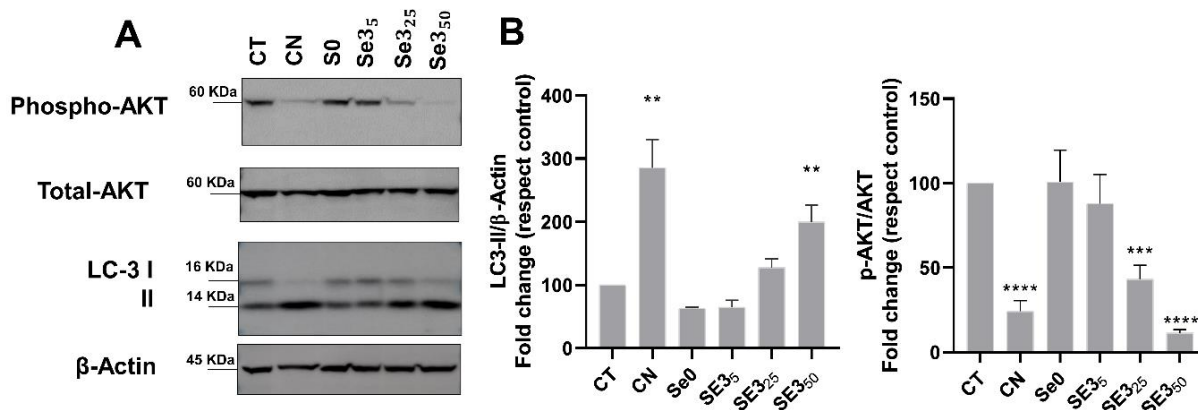
4.5.5 ANALYSIS OF CELL PROLIFERATION AND AUTOPHAGY MARKERS

THC as well as THC-enriched extracts have been shown to promote cancer cell death via inhibition of the AKT/MTORC1 axis, which leads in turn to stimulation of autophagy-mediated cancer cell death (TORRES *et al.*, 2011; VELASCO, G.; SÁNCHEZ; GUZMÁN, 2015; VELASCO, GUILLERMO; SÁNCHEZ; GUZMÁN, 2012). Therefore, we next asked whether the encapsulated extracts could also activate this signaling mechanism. To do this, we evaluated AKT phosphorylation and the levels of the autophagy marker LC3-II by Western blot in BF16F10 cells. We observed that treatment with both free CN and the encapsulated CN induced a drastic reduction in AKT phosphorylation at Ser 473 which was paralleled by the accumulation of LC3-II (the lipidated and autophagosome-associated form of LC3, a well-established readout of autophagy) (**Figure 27A and B**) (KLIONSKY *et al.*, 2021). This

suggests that our nanoformulation inhibited AKT and induced autophagy to a similar extent as free CN.

Like many pharmacological agents that act through specific molecular targets, cannabinoids are expected to engage with cannabinoid receptors and trigger a cascade of events downstream of these receptors that are responsible for their physiological effects in cancer and non cancer cells. In general, since these effects are regulated by the affinity of cannabinoids with their receptors, full activation of the signaling routes downstream of cannabinoid receptors requires reaching certain concentrations of the active principles. Therefore, lower doses of cannabinoids evoke submaximal effects, which explains the dose-dependent effects observed in this and other studies. Regarding the mechanism behind the cytotoxic effect of cannabinoids, previous studies have shown that it is related with the ability to inhibit the AKT/MTORC1 axis and induce autophagy-mediated cancer cell death. In line with this idea, in this study we found that free and encapsulated cannabinoids reduce AKT phosphorylation and induce LC3-II accumulation (two well established hallmarks of AKT inhibition and autophagy activation, respectively). Finally, it is worth pointing out that cannabinoids evoke completely different responses in transformed (cancer) and non-transformed (non-cancer cells). Whereas cannabinoid treatment induces cancer cell death, the administration of these compounds has been shown to produce a protective effect in different primary cultures of non-tumoral cells. Non-tumoral cells that are in any case immortalized (such as the 3T3 fibroblasts employed in this study) exhibit an intermediate sensitivity to cannabinoid-induced cell death. It is postulated that the different metabolic characteristics of cancer and non cancer cells, together with the presence in the former of genetic alterations that are not present in non-cancer cells, could be responsible for this differential sensitivity to cannabinoid treatment.

Figure 27- (A) BF16F10 melanoma cells were seeded in 60-mm diameter culture dishes, incubated overnight, and treated with free CN and CN encapsulated in PTEe nanoparticles (Se3) for 24 h at the concentrations indicated (5, 25, 50 $\mu\text{g}\cdot\text{mL}^{-1}$). Whole-cell extracts were processed for Western blot analysis of the indicated antibodies. β -Actin protein levels in the same extract were used as a control loading. Data are average value \pm standard deviation ($n = 5$). For statistical analysis we performed unpaired t test $**p < 0.01$; $***p = 0.0001$; $****p < 0.0001$. The bands shown in Figure 9A were scanned as digital peaks and the areas of the peaks were reported as fold induction in percentage respect to the vehicle (CT), as described in Material and Methods.



Source: Author.

4.6 CONCLUSIONS

A fully renewable α,ω -diene monomer derived from castor oil (1,3-propylene diundec-10-enoate) was successfully used in thiol-ene polymerization reactions to obtain nanoparticles by miniemulsion polymerization or emulsification/evaporation containing a full-spectrum *Cannabis* extract enriched in THC. The nanoparticles presented an average diameter between 91 - 229 nm and a high encapsulation efficiency ($> 97\%$). The thermal analysis of nanoparticles revealed that the *Cannabis* extract is acting as a plasticizer of the polymer, changing its thermal properties and also the onset of polymer degradation, as can be analyzed by TGA. The FTIR showed that CN probably was not molecularly dispersed in the polymer matrix and the GPC results demonstrated a decrease in the molecular weight, when increasing the CN concentration, in the miniemulsification formulation (Me-PTEe). The biological evaluation of such

nanostructures indicated that encapsulation of CN in PTEe nanoparticles preserved the capacity of CN to promote the apoptotic death of B16F10 melanoma cells as well as exerted strong cytotoxicity in U87 and T98 glioma cells, whereas it did not produce a significant impact on the viability of NIH3T3 cells (a model of non-tumoral cells). Also, further studies revealed that the nanostructures were able to inhibit the phosphorylation of AKT, and induce LC-3 II accumulation in BF16F10 melanoma. These results are in line with a previous observation that suggested that THC and THC-enriched extracts stimulate autophagy-mediated apoptosis in cells and suggest that a similar mechanism may operate for the THC-enriched full spectrum encapsulated *Cannabis* extract studied here. Overall results presented in this work indicate that this method of encapsulation could be effective as a nanocarrier for CN delivery that could be explored in cannabinoid-based anticancer therapies.

Chapter 5

5.0 FINAL CONSIDERATIONS

5.1 CONCLUSIONS

The necessity of releasing the polymer industry from its dependence on non-renewable resources represents a significant concern. In this way, vegetable oils represent one of the most interesting renewables classes for synthesizing sustainable monomers and polymers that can be applied for biomedical as nanoparticles containing active pharmaceutical ingredients for anticancer therapy. The objective of this research project was to study the synthesis of biobased polymeric nanoparticles containing active pharmaceutical ingredients for use as antitumor therapy.

In the first step of the present work, a renewable α,ω -diene diester monomer was efficiently produced by esterification of 10-undecenoic acid and 1,3-propanediol, derived from castor oil. Two different thiols, containing two and four thiols groups per molecule, were employed as comonomers, 1,4-butanedithiol (dithiol, molar ratio 1:1 dithiol/diene) and 3-mercaptopropionate (tetrathiol, molar ratio 1:2 tetrathiol/diene) to produce nanoparticle of poly(thioether-ester) loaded zinc phthalocyanine by thiol-ene *in situ* miniemulsion technique. Nanoparticles obtained presented an intensity average diameter of around 120 - 160 nm with a high encapsulation efficiency of ZnPc (> 98%). The ZnPc was molecularly dispersed in the polymeric matrix based on FTIR and thermal analysis. The release studies showed an initial burst effect followed by a slow-release rate of ZnPc loaded in PTEe nanoparticles. The analysis of cytotoxicity showed that the PTEe nanoparticles protect blood cells against ZnPc decreasing hemolytic damages and confirming the phototoxic effect on the cancer cell line (MDA-MB231).

In the second stage of the work, full-spectrum *Cannabis* extract was used for the encapsulation studies in the polymer poly(thioether-ester), with dithiol as comonomer, through thiol-ene *in situ* miniemulsion and solvent evaporation technique. In the case of the solvent evaporation technique, the polymer was synthesized by bulk polymerization technic. The nanoparticles containing full-spectrum *Cannabis* extract were characterized in relation to particle size and dispersion, surface load by zeta potential, gel permeation chromatography, transmission electron microscopy, thermal analyses, encapsulation efficiency and biological *in*

vitro studies. The nanoparticles presented an average diameter between 91 - 229 nm and high encapsulation efficiency (> 97%). The thermal analysis of nanoparticles revealed that the *Cannabis* extract is probably acting as a plasticizer of the polymer, changing its thermal properties as the extract was probably not molecularly dispersed in the polymer matrix. Also, the molecular weight decreased when the concentration of the CN was increased. The cytotoxicity study indicated that encapsulation of the extract in PTEe nanoparticles preserved the capacity to promote the apoptotic death of melanoma (B16F10) and glioma cells (U87 and T98). Also, did not produce a significant impact on the viability of non-tumoral cells.

Overall results presented in this work indicate that PTEe nanoparticles can be used as an effective nanocarrier for APIs delivery in anticancer therapies. The possibility of using castor oil as a renewable raw material to replace fossil-based raw material appears to be one of the strengths of the work. In addition, the use of the *in situ* miniemulsion polymerization for the encapsulation of both zinc phthalocyanine and full-spectrum *Cannabis* extract enables the production of particles and encapsulation of the actives in a single moment. It is also worth highlighting the great therapeutic potential of the full-spectrum *Cannabis* extract, still, little documented in scientific bibliography loaded polymeric nanoparticles, and so far, not produced by *in situ* techniques.

5.2 RECOMMENDATIONS FOR FUTURE WORK

- To synthesize PTEe nanoparticles with other kinds of APIs for biomedical applications.
- To study the synergism effect of combined APIs loaded in PTEe nanoparticles.
- To investigate the functionalization of PTEe nanoparticles for delivery at targeted spots.
- To extend the biological assays to *in ovo* and *in vivo* analysis to understand the action of nanoparticles for cancer treatments.
- To analyze the biodegradation of the PTEe nanoparticles by hydrolysis of the ester group in the main chain.

Chapter 6

6.0 REFERENCES

ABRAMS, D. I.; GUZMAN, M. Cannabis in Cancer Care. *Clinical Pharmacology and Therapeutics*, v. 97, n. 6, p. 575–586, 2014.

ABRAMS, Donald I. *et al.* Cancer Treatment: Preclinical & Clinical. *Journal of the National Cancer Institute - Monographs*, v. 2021, n. 58, p. 107–113, 2021.

ADAMS, Robert P. *Identification of essential oil components by gas chromatography/mass spectroscopy*. [S.l.]: Allured Pub. Corp, 2007.

AGGARWAL, S., YADAV, S. & GUPTA, S. EGFR targeted PLGA nanoparticles using gemcitabine for treatment of pancreatic cancer. *J. Biomed. Nanotechnol.*, v. 7, p. 137–138, 2011.

AHLIN GRABNAR, Pegi; KRISTL, Julijana. The manufacturing techniques of drug-loaded polymeric nanoparticles from preformed polymers. *Journal of Microencapsulation*, v. 28, n. 4, p. 323–335, 2011.

ALEXANDER, Stephen P H. Progress in Neuro-Psychopharmacology & Biological Psychiatry Therapeutic potential of cannabis-related drugs ☆. *Progress in Neuropsychopharmacology & Biological Psychiatry*, v. 64, p. 157–166, 2016. Disponível em: <<http://dx.doi.org/10.1016/j.pnpbp.2015.07.001>>.

ALVES, Rômulo C. *et al.* Cationic miniemulsion polymerization of styrene mediated by imidazolium based ionic liquid. *European Polymer Journal*, v. 104, p. 51–56, jul. 2018.

ANTONIETTI, Markus; LANDFESTER, Katharina. Polyreactions in miniemulsions. *Progress in Polymer Science (Oxford)*, v. 27, n. 4, p. 689–757, 2002.

APARICIO-BLANCO, Juan *et al.* Lipid nanocapsules decorated and loaded with cannabidiol as targeted prolonged release carriers for glioma therapy: In vitro screening of critical parameters. *European Journal of Pharmaceutics and Biopharmaceutics*, v. 134, n. November 2018, p. 126–137, 2019.

ARAVIND, A. et al. Aptamer conjugated paclitaxel and magnetic fluid loaded fluorescently tagged PLGA nanoparticles for targeted cancer therapy. *J. Magn. Magn. Mater.*, v. 344, p. 116–123, 2013.

ASUA, Jose M. Miniemulsion polymerisation. *Prog. Polym. Sci.*, v. 27, p. 1283–1346, 2002.

ATAKAN, Zerrin. Cannabis, a complex plant: Different compounds and different effects on individuals. *Therapeutic Advances in Psychopharmacology*, v. 2, n. 6, p. 241–254, 2012.

BAGHERZADEH-KHAJEHMARJAN, Elnaz *et al.* Morphology enhancement of self-assembled CH₃NH₃PbI₃ nanoparticles through customized solvent evaporation temperatures. *Journal of Crystal Growth*, v. 601, n. November 2022, p. 126970, 2023. Disponível em: <<https://doi.org/10.1016/j.jcrysgro.2022.126970>>.

BARAKAT, Nahla S.; ELBAGORY, Ibrahim M.; ALMURSHEDI, Alanood S. Controlled-release carbamazepine matrix granules and tablets comprising lipophilic and hydrophilic components. *Drug Delivery*, v. 16, n. 1, p. 57–65, 2009.

BELGACEM, Mohamed; GANDINI, Alessandro. *Monomers, Polymers and Composites from Renewable Resources*. [S.l.: s.n.], 2008. Disponível em: <<http://www.sciencedirect.com/science/article/pii/B9780080453163000132>>.

BERNARDY, Neusa *et al.* Nanoencapsulation of quercetin via miniemulsion polymerization. *Journal of Biomedical Nanotechnology*, v. 6, n. 2, p. 181–186, 2010.

BERROCOSO, Esther *et al.* Single oral dose of cannabinoid derivate loaded PLGA nanocarriers relieves neuropathic pain for eleven days. *Nanomedicine: Nanotechnology, Biology, and Medicine*, v. 13, n. 8, p. 2623–2632, 2017. Disponível em: <<https://doi.org/10.1016/j.nano.2017.07.010>>.

BIERMANN, Ursula *et al.* Oils and Fats as Renewable Raw Materials in Chemistry. *Angewandte Chemie International Edition*, v. 50, n. 17, p. 3854–3871, 2011. Disponível em: <<http://doi.wiley.com/10.1002/anie.201002767>>.

BIZZO, Humberto R. *et al.* A set of electronic sheets for the identification and quantification of constituents of essential oils. *Quimica Nova*, v. 43, n. 1, p. 98–105, 1 jan. 2020.

BLASCO-BENITO, Sandra *et al.* Appraising the “entourage effect”: Antitumor action of a pure

cannabinoid versus a botanical drug preparation in preclinical models of breast cancer. *Biochemical Pharmacology*, v. 157, n. May, p. 285–293, 2018.

BLÁZQUEZ, Cristina *et al.* Cannabinoid receptors as novel targets for the treatment of melanoma. *The FASEB Journal*, v. 20, n. 14, p. 2633–2635, 2006.

BOLFARINI, Gisele C. *et al.* In vitro evaluation of combined hyperthermia and photodynamic effects using magnetoliposomes loaded with cucurbit. *Journal of Photochemistry and Photobiology B: Biology*, v. 115, p. 1–4, 2012.

BORGES, Gabriela Ramos *et al.* Simple and straightforward analysis of cannabinoids in medicinal products by fast-GC–FID. *Forensic Toxicology*, v. 38, n. 2, p. 531–535, 2020. Disponível em: <<https://doi.org/10.1007/s11419-020-00522-1>>.

BRIGHENTI, Virginia *et al.* Journal of Pharmaceutical and Biomedical Analysis Development of a new extraction technique and HPLC method for the analysis of non-psychoactive cannabinoids in fibre-type Cannabis. *Journal of Pharmaceutical and Biomedical Analysis*, v. 143, p. 228–236, 2017. Disponível em: <<http://dx.doi.org/10.1016/j.jpba.2017.05.049>>.

BRITANNICA. *Anticancer drug*. Disponível em: <<https://www.britannica.com/science/anticancer-drug>>. Acesso em: 10 jun. 2020a.

BRITANNICA. *Green chemistry*. Disponível em: <<https://www.britannica.com/science/green-chemistry>>. Acesso em: 19 maio 2020b.

CALORI, Italo Rodrigo *et al.* Theoretical and experimental studies concerning monomer/aggregates equilibrium of zinc phthalocyanine for future photodynamic action. *Spectrochimica Acta - Part A: Molecular and Biomolecular Spectroscopy*, v. 214, p. 513–521, 2019.

CARDOSO, Priscilla B. *et al.* Biocompatible Polymeric Nanoparticles From Castor Oil Derivatives via Thiol-Ene Miniemulsion Polymerization. *European Journal of Lipid Science and Technology*, v. 120, n. 1, p. 1–8, 2018.

CARVALHO, Virgínia *et al.* QUANTIFICAÇÃO DE CANABINOIDES EM EXTRATOS MEDICINAIS DE Cannabis POR CROMATOLOGRAFIA LÍQUIDA DE ALTA EFICIÊNCIA. *Química Nova*, v. 43, n. 1, p. 90–97, 2020.

CHÁIREZ-RAMÍREZ, M. H. et al. Morphological and release characterization of nanoparticles formulated with poly (dl-lactide-co-glycolide) (PLGA) and lupeol: In vitro permeability and modulator effect on NF- κ B in Caco-2 cell system stimulated with TNF- α . *Food Chem. Toxicol.*, 2015.

CHAN, J. M. et al. PLGA-lecithin-PEG core-shell nanoparticles for controlled drug delivery. *Biomaterials*, v. 30, p. 1627–1634, 2009.

CHAN, John Zewen; DUNCAN, Robin Elaine. Regulatory effects of cannabidiol on mitochondrial functions: A review. *Cells*, v. 10, n. 5, 2021.

CHAN, Zhang *et al.* Folate-mediated poly(3-hydroxybutyrate-co-3-hydroxyoctanoate) nanoparticles for targeting drug delivery. *European Journal of Pharmaceutics and Biopharmaceutics*, v. 76, n. 1, p. 10–16, 2010.

CHAUHAN, Nidhi *et al.* An electrochemical sensor for detection of neurotransmitter-acetylcholine using metal nanoparticles, 2D material and conducting polymer modified electrode. *Biosensors and Bioelectronics*, v. 89, p. 377–383, 2017. Disponível em: <<http://dx.doi.org/10.1016/j.bios.2016.06.047>>.

CHEN, Chih Kuang *et al.* Biodegradable cationic polymeric nanocapsules for overcoming multidrug resistance and enabling drug-gene co-delivery to cancer cells. *Nanoscale*, v. 6, n. 3, p. 1567–1572, 2014.

CHEN, H. et al. Preparation and characterization of PE38KDEL-loaded anti-HER2 nanoparticles for targeted cancer therapy. *J. Control. Release*, v. 128, p. 209–216, 2008.

CHERNIAKOV, Irina *et al.* The effect of Pro NanoLipospheres (PNL) formulation containing natural absorption enhancers on the oral bioavailability of delta-9-tetrahydrocannabinol (THC) and cannabidiol (CBD) in a rat model. *European Journal of Pharmaceutical Sciences*, v. 109, n. July, p. 21–30, 2017.

CHITTASUPHO, C., LIRDPRAPAMONGKOL, K., KEWSUWAN, P. & SARISUTA, N. Targeted delivery of doxorubicin to A549 lung cancer cells by CXCR4 antagonist conjugated PLGA nanoparticles. *Eur. J. Pharm. Biopharm.*, 2014.

CHITTASUPHO, C. et al. ICAM-1 targeting of doxorubicin-loaded PLGA nanoparticles to

lung epithelial cells. *Eur. J. Pharm. Sci.*, v. 37, p. 141–150, 2009.

CHO, Wan Seob *et al.* Surface functionalization affects the zeta potential, coronal stability and membranolytic activity of polymeric nanoparticles. *Nanotoxicology*, v. 8, n. 2, p. 202–211, 2014.

CIOLINO, Laura A.; RANIERI, Tracy L.; TAYLOR, Allison M. Commercial cannabis consumer products part 1: GC–MS qualitative analysis of cannabis cannabinoids Laura. *Forensic Science International*, v. 289, p. 438–447, 2018a.

CIOLINO, Laura A.; RANIERI, Tracy L.; TAYLOR, Allison M. Commercial cannabis consumer products part 2: HPLC-DAD quantitative analysis of cannabis cannabinoids. *Forensic Science International*, v. 289, p. 438–447, 2018b.

CIRPANLI, Y., BILENSOY, E., LALE DOĞAN, A & CALIŞ, S. Comparative evaluation of polymeric and amphiphilic cyclodextrin nanoparticles for effective camptothecin delivery. *Eur. J. Pharm. Biopharm.*, v. 73, p. 82–9, 2009.

CITTI, Cinzia *et al.* Analysis of cannabinoids in commercial hemp seed oil and decarboxylation kinetics studies of cannabidiolic acid (CBDA). *Journal of Pharmaceutical and Biomedical Analysis*, v. 149, p. 532–540, 2018.

COSTA, Cristiane *et al.* Compartmentalization effects on miniemulsion polymerization with oil-soluble initiator. *Macromolecular Reaction Engineering*, v. 7, n. 5, p. 221–231, 2013.

COSTA, P; SOUSA LOBO, J M. Modeling and comparison of dissolution profiles. *European journal of pharmaceutical sciences: official journal of the European Federation for Pharmaceutical Sciences*, v. 13, n. 2, p. 123–33, maio 2001.

CUI, Y., XU, Q., CHOW, P. K.-H., WANG, D. & WANG, C.-H. Transferrin-conjugated magnetic silica PLGA nanoparticles loaded with doxorubicin and paclitaxel for brain glioma treatment. *Biomaterials*, v. 34, p. 8511–20, 2013.

DA VOLTA SOARES, Mariana *et al.* Nanostructured delivery system for zinc phthalocyanine: preparation, characterization, and phototoxicity study against human lung adenocarcinoma A549 cells. *International journal of nanomedicine*, v. 6, p. 227–238, 2011.

DANHIER, F. *et al.* Targeting of tumor endothelium by RGD-grafted PLGA-nanoparticles.

Methods Enzymol., v. 508, p. 157–175, 2012.

DANHIER, Fabienne *et al.* Paclitaxel-loaded PEGylated PLGA-based nanoparticles: In vitro and in vivo evaluation. *Journal of Controlled Release*, v. 133, n. 1, p. 11–17, 2009.

DANHIER, Fabienne; FERON, Olivier; PRÉAT, Véronique. To exploit the tumor microenvironment: Passive and active tumor targeting of nanocarriers for anti-cancer drug delivery. *Journal of Controlled Release*, v. 148, n. 2, p. 135–146, dez. 2010.

DE BACKER, Benjamin *et al.* Innovative development and validation of an HPLC/DAD method for the qualitative and quantitative determination of major cannabinoids in cannabis plant material. *Journal of Chromatography B: Analytical Technologies in the Biomedical and Life Sciences*, v. 877, n. 32, p. 4115–4124, 2009.

DE LA OSSA, Dolores Hernán Pérez *et al.* Preparation and characterization of delta9-tetrahydrocannabinol-loaded biodegradable polymeric microparticles and their antitumoral efficacy on cancer cell lines. *Journal of Drug Targeting*, v. 21, n. 8, p. 710–718, 2013.

DE MELLO, Vanessa Azevedo; RICCI-JÚNIOR, Eduardo. Encapsulation of naproxen in nanostructured system: Structural characterization and in Vitro release studies. *Quimica Nova*, v. 34, n. 6, p. 933–939, 2011.

DE OLIVEIRA DE SIQUEIRA, Luciana Betzler *et al.* Development and evaluation of zinc phthalocyanine nanoemulsions for use in photodynamic therapy for *Leishmania* spp . *Nanotechnology*, v. 28, n. 6, p. 065101, 2017. Disponível em: <<http://stacks.iop.org/0957-4484/28/i=6/a=065101?key=crossref.d4efe2383ff6a13ee1443b5d91849090>>.

DEDA, Daiana K. *et al.* A new micro/nanoencapsulated porphyrin formulation for PDT treatment. *International Journal of Pharmaceutics*, v. 376, n. 1–2, p. 76–83, 2009.

DEIDDA, Riccardo *et al.* Analytical quality by design: Development and control strategy for a LC method to evaluate the cannabinoids content in cannabis olive oil extracts. *Journal of Pharmaceutical and Biomedical Analysis*, v. 166, p. 326–335, 2019. Disponível em: <<https://doi.org/10.1016/j.jpba.2019.01.032>>.

DEL RIO, E. *et al.* Polyurethanes from polyols obtained by ADMET polymerization of a castor oil-based diene: Characterization and shape memory properties. *Journal of Polymer Science*,

Part A: Polymer Chemistry, v. 49, n. 2, p. 518–525, 2011.

DERAKHSHANDEH, K., ERFAN, M. & DADASHZADEH, S. Encapsulation of 9-nitrocamptothecin, a novel anticancer drug, in biodegradable nanoparticles: Factorial design, characterization and release kinetics. *Eur. J. Pharm. Biopharm.*, v. 66, p. 34–41, 2007.

DHANA LEKSHMI, U. M. *et al.* In vitro characterization and in vivo toxicity study of repaglinide loaded poly (methyl methacrylate) nanoparticles. *International Journal of Pharmaceutics*, v. 396, n. 1–2, p. 194–203, 2010.

DHAR, S., GU, F. X., LANGER, R., FAROKHZAD, O. C. & LIPPARD, S. J. Targeted delivery of cisplatin to prostate cancer cells by aptamer functionalized Pt(IV) prodrug-PLGA-PEG nanoparticles. *Proc. Natl. Acad. Sci. U. S. A.*, v. 105, p. 7356–7361, 2008.

DHAS, N. L., IGE, P. P. & KUDARHA, R. R. Design, optimization and in-vitro study of folic acid conjugated-chitosan functionalized PLGA nanoparticle for delivery of bicalutamide in prostate cancer. *Powder Technol.*, v. 283, p. 234–245, 2015.

DORADO, José *et al.* Infrared spectroscopy analysis of hemp (*Cannabis sativa*) after selective delignification by *Bjerkandera* sp. at different nitrogen levels. *Enzyme and Microbial Technology*, v. 28, n. 6, p. 550–559, 2001.

DOS REIS ANTUNES JUNIOR, Osmar *et al.* Preparation, physicochemical characterization and antioxidant activity of diphenyl diselenide-loaded poly(lactic acid) nanoparticles. *Journal of Trace Elements in Medicine and Biology*, v. 39, p. 176–185, 2017.

DOS SANTOS, Paula C. M. *et al.* Evaluation of in vitro cytotoxicity of superparamagnetic poly(thioether-ester) nanoparticles on erythrocytes, non-tumor (NIH3T3), tumor (HeLa) cells and hyperthermia studies. *Journal of Biomaterials Science, Polymer Edition*, v. 29, n. 16, p. 1935–1948, 2019.

DURÁN-LOBATO, Matilde *et al.* Comparative study of chitosan- and PEG-coated lipid and PLGA nanoparticles as oral delivery systems for cannabinoids. *Journal of Nanoparticle Research*, v. 17, n. 2, 2015.

DURÁN-LOBATO, Matilde *et al.* Enhanced cellular uptake and biodistribution of a synthetic cannabinoid loaded in surface-modified poly(lactic-co-glycolic acid) nanoparticles. *Journal of*

Biomedical Nanotechnology, v. 10, n. 6, p. 1068–1079, 2014.

EL-SAY, Khalid M.; EL-SAWY, Hossam S. Polymeric nanoparticles: Promising platform for drug delivery. *International Journal of Pharmaceutics*, v. 528, n. 1–2, p. 675–691, 2017. Disponível em: <<http://dx.doi.org/10.1016/j.ijpharm.2017.06.052>>.

F, Masood; P Chen; T Yasin. Encapsulation of Ellipticine in poly- (3-hydroxybutyrate-co-3-hydroxyvalerate) based nanoparticles and its in vitro application. *Mater. Sci. Eng.*, v. 33, p. 1054–106, 2013.

FEUSER, P.E. Paulo Emilio *et al.* Increased cellular uptake of lauryl gallate loaded in superparamagnetic poly(methyl methacrylate) nanoparticles due to surface modification with folic acid. *Journal of Materials Science: Materials in Medicine*, v. 27, n. 12, 2016.

FEUSER, P.E. Paulo Emilio *et al.* Simultaneous encapsulation of magnetic nanoparticles and zinc phthalocyanine in poly(methyl methacrylate) nanoparticles by miniemulsion polymerization and in vitro studies. *Colloids and Surfaces B: Biointerfaces*, v. 135, p. 357–364, 2015.

FEUSER, Paulo Emilio. Encapsulamento Simultâneo de Nanopartículas Magnéticas (NPMS) com Ftalocianina de Zinco (ZNPC) Via Polimerização em Miniemulsão. p. 120, 2012. Disponível em: <<https://repositorio.ufsc.br/handle/123456789/122562>>.

FEUSER, Paulo Emilio; BUBNIAK, Lorena Dos Santos; *et al.* In vitro cytotoxicity of poly(methyl methacrylate) nanoparticles and nanocapsules obtained by miniemulsion polymerization for drug delivery application. *Journal of Nanoscience and Nanotechnology*, v. 16, n. 7, p. 7669–7676, 2016.

FEUSER, Paulo Emilio; GASPAR, Pamela Cristina; *et al.* Synthesis of ZnPc loaded poly(methyl methacrylate) nanoparticles via miniemulsion polymerization for photodynamic therapy in leukemic cells. *Materials Science and Engineering C*, v. 60, p. 458–466, 2016.

FIRDAUS, Maulidan *et al.* Renewable co-polymers derived from castor oil and limonene. *European Journal of Lipid Science and Technology*, v. 116, n. 1, p. 31–36, 2014.

FONSECA, Laís B. *et al.* Production of PMMA Nanoparticles Loaded with Praziquantel Through “In Situ” Miniemulsion Polymerization. *Macromolecular Reaction Engineering*, v. 7,

n. 1, p. 54–63, 2013.

FORNAGUERA, Cristina *et al.* Interactions of PLGA nanoparticles with blood components: protein adsorption, coagulation, activation of the complement system and hemolysis studies. *Nanoscale*, v. 7, n. 14, p. 6045–6058, 2015.

FRAGUAS-SÁNCHEZ, Ana I. *et al.* PLGA nanoparticles for the intraperitoneal administration of CBD in the treatment of ovarian cancer: In vitro and in Ovo assessment. *Pharmaceutics*, v. 12, n. 5, p. 2–3, 2020.

FREIRE, Nathália Freitas *et al.* Zinc phthalocyanine encapsulation via thiol-ene miniemulsion polymerization and in vitro phototoxicity studies. *International Journal of Polymeric Materials and Polymeric Biomaterials*, v. 0, n. 0, p. 1–10, 2020. Disponível em: <<https://doi.org/10.1080/00914037.2020.1838517>>.

GURNY R, PEPPAS NA, HARRINGTON DD, Banker GS. Development of biodegradable and injectable latices for controlled release of potent drugs. *Drug Dev Ind Pharm*, v. 7, p. 1–25, 1981.

HAN, Lei *et al.* Inhibition of C6 glioma in vivo by combination chemotherapy of implantation of polymer wafer and intracarotid perfusion of transferrin-decorated nanoparticles. *Oncology Reports*, v. 27, n. 1, p. 121–128, 2012.

HAO, Da Cheng; GU, Xiao-Jie; XIAO, Pei Gen. *Phytochemical and biological research of Cannabis pharmaceutical resources*. [S.l: s.n.], 2015.

HAZEKAMP, Arno. *Cannabis; extracting the medicine*. [S.l: s.n.], 2007. Disponível em: <<http://hdl.handle.net/1887/12297>>.

HAZEKAMP, Arno *et al.* The Medicinal Use of Cannabis and Cannabinoids-An International Cross-Sectional Survey on Administration Forms. *Journal of Psychoactive Drugs*, v. 45, n. 3, p. 199–210, 2013.

HAZRA, Chinmay *et al.* Colloids and Surfaces A : Physicochemical and Engineering Aspects Size controlled sub-100 nm synthesis , characterization , antibacterial activity , cytotoxicity and sustained drug release behavior. *Colloids and Surfaces A: Physicochemical and Engineering Aspects*, v. 449, p. 96–113, 2014.

HE, Chunbai *et al.* Effects of particle size and surface charge on cellular uptake and biodistribution of polymeric nanoparticles. *Biomaterials*, v. 31, n. 13, p. 3657–3666, maio 2010.

HERNAN PEREZ DE LA OSSA, D. *et al.* Poly- ϵ -caprolactone microspheres as a drug delivery system for cannabinoid administration: Development, characterization and in vitro evaluation of their antitumoral efficacy. *Journal of Controlled Release*, v. 161, n. 3, p. 927–932, 2012. Disponível em: <<http://dx.doi.org/10.1016/j.jconrel.2012.05.003>>.

HERNÁN PÉREZ DE LA OSSA, Dolores *et al.* Local Delivery of Cannabinoid-Loaded Microparticles Inhibits Tumor Growth in a Murine Xenograft Model of Glioblastoma Multiforme. *PLoS ONE*, v. 8, n. 1, 2013.

HERNÁNDEZ-TIEDRA, Sonia *et al.* Dihydroceramide accumulation mediates cytotoxic autophagy of cancer cells via autolysosome destabilization. *Autophagy*, v. 12, n. 11, p. 2213–2229, 2016.

HOELSCHER, Fernanda *et al.* Enzymatically catalyzed degradation of poly (thioether-ester) nanoparticles. *Polymer Degradation and Stability*, v. 156, p. 211–217, 2018.

HOMMOSS, Ghaith; PYO, Sung Min; MÜLLER, Rainer H. Mucoadhesive tetrahydrocannabinol-loaded NLC – Formulation optimization and long-term physicochemical stability. *European Journal of Pharmaceutics and Biopharmaceutics*, v. 117, p. 408–417, 2017. Disponível em: <<http://dx.doi.org/10.1016/j.ejpb.2017.04.009>>.

HONARY, S; ZAHIR, F. Effect of Zeta Potential on the Properties of Nano-Drug Delivery Systems - A Review (Part 2). *Tropical Journal of Pharmaceutical Research*, v. 12, n. 2, p. 265–273, maio 2013.

HOYLE, Charles E.; BOWMAN, Christopher N. Thiol-ene click chemistry. *Angewandte Chemie - International Edition*, v. 49, n. 9, p. 1540–1573, 2010.

HU, Yanfang *et al.* Multi-responsive core-crosslinked poly (thioether ester) micelles for smart drug delivery. *Polymer*, v. 110, p. 235–241, 2017. Disponível em: <<http://dx.doi.org/10.1016/j.polymer.2017.01.019>>.

HUSSEIN, Mohammed T. Study β -phase Zn-Phthalocyanine nanostructure by high accuracy preparation with sublimation method. v. 1, n. 7, p. 137–141, 2011.

JAIDEV, L. R., KRISHNAN, U. M. & SETHURAMAN, S. Gemcitabine loaded biodegradable PLGA nanospheres for in vitro pancreatic cancer therapy. *Mater. Sci. Eng. C. Mater. Biol. Appl.*, v. 47, p. 40–7, 2015.

JAIN, A. K., THANKI, K. & JAIN, S. Co-encapsulation of tamoxifen and quercetin in polymeric nanoparticles: implications on oral bioavailability, antitumor efficacy, and drug-induced toxicity. *Mol. Pharm.*, v. 10, p. 3459–74, 2013.

JAIN, A. et al. Surface engineered polymeric nanocarriers mediate the delivery of transferrin-methotrexate conjugates for an improved understanding of brain cancer. *Acta Biomater.*, v. 24, p. 140–51, 2015.

KAMALI, Amir *et al.* Cannabidiol-loaded microspheres incorporated into osteoconductive scaffold enhance mesenchymal stem cell recruitment and regeneration of critical-sized bone defects. *Materials Science and Engineering C*, v. 101, n. February 2018, p. 64–75, 2019. Disponível em: <<https://doi.org/10.1016/j.msec.2019.03.070>>.

KHAN, Muhammad Muzamil *et al.* Folate targeted lipid chitosan hybrid nanoparticles for enhanced anti-tumor efficacy. *Nanomedicine: Nanotechnology, Biology, and Medicine*, v. 28, p. 102228, 2020. Disponível em: <<https://doi.org/10.1016/j.nano.2020.102228>>.

KHURROO, T. et al. Topotecan–tamoxifen duple PLGA polymeric nanoparticles: Investigation of in vitro, in vivo and cellular uptake potential. *Int. J. Pharm.*, v. 473, p. 384–394, 2014.

KILIÇAY, E. et al. Preparation and characterization of poly(3-hydroxybutyrate-co-3-hydroxyhexanoate) (PHBHHX) based nanoparticles for targeted cancer therapy. *Eur. J. Pharm. Sci.*, v. 44, p. 310–20, 2011.

KLEPAC, Damir *et al.* Interaction of spin-labeled HPMA-based nanoparticles with human blood plasma proteins-the introduction of protein-corona-free polymer nanomedicine. *Nanoscale*, v. 10, n. 13, p. 6194–6204, 2018.

KLIONSKY, Daniel J. *et al.* Guidelines for the use and interpretation of assays for monitoring autophagy (4th edition)1. *Autophagy*, v. 17, n. 1, p. 1–382, 2021.

KOCBEK, P., OBERMAJER, N., CEGNAR, M., KOS, J. & KRISTL, J. Targeting cancer cells using PLGA nanoparticles surface modified with monoclonal antibody. *J. Control. Release*, v.

120, p. 18–26, 2007.

KRATZ, Dec. *A GENERALIZATION OF THE RETENTION INDEX SYSTEM INCLUDING LINEAR TEMPERATURE PROGRAMMED GAS-LI&UID PARTITION CHROMATOGRAPHY I-I. VAN DEN DOOL AND I? JOURNAL OF CHROMATOGRAPHY.* [S.l: s.n.], [S.d.].

KREYE, Oliver; TÓTH, Tommy; MEIER, Michael A R. Poly- α,β -unsaturated aldehydes derived from castor oil via ADMET polymerization. *European Journal of Lipid Science and Technology*, v. 113, n. 1, p. 31–38, 2011.

KUCUKSAYAN, Ertan *et al.* A new combination strategy to enhance apoptosis in cancer cells by using nanoparticles as biocompatible drug delivery carriers. *Scientific Reports*, v. 11, n. 1, p. 1–19, 2021. Disponível em: <<https://doi.org/10.1038/s41598-021-92447-x>>.

KUMAR, Dev; SHAN, Li; ZHANG, Yong. Nanoparticles in photodynamic therapy: An emerging paradigm. *Advanced Drug Delivery Reviews*, v. 60, n. 15, p. 1627–1637, 2008.

LANDFESTER, K. Synthesis of Colloidal Particles in Miniemulsions. *Annual Review of Materials Research*, v. 36, n. 1, p. 231–279, 2006.

LANDFESTER, Katharina *et al.* Formulation and stability mechanisms of polymerizable miniemulsions. *Macromolecules*, v. 32, n. 16, p. 5222–5228, 1999.

LAURENTINO, Larissa S. *et al.* Synthesis of a biobased monomer derived from castor oil and copolymerization in aqueous medium. *Chemical Engineering Research and Design*, v. 137, p. 213–220, 2018. Disponível em: <<https://doi.org/10.1016/j.cherd.2018.07.014>>.

LE BROU-RYCKEWAERT, D. *et al.* Development of innovative paclitaxel-loaded small PLGA nanoparticles: study of their antiproliferative activity and their molecular interactions on prostatic cancer cells. *Int. J. Pharm.*, v. 454, p. 712–9, 2013.

LI, Chen *et al.* Tunable biphasic drug release from ethyl cellulose nanofibers fabricated using a modified coaxial electrospinning process. v. 9, n. 1, p. 1–10, 2014.

LI, L. *et al.* Epithelial cell adhesion molecule aptamer functionalized PLGA-lecithin-curcumin-PEG nanoparticles for targeted drug delivery to human colorectal adenocarcinoma cells. *Int. J. Nanomedicine*, v. 9, p. 1083–96, 2014.

LIANG, C. et al. Improved therapeutic effect of folate-decorated PLGA-PEG nanoparticles for endometrial carcinoma. *Bioorganic Med. Chem.*, v. 19, p. 4057–4066, 2011.

LLEVOT, Audrey *et al.* Renewability is not Enough: Recent Advances in the Sustainable Synthesis of Biomass-Derived Monomers and Polymers. *Chemistry - A European Journal*, v. 22, n. 33, p. 11510–11521, 2016.

LLEVOT, Audrey; MEIER, Michael A.R. Renewability-a principle of utmost importance! *Green Chemistry*, v. 18, n. 18, p. 4800–4803, 2016.

LLUCH, Cristina *et al.* Rapid approach to biobased telechelics through two one-pot thiol-ene click reactions. *Biomacromolecules*, v. 11, n. 6, p. 1646–1653, 2010.

LOWE, Andrew B. Thiol-ene “click” reactions and recent applications in polymer and materials synthesis: A first update. *Polymer Chemistry*, v. 5, n. 17, p. 4820–4870, 2014.

LOWE, Andrew B. Thiol-ene “click” reactions and recent applications in polymer and materials synthesis. *Polymer Chemistry*, v. 1, n. 1, p. 17–36, 2010.

LU, X. Y., ZHANG, Y. & WANG, L. Preparation and in vitro drug-release behavior of 5-fluorouracil-loaded poly(hydroxybutyrate-co-hydroxyhexanoate) nanoparticles and microparticles. *J. Appl. Polym. Sci.*, v. 116, p. 2944–2950, 2010.

MA, Wei *et al.* Fluoropolymer Nanoparticles Prepared Using Trifluoropropene Telomer Based Fluorosurfactants. *Langmuir*, v. 36, n. 7, p. 1754–1760, 2020.

MAAYAH, Zaid H. *et al.* The molecular mechanisms that underpin the biological benefits of full-spectrum cannabis extract in the treatment of neuropathic pain and inflammation. *Biochimica et Biophysica Acta - Molecular Basis of Disease*, v. 1866, n. 7, p. 165771, 2020. Disponível em: <<https://doi.org/10.1016/j.bbadis.2020.165771>>.

MACCALLUM, Caroline A.; RUSSO, Ethan B. Practical considerations in medical cannabis administration and dosing. *European Journal of Internal Medicine*, v. 49, n. October 2017, p. 12–19, 2018. Disponível em: <<https://doi.org/10.1016/j.ejim.2018.01.004>>.

MACHADO, Fabricio; LIMA, Enrique L.; PINTO, José Carlos. A review on suspension polymerization processes. *Polimeros*, v. 17, n. 2, p. 166–179, 2007.

MACHADO, Thiago O. *et al.* Thiol-ene miniemulsion polymerization of a biobased monomer for biomedical applications. *Colloids and Surfaces B: Biointerfaces*, v. 159, p. 509–517, 2017. Disponível em: <<https://doi.org/10.1016/j.colsurfb.2017.07.043>>.

MACHADO, Thiago O.; SAYER, Claudia; ARAUJO, Pedro H.H. Thiol-ene polymerisation: A promising technique to obtain novel biomaterials. *European Polymer Journal*, v. 86, p. 200–215, 2017. Disponível em: <<http://dx.doi.org/10.1016/j.eurpolymj.2016.02.025>>.

MANISH MUNJAL, STEVEN P. STODGHILL, MAHMOUD A. ELSOHLY, MICHAEL A. REPKA. Polymeric Systems for Amorphous D9-Tetrahydrocannabinol Produced by a Hot-Melt Method. Part I: Chemical and Thermal Stability during Processing. *Journal of pharmaceutical sciences*, v. 99, n. 5, p. 2386–2398, 2006. Disponível em: <<http://onlinelibrary.wiley.com/doi/10.1002/jps.22007/full%5Cnhttp://www.ncbi.nlm.nih.gov/pubmed/19967780>>.

MARTÍN-BANDERAS, L. *et al.* In vitro and in vivo evaluation of delta9-tetrahydrocannabinol/PLGA nanoparticles for cancer chemotherapy. *International Journal of Pharmaceutics*, v. 487, n. 1–2, p. 205–212, 2015.

MARTÍN-BANDERAS, Lucía *et al.* Engineering of delta9-tetrahydrocannabinol delivery systems based on surface modified-PLGA nanoplatfoms. *Colloids and Surfaces B: Biointerfaces*, v. 123, p. 114–122, 2014.

MASOOD, F. *et al.* Synthesis of poly-(3-hydroxybutyrate-co-12 mol % 3-hydroxyvalerate) by *Bacillus cereus* FB11: its characterization and application as a drug carrier. *J. Mater. Sci. Mater. Med.*, v. 24, p. 1927–37, 2013.

MASOOD, Farha. Polymeric nanoparticles for targeted drug delivery system for cancer therapy. *Materials Science and Engineering C*, v. 60, p. 569–578, 2016. Disponível em: <<http://dx.doi.org/10.1016/j.msec.2015.11.067>>.

MATO, Susana; VICTORIA SÁNCHEZ-GÓMEZ, María; MATUTE, Carlos. Cannabidiol induces intracellular calcium elevation and cytotoxicity in oligodendrocytes. *Glia*, v. 58, n. 14, p. 1739–1747, 2010.

MATTHEOLABAKIS, G., TAOUFIK, E., HARALAMBOUS, S., ROBERTS, M. L. & AVGOUSTAKIS, K. In vivo investigation of tolerance and antitumor activity of cisplatin-

loaded PLGA-mPEG nanoparticles. *Eur. J. Pharm. Biopharm.*, v. 71, p. 190–5, 2009.

MCALLISTER, Sean D. *et al.* Pathways mediating the effects of cannabidiol on the reduction of breast cancer cell proliferation, invasion, and metastasis. *Breast Cancer Research and Treatment*, v. 129, n. 1, p. 37–47, 2011.

MCCLEMENTS, David Julian. Nanoemulsions versus microemulsions: Terminology, differences, and similarities. *Soft Matter*, v. 8, n. 6, p. 1719–1729, 2012.

MECHOULAM, Raphael; PARKER, Linda A. The Endocannabinoid System and the Brain. *Annual Review of Psychology*, v. 64, n. 1, p. 21–47, 2013.

MEIER, Michael A.R.; METZGER, Jürgen O.; SCHUBERT, Ulrich S. Plant oil renewable resources as green alternatives in polymer science. *Chemical Society Reviews*, v. 36, n. 11, p. 1788–1802, 2007.

MENSAH, M. B.; AWUDZA, J. A.M.; O'BRIEN, P. Castor oil: A suitable green source of capping agent for nanoparticle syntheses and facile surface functionalization. *Royal Society Open Science*, v. 5, n. 8, 2018.

MIAO, Q. *et al.* Construction of hydroxypropyl- β -cyclodextrin copolymer nanoparticles and targeting delivery of paclitaxel. *J. Nanoparticle Res*, v. 14, p. 1043, 2012.

MIAO, Shida *et al.* Vegetable-oil-based polymers as future polymeric biomaterials. *Acta Biomaterialia*, v. 10, n. 4, p. 1692–1704, 2014. Disponível em: <<http://dx.doi.org/10.1016/j.actbio.2013.08.040>>.

MISHIMA, Kenji. Biodegradable particle formation for drug and gene delivery using supercritical fluid and dense gas. *Advanced Drug Delivery Reviews*, v. 60, n. 3, p. 411–432, 2008.

MONTERO DE ESPINOSA, Lucas; MEIER, Michael A.R. Plant oils: The perfect renewable resource for polymer science?! *European Polymer Journal*, v. 47, n. 5, p. 837–852, 2011. Disponível em: <<http://dx.doi.org/10.1016/j.eurpolymj.2010.11.020>>.

MOON, Hye Kyung *et al.* Significant increase in the water dispersibility of zinc phthalocyanine nanowires and applications in cancer phototherapy. *NPG Asia Materials*, v. 4, n. 4, p. e12-8, 2012. Disponível em: <<http://dx.doi.org/10.1038/am.2012.22>>.

MUTLU, Hatice; MEIER, Michael A. R. Castor oil as a renewable resource for the chemical industry. *European Journal of Lipid Science and Technology*, v. 112, n. 1, p. 10–30, 2010. Disponível em: <<http://doi.wiley.com/10.1002/ejlt.200900138>>.

NAGAVARMA, B. V.N. *et al.* Different techniques for preparation of polymeric nanoparticles- A review. *Asian Journal of Pharmaceutical and Clinical Research*, v. 5, n. SUPPL. 3, p. 16–23, 2012.

NAMDAR, Dvora *et al.* Terpenoids and phytocannabinoids co-produced in cannabis sativa strains show specific interaction for cell cytotoxic activity. *Molecules*, v. 24, n. 17, 2019.

NARAYANAN, S. *et al.* Sequential release of epigallocatechin gallate and paclitaxel from PLGA-casein core/shell nanoparticles sensitizes drug-resistant breast cancer cells. *Nanomedicine Nanotechnology, Biol. Med.*, v. 11, p. 1399–1406, 2015.

NGUYEN, Kytai Truong. Targeted nanoparticles for cancer therapy: Promises and challenges. *Journal of Nanomedicine and Nanotechnology*, v. 2, n. 5, 2011.

NIYOM, Yupaporn; CRESPIY, Daniel; FLOOD, Adrian E. Compatibility between Drugs and Polymer in Nanoparticles Produced by the Miniemulsion-Solvent Evaporation Technique. *Macromolecular Materials and Engineering*, v. 306, n. 7, p. 1–7, 2021.

NUGENT, Shannon M. *et al.* Medical cannabis use among individuals with cancer: An unresolved and timely issue. *Cancer*, v. 126, n. 9, p. 1832–1836, 2020.

OLIVAS-AGUIRRE, Miguel *et al.* Phenolic compounds cannabidiol, curcumin and quercetin cause mitochondrial dysfunction and suppress acute lymphoblastic leukemia cells. *International Journal of Molecular Sciences*, v. 22, n. 1, p. 1–13, 2021.

PAVLOVIC, Radmila *et al.* Quality traits of “cannabidiol oils”: Cannabinoids content, terpene fingerprint and oxidation stability of european commercially available preparations. *Molecules*, v. 23, n. 5, p. 1–22, 2018.

PERRET, F., DUFFOUR, M., CHEVALIER, Y. & PARROT-LOPEZ, H. Design, synthesis, and in vitro evaluation of new amphiphilic cyclodextrin-based nanoparticles for the incorporation and controlled release of acyclovir. *Eur. J. Pharm. Biopharm.*, v. 83, p. 25–32, 2013.

PETERS, Maximilian; MURILLO-RODRIGUEZ, Eric; HANUS, Lumír O. Cannabidiol – Recent Advances. v. 4, p. 1678–1692, 2007.

PICCOLO, Maria; MENALE, Ciro; CRISPI, Stefania. Combined Anticancer Therapies: An Overview of the Latest Applications. *Anti-Cancer Agents in Medicinal Chemistry*, v. 15, n. 4, p. 408–422, 2015.

PLENAGL, Nikola *et al.* Photodynamic therapy–hypericin tetraether liposome conjugates and their antitumor and antiangiogenic activity. *Drug Delivery*, v. 26, n. 1, p. 23–33, 2019. Disponível em: <<https://doi.org/10.1080/10717544.2018.1531954>>.

PRIMO, Fernando Lucas; TEDESCO, Antonio Claudio. Combining photobiology and nanobiotechnology : a step towards improving medical protocols based on advanced biological models E ditorial. *Nanomedicine*, v. 8, p. 513–515, 2013.

QUINTANAR-GUERRERO, David *et al.* Preparation techniques and mechanisms of formation of biodegradable nanoparticles from preformed polymers. *Drug Development and Industrial Pharmacy*, v. 24, n. 12, p. 1113–1128, 1998.

RAHMAN, Mustafizur; BRAZEL, Christopher S. The plasticizer market: An assessment of traditional plasticizers and research trends to meet new challenges. *Progress in Polymer Science (Oxford)*, v. 29, n. 12, p. 1223–1248, 2004.

RAJALAKSHMI, P.; MARIE, J. Margaret; MARIA XAVIER, A. John. Castor oil-derived monomer ricinoleic acid based biodegradable unsaturated polyesters. *Polymer Degradation and Stability*, v. 170, p. 109016, 2019. Disponível em: <<https://doi.org/10.1016/j.polymdegradstab.2019.109016>>.

RAO, J. Prasad; GECKELER, Kurt E. Polymer nanoparticles: Preparation techniques and size-control parameters. *Progress in Polymer Science (Oxford)*, v. 36, n. 7, p. 887–913, 2011. Disponível em: <<http://dx.doi.org/10.1016/j.progpolymsci.2011.01.001>>.

ROGUIN, Leonor P. *et al.* Zinc(II) phthalocyanines as photosensitizers for antitumor photodynamic therapy. *The International Journal of Biochemistry & Cell Biology*, v. 114, n. July, p. 105575, 2019.

ROMIO, Ana P. *et al.* Nanocapsules by miniemulsion polymerization with biodegradable

surfactant and hydrophobe. *Macromolecular Chemistry and Physics*, v. 210, n. 9, p. 747–751, 2009.

ROMIO, Ana Paula *et al.* Polymeric nanocapsules via miniemulsion polymerization using redox initiation. *Materials Science and Engineering C*, v. 29, n. 2, p. 514–518, 2009. Disponível em: <<http://dx.doi.org/10.1016/j.msec.2008.09.011>>.

SAITO, Viviane M; WOTJAK, Carsten T; MOREIRA, Fabrício A. [Pharmacological exploitation of the endocannabinoid system: new perspectives for the treatment of depression and anxiety disorders?]. *Revista brasileira de psiquiatria (Sao Paulo, Brazil : 1999)*, v. 32 Suppl 1, p. S7-14, 2010. Disponível em: <<http://www.ncbi.nlm.nih.gov/pubmed/20512266>>.

SALAZAR, María *et al.* Cannabinoid action induces autophagy-mediated cell death through stimulation of ER stress in human glioma cells. *Journal of Clinical Investigation*, v. 119, n. 5, p. 1359–1372, 2009.

SANCHEZ-RAMOS, Juan. The entourage effect of the phytocannabinoids. *Annals of Neurology*, v. 77, n. 6, p. 1083, 2015.

SANTOS, Paula Christina Mattos Dos *et al.* Evaluation of in vitro cytotoxicity of superparamagnetic poly(thioether-ester) nanoparticles on erythrocytes, non-tumor (NIH3T3), tumor (HeLa) cells and hyperthermia studies. *Journal of Biomaterials Science, Polymer Edition*, jan. 2019.

SAVAGE, Seddon R. *et al.* Cannabis in Pain Treatment: Clinical and Research Considerations. *Journal of Pain*, v. 17, n. 6, p. 654–668, 2016. Disponível em: <<http://dx.doi.org/10.1016/j.jpain.2016.02.007>>.

SCHLEICH, N. *et al.* Dual anticancer drug/superparamagnetic iron oxide-loaded PLGAbased nanoparticles for cancer therapy and magnetic resonance imaging. *Int. J. Pharm.*, v. 447, p. 94–101, 2013.

SCHORK, F. J. *et al.* Miniemulsion polymerization. *Colloids and Surfaces A: Physicochemical and Engineering Aspects*, v. 153, n. 1–3, p. 39–45, 1999.

SELTZER, Emily S *et al.* Cannabidiol (CBD) as a Promising Anti-Cancer Drug. 2020.

SHAH, M., IMRAN, M., HWAN, M., OK, M. & CHUL, S. Amphiphilic PHA – mPEG

copolymeric nanocontainers for drug delivery: Preparation , characterization and in vitro evaluation. *Int. J. Pharm.*, v. 400, p. 165–175, 2010.

SHAH, M., ULLAH, N., CHOI, M. H., KIM, M. O. & YOON, S. C. Amorphous amphiphilic P(3HV-co-4HB)-b-mPEG block copolymer synthesized from bacterial copolyester via melt transesterification: Nanoparticle preparation, cisplatin-loading for cancer therapy and in vitro evaluation. *Eur. J. Pharm. Biopharm.*, v. 80, p. 518–527, 2012.

SHEIKH, Faheem A. *et al.* Novel self-assembled amphiphilic poly(ϵ -caprolactone)-grafted-poly(vinyl alcohol) nanoparticles: Hydrophobic and hydrophilic drugs carrier nanoparticles. *Journal of Materials Science: Materials in Medicine*, v. 20, n. 3, p. 821–831, 2009.

SIAFAKA, P *et al.* Synthesis of folate- pegylated polyester nanoparticles encapsulating ixabepilone for targeting folate receptor overexpressing breast cancer cells. *Journal of Materials Science: Materials in Medicine*, 2015.

SIQUEIRA-MOURA, Marigilson P. *et al.* Development, characterization, and photocytotoxicity assessment on human melanoma of chloroaluminum phthalocyanine nanocapsules. *Materials Science and Engineering C*, v. 33, n. 3, p. 1744–1752, 2013.

ŚLEDZIŃSKI, Paweł *et al.* The current state and future perspectives of cannabinoids in cancer biology. *Cancer Medicine*, v. 7, n. 3, p. 765–775, 2018.

STAUDT, Thiago *et al.* Magnetic Polymer / Nickel Hybrid Nanoparticles Via Miniemulsion Polymerization. *Macromolecular Chemistry and Physics*, v. 214, p. 2213–2222, 2013.

SU, W.-C., SU, W.-P., CHENG, Shieh & Yeh. PLGA nanoparticles codeliver paclitaxel and Stat3 siRNA to overcome cellular resistance in lung cancer cells. *International Journal of Nanomedicine*, 2012.

TALIANOV, Pavel *et al.* Adaptive Nanoparticle-Polymer Complexes as Optical Elements: Design and Application in Nanophotonics and Nanomedicine. *Laser and Photonics Reviews*, v. 15, n. 9, p. 1–28, 2021.

TOMAZINI, Marília Vannuchi *et al.* Terapia fotodinâmica com ftalocianina de zinco tópica: Avaliação da intensidade de fluorescência, absorção cutânea, alterações histológicas e imunohistoquímicas na pele do modelo animal. *Anais Brasileiros de Dermatologia*, v. 82, n. 6, p.

535–541, 2007.

TOMKO, Andrea M *et al.* and Flavonoids Present in Cannabis. *Cancers*, v. 12, n. 1985, p. 1–68, 2020.

TORRES, Sofía *et al.* A combined preclinical therapy of cannabinoids and temozolomide against glioma. *Molecular Cancer Therapeutics*, v. 10, n. 1, p. 90–103, 2011.

TSCHAN, Mathieu J.L. *et al.* Synthesis of biodegradable polymers from renewable resources. *Polymer Chemistry*, v. 3, n. 4, p. 836–851, 2012.

TÜRÜNÇ, Oğuz; MEIER, Michael A.R. Fatty acid derived monomers and related polymers via thiol-ene (Click) additions. *Macromolecular Rapid Communications*, v. 31, n. 20, p. 1822–1826, 2010.

TÜRÜNÇ, Oğuz; MEIER, Michael A.R. A novel polymerization approach via thiol-yne addition. *Journal of Polymer Science, Part A: Polymer Chemistry*, v. 50, n. 9, p. 1689–1695, 2012.

UENO, Leonardo T.; MACHADO, Antonio E.H.; MACHADO, Francisco B.C. Theoretical studies of zinc phthalocyanine monomer, dimer and trimer forms. *Journal of Molecular Structure: THEOCHEM*, v. 899, n. 1–3, p. 71–78, 2009.

UGELSTAD, J.; EL-AASSER, MS.; VANDERHOFF, JW. Emulsion polymerization: initiation of polymerization in monomer droplets. *J Polym Sci Polym Lett*, v. 11, p. 503–2013, 1973.

UZIEL, Almog *et al.* Full-Spectrum Cannabis Extract Microdepots Support Controlled Release of Multiple Phytocannabinoids for Extended Therapeutic Effect. *ACS Applied Materials and Interfaces*, v. 12, n. 21, p. 23707–23716, 2020.

VACCARO, Luigi. Green chemistry. *Beilstein Journal of Organic Chemistry*, v. 12, p. 2763–2765, 2016.

VALÉRIO, Alexandra; ARAÚJO, Pedro H.H.; SAYER, Claudia. Preparation of poly(urethane-urea) nanoparticles containing Açaí oil by miniemulsion polymerization. *Polimeros*, v. 23, n. 4, p. 451–455, 2013.

VANDENBERGH, Joke *et al.* Cross-linked degradable poly(β -thioester) networks via amine-catalyzed thiol-ene click polymerization. *Polymer*, v. 55, n. 16, p. 3525–3532, 2014. Disponível em: <<http://dx.doi.org/10.1016/j.polymer.2014.05.043>>.

VANDENBERGH, Joke; RANIERI, Kayte; JUNKERS, Thomas. Synthesis of (bio)-degradable poly(β -thioester)s via amine catalyzed thiol-ene click polymerization. *Macromolecular Chemistry and Physics*, v. 213, n. 24, p. 2611–2617, 2012.

VANGARA, K. K., LIU, J. L. & PALAKURTHI, S. Hyaluronic Acid-decorated PLGAPEG Nanoparticles for Targeted Delivery of SN-38 to Ovarian Cancer. *Anticancer Res.*, v. 33, p. 2425–2434, 2013.

VARAN, C. & BILENSOY, E. Development of implantable hydroxypropyl- β -cyclodextrin coated polycaprolactone nanoparticles for the controlled delivery of docetaxel to solid tumors. *J. Incl. Phenom. Macrocycl. Chem.*, p. 1–7, 2014.

VELASCO, G.; SÁNCHEZ, C.; GUZMÁN, M. Anticancer mechanisms of cannabinoids. *Current Oncology*, v. 23, n. March, p. S23–S32, 2016.

VELASCO, G.; SÁNCHEZ, C.; GUZMÁN, M. Endocannabinoids and cancer. *Handbook of Experimental Pharmacology*. [S.l.]: Springer New York LLC, 2015. p. 449–472.

VELASCO, Guillermo *et al.* The use of cannabinoids as anticancer agents. *Progress in Neuro-Psychopharmacology and Biological Psychiatry*, v. 64, p. 259–266, 2016. Disponível em: <<http://dx.doi.org/10.1016/j.pnpbp.2015.05.010>>.

VELASCO, Guillermo; SÁNCHEZ, Cristina; GUZMÁN, Manuel. Towards the use of cannabinoids as antitumour agents. *Nature Reviews Cancer*, v. 12, n. 6, p. 436–444, 2012. Disponível em: <<http://dx.doi.org/10.1038/nrc3247>>.

VILOS, C. *et al.* Paclitaxel-PHBV nanoparticles and their toxicity to endometrial and primary ovarian cancer cells. *Biomaterials*, v. 34, p. 4098–4108, 2013.

VIVEK, Raju *et al.* Multifunctional HER2-Antibody conjugated polymeric nanocarrier-based drug delivery system for multi-drug-resistant breast cancer therapy. *ACS Applied Materials and Interfaces*, v. 6, n. 9, p. 6469–6480, 2014.

WANG, H. *et al.* Enhanced anti-tumor efficacy by co-delivery of doxorubicin and paclitaxel

with amphiphilic methoxy PEG-PLGA copolymer nanoparticles. *Biomaterials*, v. 32, p. 8281–90, 2011.

WEI, K., PENG, X. & ZOU, F. Folate-decorated PEG-PLGA nanoparticles with silica shells for capecitabine controlled and targeted delivery. *Int. J. Pharm.*, v. 464, p. 225–233, 2014.

WORLD HEALTH ORGANIZATION. Definition of Active Pharmaceutical Ingredient. *World Health Organization*, n. July, p. 1–4, 2011. Disponível em: <http://www.who.int/medicines/areas/quality_safety/quality_assurance/DefinitionAPI-QAS11-426Rev1-08082011.pdf>.

YAO, Y. et al. A specific drug targeting system based on polyhydroxyalkanoate granule binding protein PhaP fused with targeted cell ligands. *Biomaterials*, v. 29, p. 4823–4830, 2008.

YUAN, Q. et al. Controlled and extended drug release behavior of chitosan-based nanoparticle carrier. *Acta Biomaterialia*, v. 6, n. 3, p. 1140–1148, 2010.

ZEKIČ, Jure; KRIŽMAN, Mitja. Development of Gas-Chromatographic Method for Simultaneous Determination of Cannabinoids and Terpenes in Hemp. *Molecules (Basel, Switzerland)*, v. 25, n. 24, p. 19–27, 2020.

ZHANG, Jian et al. A PIID-DTBT based semi-conducting polymer dots with broad and strong optical absorption in the visible-light region: Highly effective contrast agents for multiscale and multi-spectral photoacoustic imaging. *Nano Research*, v. 10, n. 1, p. 64–76, 2017.

ZHANG, Yu; YANG, Mo; PORTNEY, Nathaniel G. Zeta potential: a surface electrical characteristic to probe the interaction of nanoparticles with normal and cancer human breast epithelial cells. p. 321–328, 2008.

ZHANG, Zheng; GRIJPMAN, Dirk W.; FEIJEN, Jan. Poly(trimethylene carbonate) and monomethoxy poly(ethylene glycol)-block-poly(trimethylene carbonate) nanoparticles for the controlled release of dexamethasone. *Journal of Controlled Release*, v. 111, n. 3, p. 263–270, 2006.

ZHU, Yunqing; ROMAIN, Charles; WILLIAMS, Charlotte K. Sustainable polymers from renewable resources. *Nature*, v. 540, n. 7633, p. 354–362, 2016.

ZIVOVINOVIC, Sanja et al. Determination of cannabinoids in Cannabis sativa L. samples for

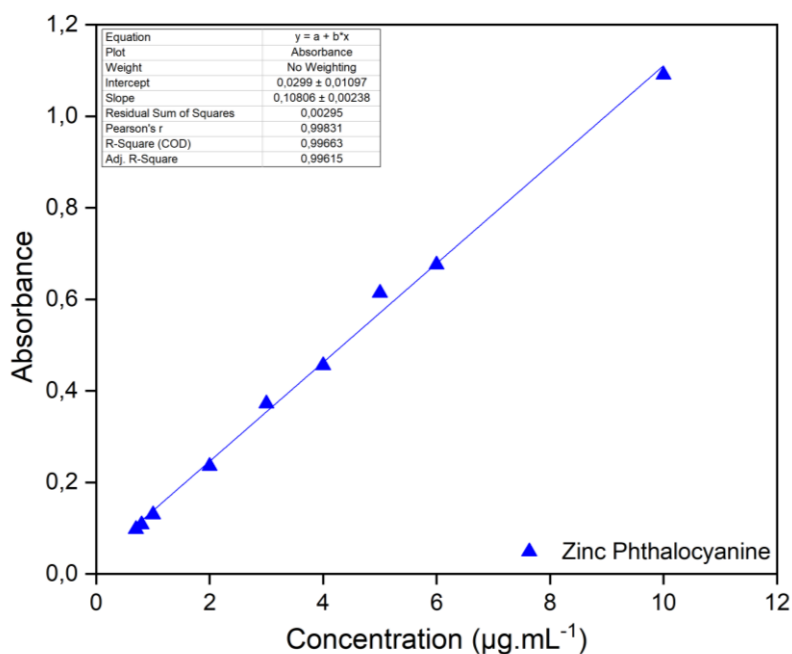
recreational, medical, and forensic purposes by reversed-phase liquid chromatography-ultraviolet detection. *Journal of Analytical Science and Technology*, v. 9, n. 1, 2018.

ZUARDI, Antonio Waldo. History of cannabis as a medicine: A review. *Revista Brasileira de Psiquiatria*, v. 28, n. 2, p. 153–157, 2006.

Appendix

Calibration curves were developed for the analysis of Zinc phthalocyanine and *Cannabis* extract encapsulation efficiency. In Figure A.1 the calibration curve was prepared using dimethylsulfoxide as a solvent and Zinc phthalocyanine as standard for the analyzes carried out on a 672 nm Spectroscopy in visible ultraviolet.

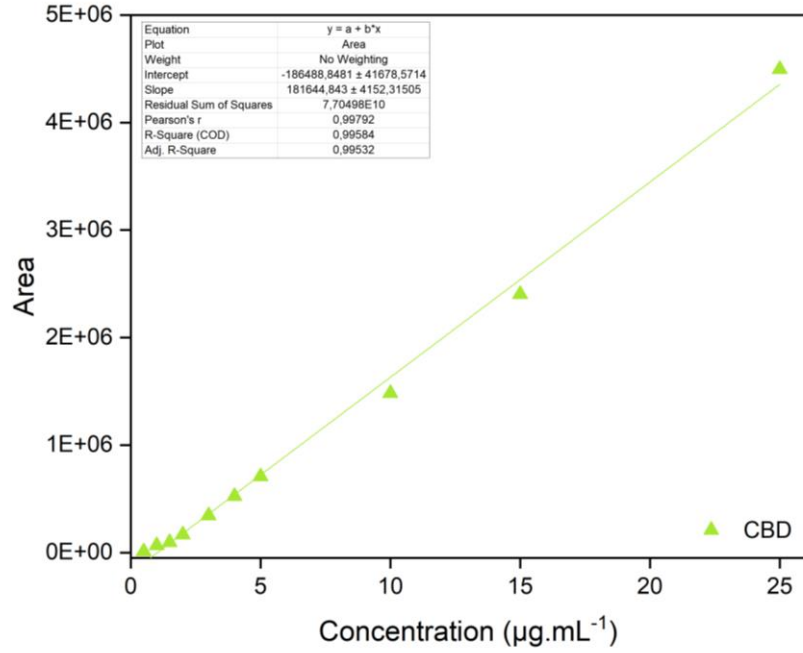
Figure A.1- Calibration curve of Zinc Phthalocyanine produced with dimethylsulfoxide as solvent for analysis of encapsulation efficiency.



Source: Author.

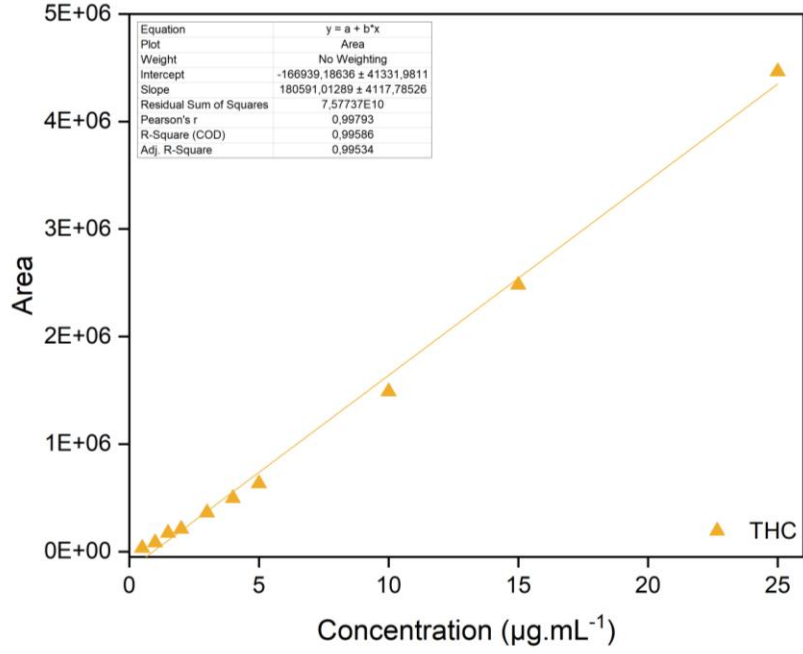
In Figure A.2, A.3 and A.4 calibration curve was prepared using methanol as a solvent and analyzed by Gas Chromatography.

Figure A.2- Calibration curve of CBD produced with metanol as solvent for analysis of encapsulation efficiency.



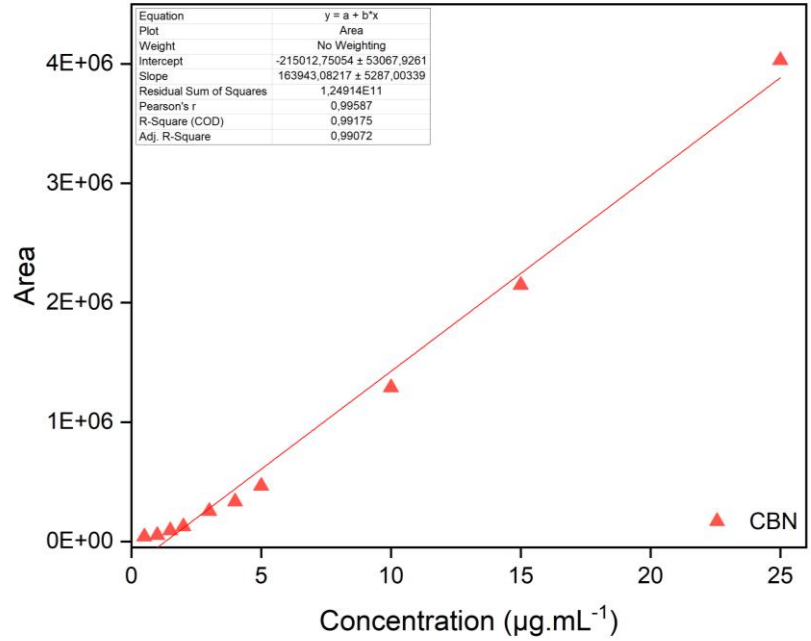
Source: Author.

Figure A.3- Calibration curve of THC produced with metanol as solvent for analysis of encapsulation efficiency.



Source: Author.

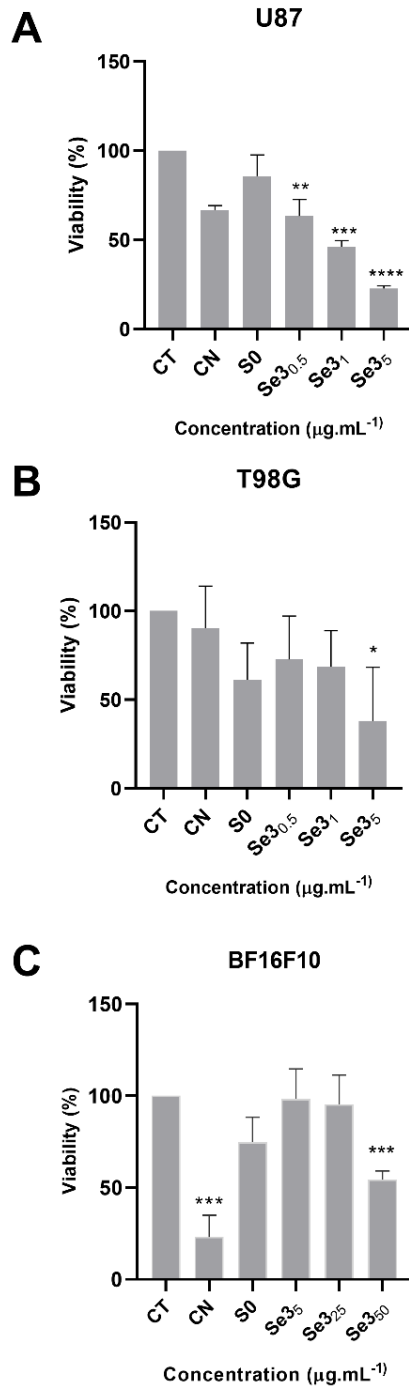
Figure A.4- Calibration curve of CBN produced with metanol as solvent for analysis of encapsulation efficiency.



Source: Author.

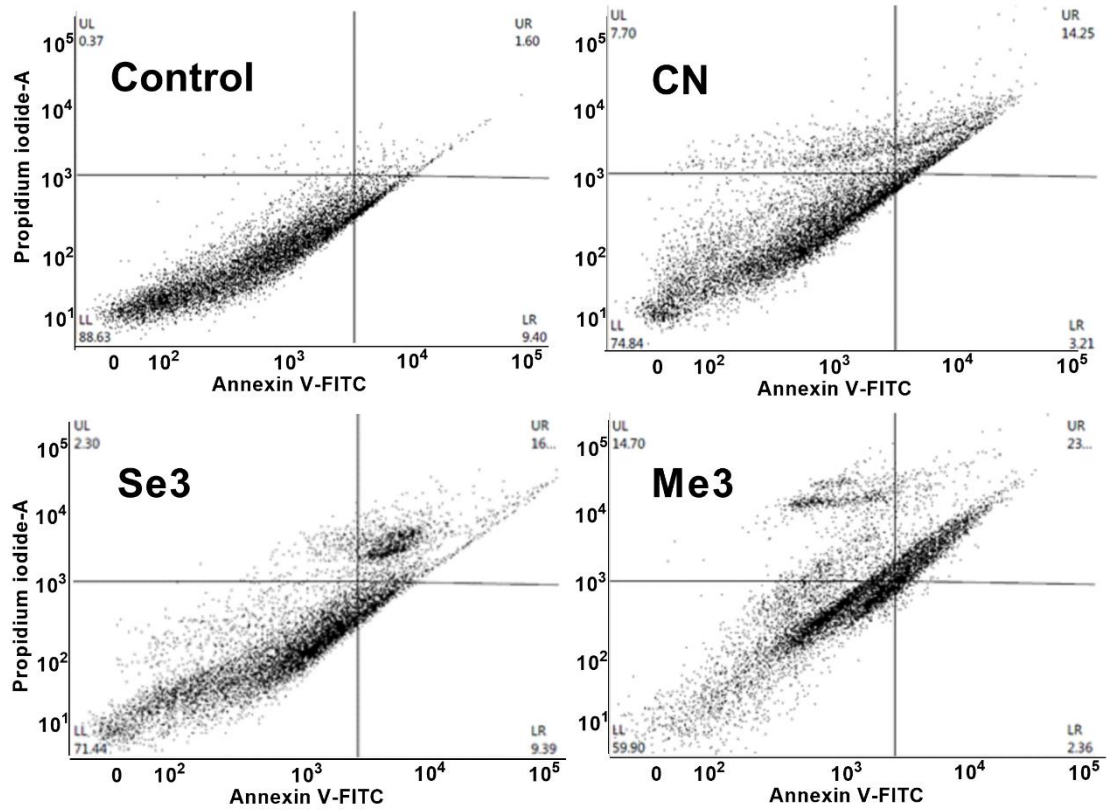
Figure A.5 and A.6 show the results of *in vitro* cytotoxicity assay of free CN and CN encapsulated in PTEe nanoparticles (Se3) of different cells line and dot plot of flow cytometry analysis.

Figure A.5- T98G (A), U87 (B) and BF16f10 (C) cells. In vitro cytotoxicity assay of free CN and CN encapsulated in PTEe nanoparticles, Se3. All assays were performed at equivalent to THC concentrations. Data are average value \pm standard deviation (n = 3). For statistical analysis we performed unpaired t test * $p < 0.05$; ** $p < 0.01$; *** $p = 0.0001$; **** $p < 0.0001$.



Source: Author.

Figure A.6- Dot plot. Flow cytometry analysis. B16F10 cells were stained with an Annexin V-FITC and propidium iodide (PI) at different incubation times after treatment with CN, Se3 and Me3 at nearly the IC50 concentration.



Source: Author.



UFBA
UNIVERSIDADE FEDERAL DA BAHIA
ESCOLA POLITÉCNICA

PROGRAMA DE PÓS GRADUAÇÃO EM ENGENHARIA INDUSTRIAL - PEI

Rua Aristides Novis, 02, 6º andar, Federação, Salvador BA

CEP: 40.210-630

Telefone: (71) 3283-9800

E-mail: pei@ufba.br

Home page: <http://www.pei.ufba.br>